Tat-translocase composition in *Corynebacterium glutamicum* and the effect of TorD coexpression

Inaugural-Dissertation

zur Erlangung des Doktorgrades
der Mathematisch-Naturwissenschaftlichen Fakultät
der Heinrich-Heine-Universität Düsseldorf

vorgelegt von

Dan Oertel
aus Hannover

Jülich, Juni 2014

aus dem Institut für Bio- und Geowissenschaften IBG-1: Biotechnologie,
Forschungszentrum Jülich GmbH
Mitglied der Helmholtz-Gemeinschaft

Gedruckt mit der Genehmigung der
Mathematisch-Naturwissenschaftlichen Fakultät der
Heinrich-Heine-Universität Düsseldorf

Referent: Prof. Dr. R. Freudl
IBG-1:Biotechnologie
Forschungszentrum Jülich GmbH

Korreferent: Prof. Dr. J. F. Ernst
Institut für Mikrobiologie
Heinrich-Heine-Universität Düsseldorf

Tag der mündlichen Prüfung: 18. September 2014

Table of contents

List of abbreviations

A. bidest	double distilled water	MOPS	3-(N-morpholino)propanesulfonic acid
APS	Ammonium persulfate	NBT	Nitro blue tetrazolium chloride
ATP	adenosine triphosphate	NMR	nuclear magnetic resonance
BCIP	5-Bromo-4-chloro-3-indolyl phosphate	OD	optical density
C.g.	*Corynebacterium glutamicum*	PAGE	polyacrylamide gel electrophoresis
Cm	Chloramphenicol	PMF	proton motive force
Da	Dalton (atomic mass unit)	REMP	Redox enzyme maturation protein
DNA	Deoxyribonucleic acid	rpm	rounds per minute
dNTP	Deoxyribonucleotide	RT	room temperature
DMF	Dimethylformamide	SD	Shine-Dalgarno sequence
DMSO	Dimethylsulfoxide	SDS	Sodium dodecyl sulfate
DTT	Dithiothreitol	SP	signal peptide
E.c.	*Escherichia coli*	TCA	Trichloracetic acid
EDTA	Ethylenediaminetetraacetic acid	TEMED	Tetramethylethylenediamine
ep	error prone (PCR method)	TMAO	trimethylamine N-oxide
FAD	Flavin adenine dinucleotide (co-factor)	TMD	transmembrane domain
GFP	Green fluorescent protein	Tris	Tris(hydroxymethyl)-aminomethan
GTP	Guanosine triphosphate	TS	temperature sensitive
IPTG	Isopropyl-β-D-thiogalactopyranosid	UV	ultraviolet
kb	kilo base	v/v	volume per volume
Km	Kanamycin	wt	wild-type
MM	minimal medium	w/v	weight per volume

Amino acid code

Alanine	Ala	A	Leucine	Leu	L
Arginine	Arg	R	Lysine	Lys	K
Asparagine	Asn	N	Methionine	Met	M
Aspartic Acid	Asp	D	Phenylalanine	Phe	F
Cysteine	Cys	C	Proline	Pro	P
Glutamic Acid	Glu	E	Serine	Ser	S
Glutamine	Gln	Q	Threonine	Thr	T
Glycine	Gly	G	Tryptophan	Trp	W
Histidine	His	H	Tyrosine	Tyr	Y
Isoleucine	Ile	I	Valine	Val	V

1. Introduction

White biotechnology employs microorganisms or microbial-derived enzymes for the production of valuable chemicals. The significance of bio-based industrial processes has been steadily increasing during the last decades; especially in facing the risks and challenges of a growing world population and being able to satisfy the growing demand for fine chemicals, food additives for humans and livestock and pharmaceutical products.

Modern biotechnology tries to address these needs by presenting bio-based production solutions which are independent of fossil-fuel carbon-sources and thus not only more sustainable but also less hazardous in their waste production. In the course of this development, the biotechnological production of proteins and peptides has rapidly grown in importance. While the market for industrial enzymes was around US$ 3.3 billion in 2010 it is estimated to reach a value of US$ 4.4 billion by 2015 (Adrio and Demain, 2014). Today, technical enzymes are being employed in a multitude of ways, e.g. amylases, xylanases and lipases for the baking industry, pectinases and cellulases for vegetable, fruit and wine processing and amylases and cellulases in the textile industry, many of which are produced in *Bacillus spec.* and fungi such as *Aspergillus spec.* or *Trichoderma spec.* (Sarrouh et al., 2012). Also products of pharmaceutical relevance such as recombinant human insulin produced in *Escherichia coli* (Schmidt, 2004) or human Interferon (IFN)-γ in *B. subtilis* (Rojas Contreras et al., 2010) have a large demand.

Advantageous for downstream processing is the direct secretion of the desired polypeptide product into the culture supernatant which can be accomplished with G ram-positive secretion hosts such as *Bacillus ssp.* or *Corynebacterium glutamicum*.

1.1. *Corynebacterium glutamicum*

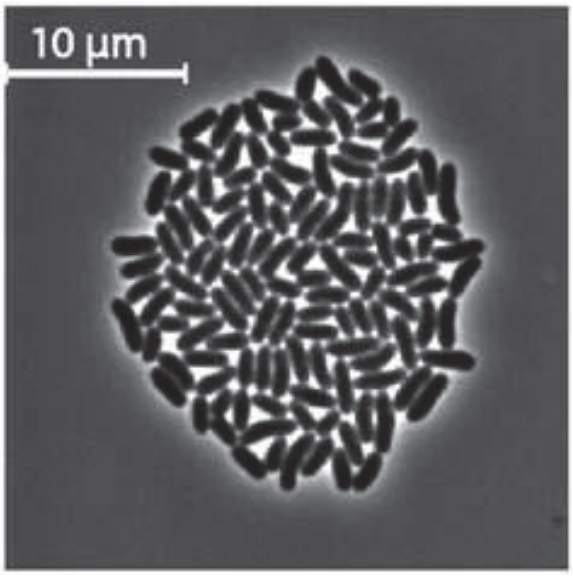

The Gram-positive soil bacterium *Corynebacterium glutamicum* is a rod-shaped organism (image courtesy of A. Grünberger) belonging to the suborder *Corynebacterineae* of the class *Actinobacteria*, to which organisms such as *Mycobacterium ssp., Nocardia ssp.* or *Rhodococcus ssp.* also belong.

C. glutamicum was originally isolated in the 1950's as a natural producer of large quantities of L-glutamate (Kinoshita et al., 1958). Today, *C. glutamicum* is widely used for the bulk production of small molecules such as L-glutamate, the salt of which is used as a *umami*-flavor enhancer (2.6 million tons/ year[1]) and L-lysine, a livestock feed additive (2.1 million tons/ year) (Vogt et al., 2013). It has GRAS status (Generally Regarded As Safe), making it an ideal biotechnological production organism. *C. glutamicum* has been fully sequenced and has a genome size of 3,28 Mb with roughly 3000 protein-encoding

1. source: http://www.ajinomoto.com (2013)

genes and a G/C content of 53,8% (Kalinowski et al., 2003).
Due to its close relation to human pathogens such as *Mycobacterium tuberculosis, Mycobacterium leprae* and *Corynebacterium diphteria*, *C. glutamicum* has also evolved as a model organisms for these pathogenic *Actinobacteria* (Kalinowski et al., 2003; Varela et al., 2012).

1.1.1 The cell envelope of *C. glutamicum*

Although Gram-positive by the classical staining method (Gram, 1884), several characteristics place *C. glutamicum,* and *Actinobacteria* in general, in between Gram-positive and -negative bacteria. One of the most noticeable features is the composition of their cell envelope.
Gram-negative bacteria such as *E. coli* have a diderm cell envelope organization. Between an outer membrane and the inner cytoplasmic membrane, a layer of peptidoglycan and an aqueous compartment, termed the periplasm are found (see figure 1). The distinguishing feature of a Gram-negative cell envelope is the outer membrane of which only the inner leaflet is composed of phospholipids, the outer leaflet is composed of glycolipids, mainly lipopolysaccharides (Silhavy et al., 2010). The outer membrane contains lipoproteins and an abundance of β-barrel proteins (Nikaido, 2003). The periplasm is thought to be of high viscosity (Mullineaux et al., 2006), densely filled with proteins and can functionally be considered as a cellular compartment (Desvaux et al., 2009).
Most Gram-positive bacteria on the other hand do not possess an outer membrane and are therefore monoderm. To protect the cell from osmotic pressure and to retain its shape, they instead have a thick peptidoglycan cell wall which is many times thicker than that of Gram-negative bacteria (see figure 1). The peptidoglycan cell wall is interspersed with proteins as well as with long anionic polymers called teichoic acids which are either joined covalently to the peptidoglycan or, as lipoteichoic acids, attached to the inner membrane (Silhavy et al., 2010). Due to the absence of a periplasm as well as a diffusion barrier to the outside of the cell wall, proteins not intended to diffuse into the extracellular milieu have to be either attached to the cytoplasmic membrane by membrane-spanning helices or lipid

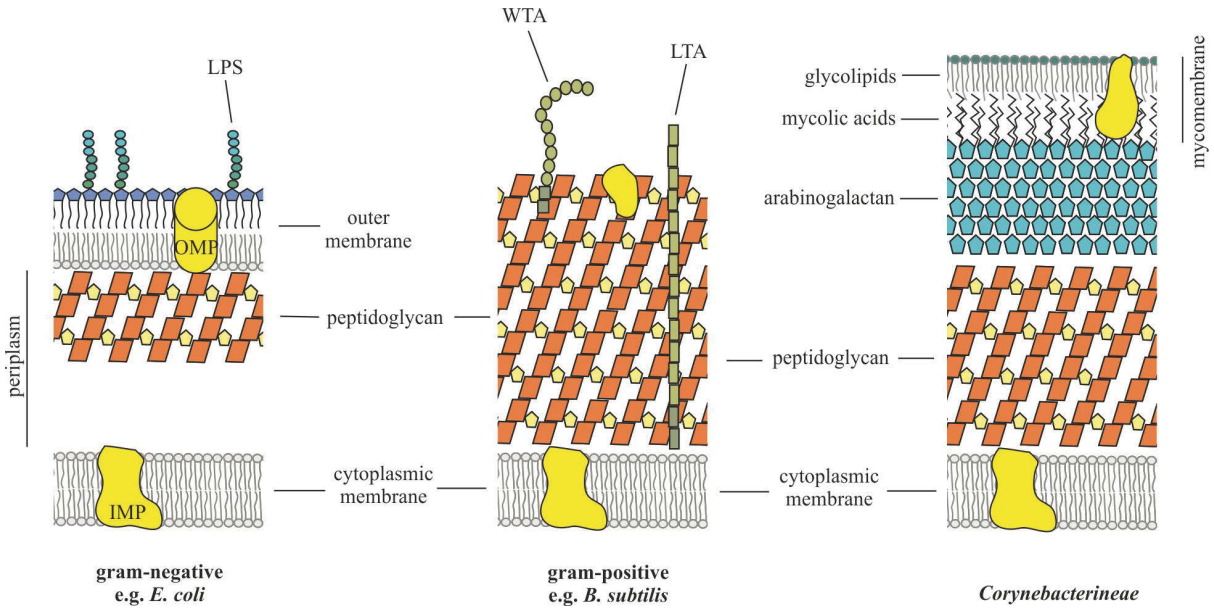

Figure 1: The cell envelope of Gram-negative and Gram-positive bacteria in comparison to *Corynebacterineae*. Inner membrane protein (IMP), outer membrane protein (OMP), lipopolysachcharides (LPS), wall teichoic acids (WTA), lipoteichoic acids (LTA).

anchors or covalently attached to the peptidoglycan or to teichoic acids (Scott and Barnett, 2006).
The cell envelope of *C. glutamicum* is fundamentally different from Gram-positive and -negative bacteria. The peptidoglycan that surrounds the cytoplasmic membrane is covalently attached to a layer of arabinogalactan (a polymer of arabinose and galactose) which is in turn attached to mycolic acids (Silhavy et al., 2010). These mycolic acids, which are long chain fatty acids (up to C_{90} in mycobacteria), make up a majority of the lipids of the inner leaflet of the outer membrane (see figure 1) (Zuber et al., 2008). The outer leaflet of the outer membrane of *C. glutamicum* is mainly composed of trehalose dimycolates, phosphatidylinositol mannosides and highly apolar lipids and also contains outer membrane proteins (Hoffmann et al., 2008; Bansal-Mutalik and Nikaido, 2011). A further outer layer has been reported for several members of *Corynebacterineae*, the S-layer, the thickness of which varies greatly from 2 to 35 nm depending on the method used for measuring it (Bayan et al., 2003). It is supposedly an envelope layer composed of carbohydrates and glycoproteins (Bayan et al., 2003). This S-layer is not present in the strain *C. glutamicum* ATCC 13032 used in this study (Hansmeier et al., 2006).
The mechanism of small molecule in- and efflux as well as mycomembrane permeability is still poorly understood. For example, it could be shown that in mycobacteria the permeability of the outer membrane for β-lactams is three orders of magnitude lower than in *E. coli* (Jarlier and Nikaido, 1990). The mechanism by which large molecules such as proteins are able to pass through this mycomembrane is even more mysterious despite the fact that *C. glutamicum* as well as mycobacteria are very efficiently able to do so (Meissner et al., 2007; Niederweis et al., 2010).

1.2. Sec-dependent protein translocation

The majority of proteins in bacteria are translocated across the cytoplasmic membrane via the general Sec pathway. This pathway is also responsible for the integration of most transmembrane domain-containing integral membrane proteins and membrane-anchored proteins such as lipoproteins (Freudl, 2013). The bacterial Sec translocase is homologous to the Sec61αβγ translocation apparatus of the eukaryotic endoplasmatic reticulum (du Plessis et al., 2010).
Proteins are targeted to the membrane by an N-terminal signal peptide which has a tripartite structure, an N-terminal basic n-region, a hydrophobic h-region and a C-terminal polar c-region. The c-region contains a cleavage site which is recognized by a signal peptidase to remove the signal peptide after translocation has occured (Rusch and Kendall, 2007).
The targeting of the substrate to the translocase can be realized by two different mechanisms, depending on the hydrophobicity of the signal peptide. Proteins posessing highly hydrophobic signal peptides or transmembrane segments intended for incorporation into the cytoplasmic membrane are targeted co-translationally by a signal recognition particle (SRP). The polypeptide emerging from the ribosome, a so-called ribosome nascent chain complex (RNC), is recognized by the SRP which is a ribonucleoprotein composed of the Ffh protein (fifty-four homologue) and a small cytoplasmic RNA (4.5S RNA in *E. coli*) (Poritz et al., 1990). This RNC-SRP complex is then targeted to the membrane associated SRP receptor FtsY from where, after binding and GTP-hydrolysis, the RNC is transferred to the translocon (Valent et al., 1998).
An alternative targeting pathway to the Sec translocase exists in *E. coli* and also other proteobacteria for substrates with less hydrophobic signal peptides which is dependent on the cytoplasmic chaperone SecB. Posttranslationally, SecB binds to the substrate to protect it from intracellular proteolysis and premature folding (Bechtluft et al., 2007). Next, the bound substrate is targeted to the translocase

component SecA and translocation is initiated (Valent et al., 1998). All Gram-positive bacteria are missing a SecB, the only known exception being *M. tuberculosis,* where a homologue called Rv1957 was identified which can functionally substitute for SecB in *E. coli* (Bordes et al., 2011). To date, *C. glutamicum* is not known to possess a SecB homologue or a functional analogue.
The Sec translocase itself is composed of the translocation pore forming components SecYEG which build up a dynamic channel of approximately 5-9Å (Lycklama a Nijholt and Driessen, 2012). In the SRP-dependent co-translational translocation mode the substrate is thought to be "pushed" through the SecYEG channel by the force of the polypeptide elongation within the ribosome (du Plessis et al., 2010). The integration of hydrophobic transmembrane segments is achieved by releasing these polypeptide stretches into the lipid bilayer through a lateral gate in the translocation pore (Dalbey et al., 2011). In SRP-independent post translational targeting of Sec-dependent translocation substrates (with the aid of SecB in proteobacteria), the translocation of the substrate is facilitated with the help of the "motor protein" SecA which has ATPase activity and pushes the substrate through the SecYEG pore in a stepwise manner (du Plessis et al., 2010).
Further components involved in Sec-dependent translocation are the accessory components YidC and SecDF. YidC is an essential gene product which has a membrane protein insertase function. It functions in conjunction with the Sec-translocase as well as independently and also participates in inner membrane protein folding (Kol et al., 2008). SecDF plays an important role in later stages of Sec-dependent protein translocation and membrane protein biogenesis (Lycklama a Nijholt and Driessen, 2012). Although deletion of *secDF* is possible in *E. coli*, translocation is drastically reduced (Pogliano and Beckwith, 1994). It has been shown that SecDF assists in the translocation of some substrates in a PMF-dependent manner (Tsukazaki et al., 2011) and increases the efficiency of membrane protein insertion by the Sec translocase (Schulze et al., 2014).
A distinctive feature of some, mainly pathogenic, Gram-positive bacteria is the presence of a second copy of *secA*. In *M. tuberculosis*, where SecA2 was first discovered, it is responsible for the translocation of a subset of substrates (SecA2-only) some of these, remarkably, not containing a signal peptide (Freudl, 2013). *C. glutamicum* also possesses an accessory SecA2 which, markedly, turned out to be just as essential for viability as SecA1 (Caspers and Freudl, 2008).

1.3. Tat-dependent protein translocation

In contrast to the Sec-pathway that translocates proteins in an unfolded state, the twin-arginine protein translocation (Tat) pathway has the remarkable ability to translocate fully folded, co-factor containing and even oligomerized proteins across the cytoplasmic membrane. The pathway was first identified being responsible for protein import into thylakoids of plant chloroplasts and termed ΔpH-dependent pathway due to its sole energetic reliance on the proton gradient across the thylakoidal membrane (Chaddock et al., 1995; Settles et al., 1997).
In plants, the Tat-pathway could be shown to ubiquitously present. Due to its localization in thylakoids of chloroplasts, it was probably evolutionarily obtained by endosymbiosis of an ancestral cyanobacterium (Dyall et al., 2004). It is essential for the assembly of the photosystem II and the cytochrome b_6f complex and thus a prerequisite for photosynthesis (Molik et al., 2001). Rudimentary remains of the Tat-pathway could also be identified in some mitochondria of plants and protists. In most of these organisms the function is not known (Yen et al., 2002).
In bacteria, the Tat-pathway translocates a wide variety of substrates encompassing proteins involved in e.g. energy metabolism, cell division, cell motility, iron- and phosphate uptake, quorum sensing and

resistance against antimicrobial peptides (Palmer and Berks, 2012). In most bacteria the pathway is not essential with a notable exception being *Mycobacterium tuberculosis* (Saint-Joanis et al., 2006). In this organism, as in many other plant and animal pathogens, the Tat-pathway plays an important role in pathogenicity (De Buck et al., 2008).

1.3.1 The Tat signal peptide

The targeting of a substrate to the Tat-translocase occurs, in most cases, via an N-terminal signal peptide. These signal peptides are approximately 25 to 45 amino acids long and of a tripartite structure. They have similarities to the Sec signal peptides, possessing an N-terminal basic n-region, a hydrophobic h-region and a C-terminal polar c-region (see figure 2 for some examples relevant to this work). The characteristic feature of Tat-signal peptides is the highly conserved twin-arginine motif S/T-R-R-x-F-L-K found towards the end of the n-region. The two arginine residues are practically invariant and the amino acid at position x can be any amino acid (Stanley et al., 2000; Palmer and Berks, 2012). Remarkably, some Tat-dependent substrates without a Tat signal peptide can be exported in a "hitchhiking"-manner. They oligomerize with another substrate which possesses a Tat signal peptide such as the small subunit of hydrogenase 2 HybO which is co-translocated with its large subunit HybC in *E. coli* (Rodrigue et al., 1999).
At the end of the c-region a cleavage site for a signal peptidase, such as the type I signal peptidase LepB in *E. coli*, which recognizes a A-x-A consensus motif is located (Lüke et al., 2009). If the Tat substrate is to be attached to the *trans* side of the cytoplasmic membrane, a type II lipoprotein signal peptidase recognizes a cleavage site with a consensus motif of L-A/S/T-G/A. If this is the case, the +1 residue of the mature protein is invariably a cysteine which is modified by addition of a fatty acid (lipidation) prior to cleavage (Babu et al., 2006; Rezwan et al., 2007).

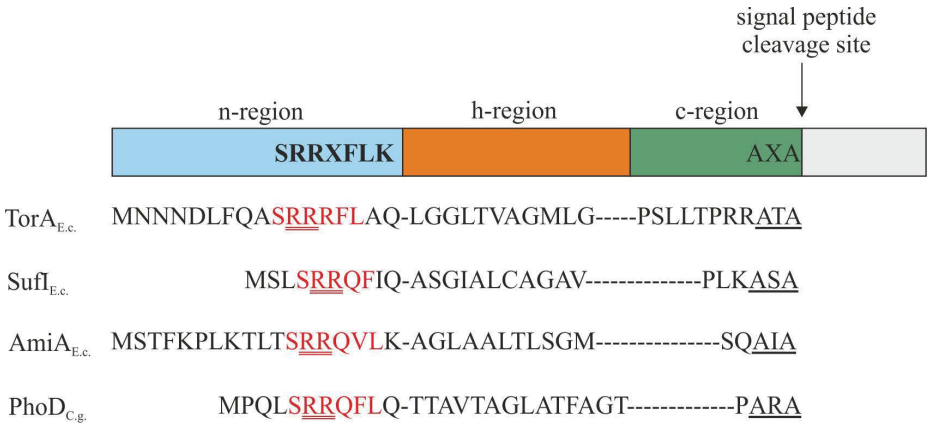

Figure 2: Schematic composition (top) and amino acid sequence of the Tat signal peptides of the TMAO reductase TorA, a member of the multi copper oxidase superfamily SufI, the amidase AmiA (*E. coli*) and the alkaline phosphatase PhoD (*C. glutamicum*). The Tat consensus motiv is highlighted in red, the twin-arginine residues are double-underlined and the recognition site for the signal peptidase is single-underlined.

As the signal peptides of the general Sec and the twin-arginine pathways resemble each other in general structure, unwanted translocation of Tat-substrates via the Sec pathway has to be prevented. This is accomplished by a lower hydrophobicity of the h-region of the Tat signal peptide and sometimes by the presence of basic amino acid residues within the c-region of the Tat signal peptide (Bogsch et al., 1997; Cristóbal et al., 1999; Blaudeck et al., 2003). Furthermore, a positive charge within the extreme

N-terminus of the mature protein part can prevent targeting to the Sec translocase (Tullman-Ercek et al., 2007). These loosely defined attributes of the Tat precursor proteins have been termed "Sec-avoidance" properties (Bogsch et al., 1997) and are thought to possibly prevent proper channeling of the substrate into the SecYEG translocon (Blaudeck et al., 2003).

1.3.2 The Tat translocase of *E. coli* and plant thylakoids

The twin-arginine translocation pathway has been most extensively studied in the Gram-negative model organism *Escherichia coli* and in the thylakoid membrane of plant chloroplasts. The translocase is composed of the three integral membrane proteins TatA, TatB and TatC (Sargent et al., 1999). In plant thylakoids these are termed Tha4 (thylakoid assembly), Hcf106 (high-chlorophyll fluorescent) and cpTatC, respectively (Settles et al., 1997; Walker et al., 1999; Mori et al., 2001).
The components TatA and TatB are homologous and have a very similar overall structure (Barnett et al., 2011). Both possess an N-terminal transmembrane domain followed by a hinge region, an amphipathic helix and an unstructured C-terminus. It could be determined that both components have a N-out/C-in topology, orienting the amphipathic helix into the cytoplasm (Koch et al., 2012). In *E. coli* and some other organisms, a cryptic gene duplication of *tatA*, termed *tatE*, can be found. In *E. coli*, TatE, which has over 50% sequence identity to TatA (Sargent et al., 1998), can functionally replace TatA in a *tatA*-mutant strain (Sargent et al., 1999). Albeit, the expression level of *tatE* is significantly lower than that of *tatA* in *E. coli* and a physiological role has not yet been identified (Jack et al., 2001; Baglieri et al., 2012).
TatC is the largest of the Tat components and possesses six transmembrane domains. The insertion of TatC into the cytoplasmic membrane is dependent on the Sec-pathway (Zhu et al., 2012). A crystal structure of TatC of *Aquifex aeolicus* was recently obtained which showed that it forms a " baseball glove-like structure" in which the open palm is the proposed binding pocket for the signal peptide of the substrate (Ramasamy et al., 2013).
The translocation process in itself has not yet been fully understood. It could be shown that the translocation of substrates is solely energized by the proton motive force (PMF) (Yahr and Wickner, 2001). At the same time it has to be considered that *E. coli* for example is able to translocate substrates ranging in size from 10 kDa high potential iron-sulfur proteins (Bruser et al., 2003) to a nearly 150 kDa heterodimeric formate dehydrogenase (Sargent et al., 2002). These fully folded substrates, varying in diameter from 20 to 70 Å, have to be exported through an intact cytoplasmic membrane (Palmer and Berks, 2012). It is imperative for the cell to accomplish this without significant ion-leakage from or into the cytoplasm. This astonishing feat of having such a variety in the size of exported substrates and at the same time having to protect the integrity of the membrane is accomplished by a highly dynamic array of small membrane spanning proteins, the Tat components.
One possible mechanism of the translocation process can be seen schematically in figure 3. First, the signal peptide of the substrate is recognized by a TatBC receptor complex. This complex within the membrane has a TatB:TatC stochiometry of 1:1 (Bolhuis et al., 2001) and both components together have contact to the signal peptide (Alami et al., 2003; Lausberg et al., 2012). In plant thylakoids it has been shown that the binding of the signal peptide into a pocket formed by the TatBC receptor complex is strengthened by the presence of a proton gradient (Gerard and Cline, 2007). Next, recruitment of TatA multimers, which comprise the actual translocation "channel", takes place PMF-dependently (Dabney-Smith and Cline, 2009). The nature of this event has not been fully elucidated but one model suggests the assembly of differently sized TatA complexes to build up individual protein channels to accommodate the differing sizes of substrates. These TatA complexes can be visualized by single par

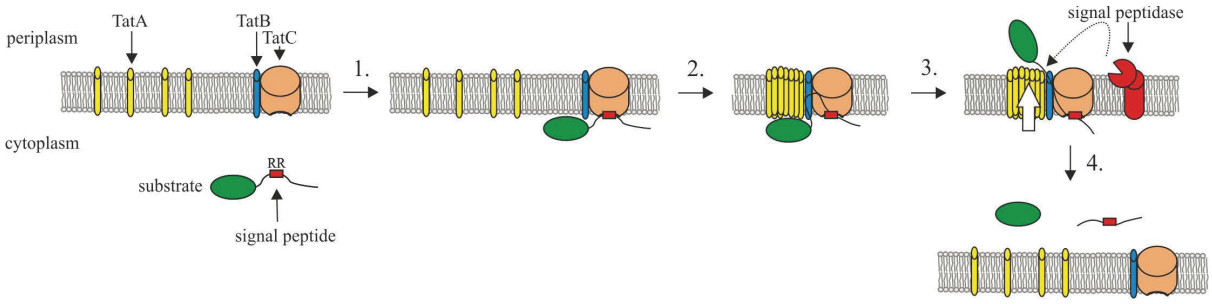

Figure 3: Tat-dependent translocation. **1.** The substrate, which has an N-terminal signal peptide containing the twin-arginine motiv, is recognized and bound by a TatBC receptor complex. **2.** TatA multimers are recruited to the TatBC/substrate complex and form a protein conducting channel. **3.** Translocation of the substrate across the cytoplasmic membrane takes place (possibly energized by the proton motive force). **4.** After translocation, the signal peptide is cleaved by signal peptidase and the substrate is released into the extracytoplasmic space.

ticle electron microscopy (Gohlke et al., 2005).
Another translocation model suggests a local "weakening" of the membrane (Brüser and Sanders, 2003). By solution NMR it could be shown that the ring-like TatA multimers have an orientation where the transmembrane domains are located in the centre and the amphipathic helices are oriented radially to the outside of this ring. These ring-like structures can be assembled with varying numbers of TatA molecules to adapt to different cargo sizes. Now, as the transmembrane domains of TatA are too short to fully span the membrane, in the center of this ring-like structure the cytoplasmic membrane is thinned and distorted. At this point the translocation substrate lies against the amphipathic helices of this TatA ring and is then pulled through the destabilized patch of membrane in the centre which ruptures and allows the substrate to exit the cytoplasm (Rodriguez et al., 2013).
Whatever the exact translocation mechanism is, when the translocase is assembled, the substrate is transported to the *trans* side of the membrane and the signal peptide is cleaved by a signal peptidase (Lüke et al., 2009). Directly after the translocation process, the TatABC complexes redissociate into TatA and TatBC complexes (Mori and Cline, 2002). The amount of energy required for translocation is significant. In plant thylakoids it has been estimated that the export of a single substrate removes around 10^5 protons from the gradient which is an energetic equivalent to around 10^4 molecules of ATP per substrate translocated (Alder and Theg, 2003).

1.3.3 Evolutionary diversity of the Tat-pathway

As mentioned above, the Tat pathway can be found in the cytoplasmic membranes of many eubacteria and archae as well as in the thylakoid membranes of plant chloroplasts (Simone et al., 2013). In some mitochondria of plants and protists, a copy of *tatC* has been found (Yen et al., 2002), one example being the homoscleromorph sponge *Oscarella* (Pett and Lavrov, 2013). Bacteria missing the Tat-pathway altogether generally have a genome size of less than 2 Mb or occur as obligate intracellular parasites (Simone et al., 2013).
Interestingly, not all of the organisms containing a Tat-pathway possess the three translocase components TatA, TatB and TatC as described in the previous section. Also, the genetic organization of the *tat*-genes is very diverse, indicating different time-points and sources of *tat*-gene acquisition during evolution (some examples are shown in the table below).

	Organism	TatA/E	TatB	TatC	*tat* operon arrangement
Gram-negative eubacteria	*Escherichia coli*	2	1	1	*tatABC* ⦚ *tatE*
	Salmonella enterica	2	1	1	*tatABC* ⦚ *tatE*
	Campylobacter jejuni	1	1	1	*tatBC* ⦚ *tatA*
	Ricketisia conorii	1		1	*tatA* ⦚ *tatC*
Gram-positive eubacteria	*Bacillus subtilis*	3		2	$tatA_yC_Y$ ⦚ $tatA_DC_D$ ⦚ $tatA_C$
	Staphylococcus aureus	1		1	*tatAC*
	Corynebacterium glutamicum	2	1	1	*tatAC* ⦚ *tatB* ⦚ *tatE*
	Mycobacterium tuberculosis	1	1	1	*tatAC* ⦚ *tatB*
Archae	*Archaeoglobus fulgidus*	2		2	*tatA1* ⦚ *tatA2* ⦚ *tatC1* ⦚ *tatC2*
Plant chloroplasts	*Arabidopsis thaliana*[2]	1	1	1	*cpTatC* ⦚ *Hcf106* ⦚ *Tha4*
	Zea mays[3]	1	2	2	*Tha4* ⦚ $cpTatC_1$ ⦚ $Hcf106_1$ ⦚ $cpTatC_2$ ⦚ $Hcf106_2$

Figure 4: Tat-translocase components are found throughout bacteria, archae and plant chloroplast but the number of components and *tat* gene arrangement vary greatly.

While most proteobacteria and plant chloroplasts use a TatABC-type translocase, phylogenetic analysis has revealed that a significant number of eubacterial and all archaeal genomes are missing a copy of *tatB* (Simone et al., 2013). Translocases missing TatB were termed TatAC-type translocases and will be discussed in more detail on the example of *Bacillus subtilis* in the next section. A further simplification of the Tat-pathway is observed in some eukaryotic organisms where the mitochondrial genome only codes for a copy of *tatC*. It has been suggested that in these organisms the one-component translocase serves solely as an insertase of specific membrane proteins and is incapable of fully translocating substrates across the membrane (Pett and Lavrov, 2013).

1.3.4 The TatAC-type translocases of *Bacillus subtilis*

In *E. coli*, although their structure is very similar, TatA and TatB have very distinct functions and cannot replace each other (Sargent et al., 1999). While TatA multimers constitute the protein conducting channel, TatB serves, together with TatC, in the recognition of the substrate. Thus, deletion of either *tatA* or *tatB* renders the *E. coli* Tat-translocase virtually incapable of translocating natural substrates (Sargent et al., 1999). Only reduced amounts of highly-sensitive artificial model substrates can be still be exported in an *E. coli* Δ*tatB* strain in comparison to the wild-type strain (Ize et al., 2002; Blaudeck et al., 2005).
In many organisms, the TatB component of the Tat translocase is missing. Here, both the TatA and

2. *Arabidopsis thaliana* is diploid and has 5 chromosomes. *Tha4* is on chromosome 4, *Hcf106* on chromosome 5 and *cpTatC* is on chromosome 2.

3. *Zea mays* is diploid and has 10 chromosomes. *Tha4* is on chromosome 1, one copy each of *Hcf106* on chromosomes 2 and 10 and one copy of *cpTatC* on chromosomes 1 and 9.

TatB function are fulfilled by a single "bifunctional" TatA molecule (Barnett et al., 2008). This means that a bifunctional TatA component is able to both act within the receptor complex in signal peptide recognition as well as form the actual protein conducting channel. Interestingly, because this emphasizes the structural resemblance of TatA and TatB molecules, in *E. coli* it was possible to generate bifunctional TatA molecules by mutagenesis. Only one or two mutations within the extreme N-terminus of TatA are necessary to promote near wild-type export in the absence of TatB (Blaudeck et al., 2005).
The best understood Tat-translocases of the AC-type have been investigated in the model organism *Bacillus subtilis*. This prototypical low-G/C Gram-positive bacterium encodes three copies of *tatA* and two copies of *tatC*. These five Tat-components have been termed $TatA_Y$, $TatA_D$, $TatA_C$, $TatC_Y$ and $TatC_D$. Two physiologically relevant translocases have been identified in *B. subtilis*. The first being $TatA_YC_Y$, the two components of which are encoded in one $tatA_YC_Y$ operon (Jongbloed et al., 2004). The translocase $TatA_YC_Y$ is expressed under all conditions and has been shown to translocate YwbN, a Dyp-type peroxidase, and YkuE, a metal-dependent phosphoesterase (Monteferrante et al., 2012b). The second translocase is $TatA_DC_D$, also encoded in one operon $tatA_DC_D$, which is only expressed under conditions of phosphate starvation and only one natural substrate, the phosphodiesterase PhoD, has been allocated to it (Jongbloed et al., 2000; Pop et al., 2002). The third TatA molecule called $TatA_C$ is not found in an operon and its physiological role is still unclear (Monteferrante et al., 2012a).
The reason why *B. subtilis* maintains two Tat-translocases is unclear but it has given rise to some very interesting investigations into the diversity of the Tat-pathway. It could be shown that, next to the two already observed physiologically relevant translocases $TatA_YC_Y$ and $TatA_DC_D$, further combinations can constitute functional translocases. While a $TatA_YC_D$ translocase does not seem to be functional (Barnett et al., 2008), the overexpression of $TatA_D$ in a *B. subtilis* $tatA_Y$ mutant allows export of the *B. subtilis* peroxidase YwbN via a $TatA_DC_Y$ translocase (Eijlander et al., 2009). It could also be shown that the third TatA copy of *B. subtilis,* $TatA_C$, can assemble functional translocases with both *B. subtilis* TatC molecules (resulting in $TatA_CC_Y$ and $TatA_CC_D$) in an *E. coli tatABCD*-mutant (Monteferrante et al., 2012a).
In summary, out of three TatA and two TatC molecules, five out of six theoretically possible TatAC translocases can be functionally assembled. Furthermore, yeast-two-hybrid analysis revealed that all three TatA variants can form not only homo- but also heterooligomers (Monteferrante et al., 2012b). This inter-compatibility of the *B. subtilis* Tat-components gave rise to speculation that a diverse subset of Tat-translocases could form an intricate network of specific translocases for specific substrates (Monteferrante et al., 2012b).

1.3.5 The Tat-translocase of *Corynebacterium glutamicum*

C. glutamicum translocates proteins very efficiently across the cytoplasmic membrane using the Tat-pathway. This could be shown for several heterologous substrates such as *Streptomyces mobaraensis* transglutaminase (Date et al., 2004), human epidermal growth factor (Date et al., 2006) and also an FAD co-factor containing *Streptomyces coelicolor* sorbitol/xylitol oxidase (Scheele et al., 2013). In a comparative analysis of Tat-dependent translocation in Gram-positive bacteria between *C. glutamicum*, *B. subtilis* and *Staphylococcus carnosus*, only *C. glutamicum* was able to secrete the green fluorescent protein GFP into the culture supernatant in an active, fluorescing form (Meissner et al., 2007). Already being an established industrial production organism for the production of small molecules such as bulk amino acids, *C. glutamicum* is also beginning to be used for the industrial production of

proteins and peptides[4]. The major advantages of using *C. glutamicum* as an industrial producer of proteins are that secreted proteins can be directly isolated from the culture supernatant, omitting time-consuming and costly downstream-processing steps as well as the fact that the proteolytic activity in the culture supernatant is very low (Billman-Jacobe et al., 1995).

In the genome of *Corynebacterium glutamicum,* four *tat*-genes are found. As in most other Gram-positive organisms a *tatAC* (*cg1685, cg1684*) operon is found but, until recently, the presence of *tatB* (*cg1273*) and *tatE* (*cg3381*) (which are both not encoded in proximity to *tatAC*) had been overlooked (Dilks et al., 2003). A first comprehensive analysis of the Tat-translocase of *C. glutamicum* ATCC 13869 revealed that the deletion of *tatA* and *tatC* resulted into a serious growth defect. This indicates that a physiologically important substrate is translocated via the Tat-pathway of *C. glutamicum*. Furthermore, these deletions disallow the translocation of the artificial substrate $TorA^{SP}$-GFP, the signal peptide of *E. coli* TMAO reductase TorA fused to the green fluorescent protein (Kikuchi et al., 2006). The deletion of *tatE* has no effect on the growth phenotype and still allowed translocation of $TorA^{SP}$-GFP. This indicates that *C. glutamicum tatE* is, analogous to the situation in *E. coli*, a cryptic gene duplication of *tatA* and not necessary for functionality of the Tat-translocase. The deletion of *tatB* leads to an only slightly inhibited growth phenotype and significant export of the heterologous substrate $TorA^{SP}$-GFP still occured (Kikuchi et al., 2006). This result is surprising as in the closely related *M. tuberculosis tatB* deletion is not possible which means that it is an essential gene (Saint-Joanis et al., 2006) and a similar situation would have been expected for *C. glutamicum*.

These results are obscure regarding the role of TatB in *Corynebacterium glutamicum*. On the one hand the genomic organization of the *tatAC* operon, the good translocation of $TorA^{SP}$-GFP in absence of TatB and the near wild-type strain like growth behavior of a *tatB*-mutant leads to believe that *C. glutamicum* is utilizing a TatAC-type translocase like most other nominally Gram-positive bacteria. On the other hand, alignments of the amino acid sequence of *C. glutamicum* Cg1273 to heterologous proteins of the TatA/B-family distinguished it as a *bona fide* TatB; for which in *E. coli* and plant thylakoids a clear functional role as part of the substrate receptor complex is defined (Sargent et al., 1999; Cline and Mori, 2001). Also, it cannot be neglected that the deletion of *tatB* does have a slight inhibitory effect on growth in complex medium, leading to delayed growth in the exponential growth phase and a ~10% reduced end-OD (optical density) in comparison to the wild-type strain (Kikuchi et al., 2006). This indicates that TatB is in fact somehow involved in the translocation of a physiologically important substrate as well as increasing the amount of translocated $TorA^{SP}$-GFP (Kikuchi et al., 2006).

The assessment of these results points towards the following conclusions: *C. glutamicum* could, just like in *B. subtilis* (see page 8), utilize a translocase of the AC-type in which *C. glutamicum* TatA (Cg1685) is bifunctional. This TatAC translocase would then be responsible for translocating a physiologically relevant substrate, indicated by the growth defect in the *tatA*- and *tatC*-mutant strains. As the *tatB*-mutant strain also shows a slight growth defect, an involvement of TatB in the translocation of this substrate seems probable, but non-essential.

Given the fact that *C. glutamicum* putative *tatB* (*cg1273*) is a monocistronic gene not in proximity to other *tat*-genes, it could be speculated that it was acquired via horizontal gene transfer at a different time point during evolution than the operon *tatAC*. This could indicate that putative *C. glutamicum* TatB (Cg1273), unlike in *E. coli*, could then either be some sort of novel accessorial factor which improves Tat-dependent translocation of the AC-type translocase. For example, by taking part in Tat-de-

4. Corynex™, Ajinomoto co. Inc. (www.corynex.com)

pendent translocation only for a subset of substrates. Otherwise it could be that Cg1273 (putative TatB) and Cg1685 (TatA) are both bifunctional. This would mean that *C. glutamicum* can operate two different translocases in parallel, again like in *B. subtilis*; one TatAC translocase for the majority of substrates and one "TatBC"-translocase possibly utilized for one or several special substrates still to be identified.

1.4. The Redox enzyme maturation protein TorD

Redox enzyme maturation proteins (REMPs) are highly specific chaperones for cofactor-containing substrates translocated by the Tat-pathway; usually encoded together in one operon, one REMP is responsible for one substrate (Turner et al., 2004). One of the best examined REMPs is *E. coli* TorD which assists in the maturation of the molybdenum-dependent trimethylamine-N-oxide (TMAO) reductase TorA (Pommier et al., 1998). In the presence of TMAO, the *torCAD* operon is induced in *E. coli* (Simon et al., 1994). If furthermore oxygen is absent, TMAO can be used as an alternative terminal electron acceptor in the presence of a non-fermentable carbon source such as glycerol (Méjean et al., 1994). For this, TorC, a membrane anchored pentahemic c-type cytochrome as well as the periplasmic TMAO reductase TorA are necessary (Mejean et al., 1994). TorA is a 94,5 kDa protein containing a complex *bis*-MGD cofactor (*bis*-Molybtopterin guanidine dinucleotide). This cofactor is synthesized in a multi-step process within the cytoplasm and is extremely susceptible to oxidation (Schwarz, 2005).
To ensure the correct cytoplasmic insertion of *bis*-MGD into TorA, the dedicated chaperone TorD protects *apo*TorA from proteolysis, prevents premature export of *apo*TorA and possibly even actively assists in the insertion process of *bis*-MGD into the *apo*-protein (Genest et al., 2005; Genest et al., 2008); (see figure 6 for a schematic overview of this process).

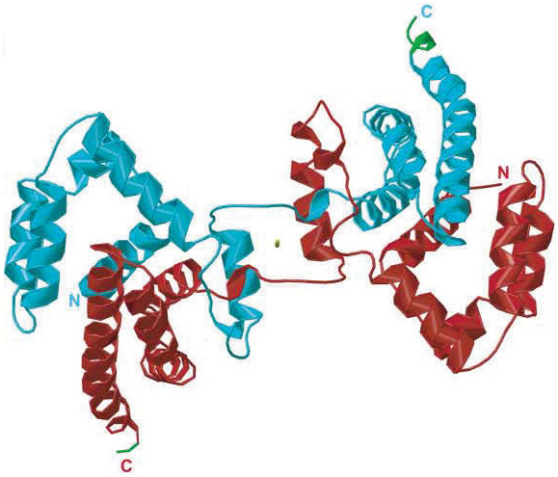

Figure 5: The crystal structure of homodimeric Redox enzyme maturation protein TorD from *Shewanella massilia* (Tranier et al., 2003). One monomer is colored in red, the other in cyan.

The crystal structure of TorD from *Shewanella massilia* (see figure 5) reveals an all-α-helical structure with one smaller and one larger domain connected by an unstructured polypeptide linker in the middle (Tranier et al., 2003). At least two different confirmations of the active chaperone seem to be possible. Firstly, the monomeric form in which the two domains together form one globular domain. Secondly,

a dimeric form (see image) in which the N-terminal domain of one monomer associates to the C-terminal domain of a second monomer and *vice versa,* resulting in two identical globular domains - this is referred to as domain-swapping (Tranier et al., 2003).
It has been shown that TorD can bind the hydrophobic h-region of the TorA signal peptide as well as parts of *apo*TorA (Jack et al., 2004; Buchanan et al., 2008). The proposed binding interface of TorD for the signal peptide of TorA is an acidic patch on the outside of the globular domain; both the monomeric and the dimeric form of TorD are able to do so (Tranier et al., 2002; Tranier et al., 2003). Binding of (monomeric) *E. coli* TorD to native TorA resulted in an apparent K_d (dissociation constant) of 59 nM (Buchanan et al., 2008). Whether *in vivo* TorA is bound by a single TorD monomer, a single dimer or possibly even two or more monomers is presently still unclear (Dow et al., 2013). The deletion of *torD* in *E. coli* does not abolish the export of TorA but significantly reduces the amount of TMAO reductase found in the periplasm (Genest et al., 2005). Furthermore, it could be shown that in absence of TorD an increased intracellular degradation of *apo*TorA by the *E. coli* Lon protease occurs (Redelberger et al., 2013).

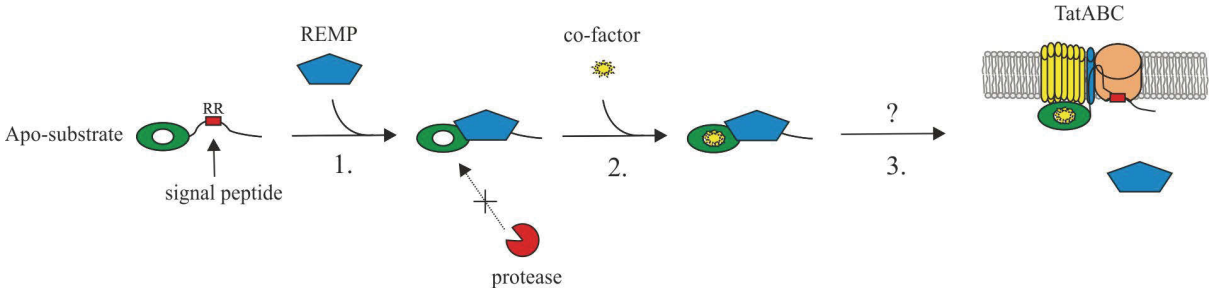

Figure 6: The proofreading mechanism of redox enzyme maturation proteins (REMP). **1.** The substrate is recognized and bound via its signal peptide by the REMP and protected against premature proteolysis. **2.** The redox co-factor is inserted into the catalytic site of the substrate. **3.** The REMP is released from the cofactor-containing substrate by an unknown mechanism and the substrate is subsequently handed off to the Tat-translocase for export over the cytoplasmic membrane.

Preventing the export of malfolded or co-factor missing proteins means preventing the waste of energy for the cell. It has been postulated that the Tat-translocase has an intrinsic folding quality control mechanism which allows only the export of correctly folded proteins (DeLisa et al., 2003). In the following years an additional quality control mechanism, termed "Tat-proofreading", was proposed (Sargent, 2007). This model assigns to REMPs like TorD, next to their role in assisting co-factor insertion and protecting their substrate from premature proteolysis, a quality control function wherein their cognate substrates are only handed off to the translocase when maturation is complete (Sargent, 2007). One interesting study that led to this theory was the investigation of the periplasmic *E. coli* substrate (NiFe) hydrogenase-2 which is translocated Tat-dependently. This hydrogenase is composed of two subunits, the smaller α-subunit HybO which has an associated nickel co-factor and possesses an N-terminal Tat signal peptide and the larger β-subunit HybC which contains an iron-sulfur cluster. HybC does not have a signal peptide and needs to oligomerize with HybO within the cytoplasm prior to translocation via the Tat-pathway in a "hitchhiking"-manner (Rodrigue et al., 1999). Within the *hyb* operon a gene is found which codes for HybE, the cognate hydrogenase-2 REMP (Rodrigue et al., 1999). When the Tat signal peptide of hydrogenase-2 α-subunit HybO was exchanged for the TorA signal peptide the cellular hydrogenase activity decreased to one quarter of the wild-type strain (Jack et al., 2004). This is due to the corresponding REMP HybE not being able to bind the TorA signal

peptide of the chimeric substrate TorA^{SP}-HybO as HybE is highly specific for only the HybO signal peptide. The missing interaction of HybO with its cognate REMP HybE leads to the complex co-factor containing heterodimeric HybOC not being assembled correctly and premature targeting of HybO to the Tat-translocase (Jack et al., 2004).
Surprisingly, upon additional overexpression of TorD, the hydrogenase activity could be restored to near wild-type level (Jack et al., 2004). This experiment firstly demonstrated that TorD, although TorA being its only known natural substrate, is not specific only for molybdoenzymes but could fulfill chaperone activity for other completely unrelated "foreign" substrates possessing different co-factors. Secondly, it showed that the specificity of TorD activity was towards the TorA signal peptide. Whether TorD can actively assist in the insertion of nickel co-factors and Fe/S-clusters is unlikely. Surely, it can protect its TorA^{SP}-substrate from cytoplasmic proteolysis so as to allow the substrate to fold correctly, associate with its co-factor(s), oligomerize and possibly even assist in targeting it to the Tat-translocase.
This finding was further supported by Li et al. (2006) who demonstrated in *E. coli* that coexpression of TorD and the chimeric substrate TorA^{SP}-GFP led to a 3-fold increase of GFP export into the periplasm. TorA^{SP}-GFP obviously does not contain a co-factor but the GFP variant used for this study (GFPmut2) is a relatively slow folding protein with an *in vitro* refolding kinetics $t_{½}$ of 33±2 minutes (Fisher and DeLisa, 2008). Thus, the enhancing effect of TorD coexpression was probably due to protection of TorA^{SP}-GFP from proteolysis and premature targeting to the Tat-translocase.
How the release of the substrate from TorD is triggered and whether an interaction of the TorD/substrate complex with the Tat translocase is required for this event is unclear. The only evidence of an interaction of a REMP with components of the Tat translocase are from bimolecular fluorescence complementation experiments. Herein it was demonstrated that DmsD, the specific REMP for the *E. coli* dimethyl sulfoxide reductase DmsA, comes into proximity of the TatBC receptor complex (Papish et al., 2003; Kostecki et al., 2010). It has furthermore been suggested that nucleotide binding could be involved as it could be shown *in vitro* that the TorD dimer can bind GTP with low affinity albeit not showing GTP-hydrolysis activity (Hatzixanthis et al., 2005; Guymer et al., 2010).
Regardless of how the TorD-release mechanism works, these previous data suggest that TorD coexpression could be beneficial in a biotechnological production background to improve the yield of heterologously secreted proteins

1.4.1 Expression of TorD in *C. glutamicum*

The coexpression of TorD and TorA^{SP}-GFP has been reported to lead to a two- to four-fold increase in the amount of Tat-dependently exported GFP in *E. coli* (Li et al., 2006). For this reason, it was investigated whether this beneficial effect of TorD expression could also be applied to a heterologous expression system. Presumably, TorD can protect a heterologous TorA^{SP}-substrate from proteolysis and premature targeting to the Tat-translocase which results in a net increase of translocated protein. In the course of her dissertation, H. Brundiek therefore tested TorD coexpression in *C. glutamicum* to see whether it could improve Tat-dependent protein secretion of heterologous proteins (Brundiek, 2008).
Surprisingly, TorD coexpression resulted in a complete export block of three investigated fusion proteins, TorA^{SP}-GFP, TorA^{SP}-Cut and TorA^{SP}-GTL. These are the green fluorescent protein (GFP), *Fusarium solani pisi* cutinase (Cut) and thermostable *Geobacillus thermoleovorans* lipase (GTL) respectively, fused to the TorA signal peptide. From this unexpected result it was deduced that the release of the substrate to the translocase from the chaperone TorD did not function properly. As the mechanism of how and when TorD (or any other REMP for that matter) releases its substrate is hither-

to not understood (Sargent, 2007), this phenotype presented a unique opportunity to study this mechanism.
In the course of the following investigation, it was possible to revert the export block of TorA^{SP}-GFP when, additionally to TorD, the whole *E. coli* Tat-translocase TatABC was coexpressed in a *C. glutamicum* wild-type strain. Neither the coexpression of *E. coli* TatAC nor TatC alone led to the release of the TorD-mediated TorA^{SP}-GFP export block (Brundiek, 2008). This finding indicated that, for some reason, the release of TorD from the TorA^{SP}-substrate requires the cognate (*E. coli*) Tat-translocase. As it has been reported that the REMP DmsD can interact with the Tat-translocase *in vitro* (Kostecki et al., 2010), it was speculated that the release of TorD from the TorA signal peptide might require an interaction between the TorD/substrate complex and the *E. coli* translocase which the homologous *C. glutamicum* translocase is not able to mediate. As the nature of this hypothetical interaction is to date unknown, two reasons for why the *C. glutamcium* Tat-translocase is unable to fulfill it are thinkable. Either, this release mechanism requires a specific interaction interface within the translocase, such as one or several specific residues or a secondary structure elements, which the *C. glutamicum* translocase simply does not posess. Otherwise, it could be that the *C. glutamicum* translocase specifically contains an element, for example a charged amino acid residue at the wrong position, which prevents an interaction of the translocase with the TorD/substrate complex from happening and thus translocation taking place.

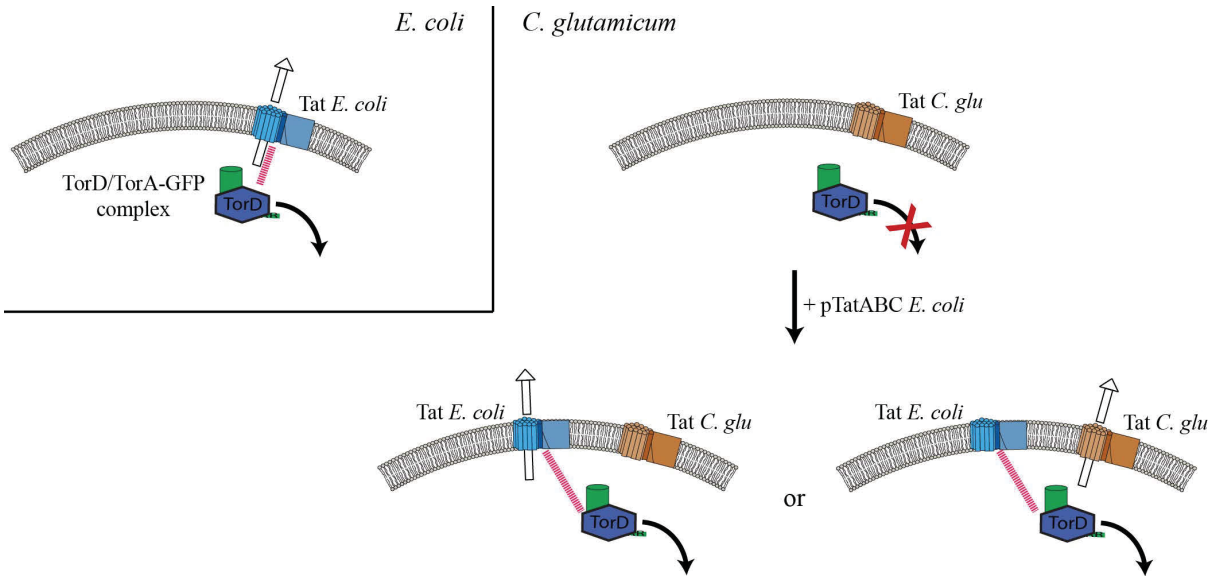

Figure 7: The effect of TorD overexpression in *E. coli* (top left) and *C. glutamicum* (right). In *E. coli* the TorD-bound TorA^{SP}-GFP is released and translocated. In *C. glutamicum* the release of TorD from the substrate does not take place, presumably because the translocase is not able to mediate this release, resulting in an export block of TorA^{SP}-GFP. The additional expression of plasmid-expressed *E. coli* TatABC leads to export of TorA^{SP}-GFP. This is hypothesized to happen because the *E. coli* translocase can mediate the release of TorD (red dotted line). Whether the actual translocation occurs via the homologous *C. glutamicum* or the heterologous *E. coli* translocase is unclear (Brundiek, 2008).

For one reason, the evaluation of this hypothesis is difficult. It cannot be said whether the *E. coli* translocase is actively translocating TorA^{SP}-GFP under these conditions because of the presence of two translocases - the genomically encoded *C. glutamicum* translocase and the plasmid-encoded *E. coli* translocase (this conundrum is depicted in figure 7). Further cross-complementation experiments

in *C. glutamicum* had shown that the simultaneous presence of Tat components from both *E. coli* and *C. glutamicum* lead to mixed translocases in the membrane which, in some combinations, abolish Tat-dependent export (Brundiek, 2008).
As improbable as it may seem, it cannot be ruled out that the release of TorD from the substrate is triggered by the *E. coli* translocase and translocation occurs via the endogenous *C. glutamicum* translocase. For this reason it was imperative for this work to test the Tat-proofreading capabilities of TorD in a clean genomic background.
It was postulated that TatB could be the candidate Tat component involved in this release mechanism of TorD from the TorD/TorA^{SP}-substrate complex. Firstly, a requirement of $TatB_{E.c.}$ had been observed for functioning release of TorA^{SP}-GFP in *C. glutamicum* in presence of TorD. Only when the whole *E. coli* Tat-translocase including *E. coli* TatB was coexpressed did this result in export of TorA^{SP}-GFP, which would imply that *E. coli* TatB participates in this interaction required for release (Brundiek, 2008). As the *C. glutamicum* wildtype strain ATCC 13032 in which these studies were carried out also expressed a homologous TatB component at all times, it was furthermore speculated that *C. glutamicum* TatB might be the counterpart to its *E. coli* homologue which could in turn be responsible for the TorD-induced export block because it either misses a specificity (in comparison to *E. coli* TatB) necessary for the release mechanism or otherwise possibly be the Tat-component responsible for preventing this interaction from taking place. Regardless, it was crucial to test these two TatB molecules in regard to their behavior with TorD in isolation of each other.

1.5. Aims of this work

1. The elucidation of the actual composition of the Tat-translocase of *Corynebacterium glutamicum* to determine whether a Gram-positive style TatAC-type or a Gram-negative-/ plant thylakoid-style TatABC-type translocase is utilized. This necessitates the evaluation of putative TatB (Cg1273) functionality for which current literature is ambiguous. By investigating a possible $TatB_{C.g.}$ bifunctionality it can furthermore be assessed whether *C. glutamicum* employs only one translocase or whether different two-component Tat-translocases are present as e.g. in *Bacillus subtilis*.
2. Investigation of what role TatB plays in the TorD-induced export block of substrates bearing the TorA signal peptide that was observed in *C. glutamicum*. Defining the critical component in the export block observed by Brundiek (2008) could shed light on the hitherto not very well understood release mechanism of the substrates of redox enzyme maturation proteins and their subsequent transfer to the Tat-translocase.

2. Material & Methods

2.1. Chemicals and Enzymes

All chemicals (analytically pure grade) used in this work were obtained from the companies AppliChem GmbH (Darmstadt), Carl Roth GmbH (Karlsruhe), Merck KgaA (Darmstadt), Sigma-Aldrich Chemie GmbH (Steinheim) and SERVA Electrophoresis GmbH (Heidelberg). Biochemicals, enzymes and their respective buffers were obtained from the companies Thermo Fisher Scientific Inc. (Schwerte), GE Healthcare (Munich), Life Technologies GmbH (Darmstadt), New England Biolabs GmbH (Frankfurt/Main), Qiagen (Hilden), Roche Diagnostics GmbH (Mannheim) IBA Life Sciences (Göttingen) and Agilent Technologies GmbH (Böblingen). Culture media components were obtained from Becton Dickinson/Difco GmbH (Heidelberg) and nitrocellulose membranes from GE Healthcare (München). The synthesis of oligonucleotides as well as DNA-sequencing was carried out by Eurofins MWG Operon (Ebersberg).

2.2. Strains, plasmids and oligonucleotides

2.2.1 Strains

2.2.1.1 *Escherichia coli*

Strain	Genotype	Reference
XL1-blue	*endA1 gyrA96(nal^R) thi-1 recA1 relA1 lac glnV44 F'[::Tn10 proAB$^+$ lacI^q Δ(lacZ)M15] hsdR17(r_K^- m_K^+)*	(Bullock et al., 1987)
MC4100		(Casadaban, 1976)
DH5α	*supE44 ΔlacU169 (Φ80 lacZΔM15) hsdR17 recA1endA1 gyrA96 thi-I relA1*	(Hanahan, 1983)
DADE	*MC4100 ΔtatABCE ΔtatE*	(Wexler et al., 2000)
GSJ100	*MC4100 x P1.MM129>TetR ΔmalE444 zjb729::Tn10*	(Blaudeck et al., 2003)
GSJ101	*DADE x P1.MM129>TetR ΔmalE444 zjb729::Tn10*	(Blaudeck et al., 2003)
JARV15	*MC4100 ΔtatA/E*	(Sargent et al., 1999)
BØD	*MC4100 ΔtatB*	(Sargent et al., 1999)
B1LK0	*MC4100 ΔtatC*	(Bogsch et al., 1998)
BØD malE$^-$	*BØD ΔmalE*	this work
B1LK0 malE$^-$	*B1LK0 ΔmalE*	this work

2.2.1.2 *Corynebacterium glutamicum*

Strain	Genotype	Reference
ATCC 13032	*wild-type*	(Kinoshita et al., 1958)
Δ*tatAC*	*ATCC13032 ΔtatAC* (*cg1685, cg1684*)	(Meissner, 2005)
Δ*tatB*	*ATCC 13032 ΔtatB* (*cg1273*)	this work
Δ*tatE*	*ATCC 13032 ΔtatE* (*cg3381*)	this work
Δ*tatA/E*	*ΔtatE ΔtatA* (*cg3381/cg1685*)	this work
Δ*qcrA*	*ATCC 13032 ΔqcrA* (*cg2404*)	(Chattopadhyay, 2013)
Δ*qcrA* Δ*tatB*	*ΔqcrA ΔtatB* (*cg2404/cg1273*)	this work

2.2.2 Plasmids

2.2.2.1 Expression in *E. coli*

Name	Description	Reference
pBBR1MCS2	*mob rep lacZα*$^{+}$ *Km*^{R}	(Kovach et al., 1995)
pBBR_TorA-MalE	expression of TorA^{SP}-MalE	(Blaudeck et al., 2003)
pBBR_TorA-Bla	expression of TorA^{SP}-Bla (TEM1)	this work
pBBR_TorA-GFP	expression of TorA^{SP}-GFP	unpublished, F. Lausberg
pHSG575	*pSC101-ori lacI + Zα*$^{+}$ *pUC8/9-type polylinker Cm*^{R}	(Takeshita et al., 1987)
pHSG_TatA$_{E.c.}$	expression of *E.c. MC4100* TatA	(Blaudeck, 2001)
pHSG_TatA$_{C.g.}$	expression of *C.g.* TatA (Cg1685)	this work
pHSG_TatB$_{E.c.}$	expression of *E.c. MC4100* TatB	this work
pHSG_TatB$_{C.g.}$	expression of *C.g.* TatB (Cg1273)	this work
pHSG_TatB1-2	expression of TatB hybrid TatB$_{E.c.\ 1\text{-}21}$-TatB$_{C.g.\ 22\text{-}156}$	this work
pHSG_TatB3-4	expression of TatB hybrid TatB$_{E.c.\ 1\text{-}54}$-TatB$_{C.g.\ 56\text{-}156}$	this work
pHSG_TatB5-6	expression of TatB hybrid TatB$_{E.c.\ 1\text{-}72}$-TatB$_{C.g.\ 74\text{-}156}$	this work
pHSG_TatB7-8	expression of TatB hybrid TatB$_{E.c.\ 1\text{-}95}$-TatB$_{C.g.\ 86\text{-}156}$	this work
pHSG_TatB$_{C.g.}^{-n}$	expression of truncated TatB$_{C.g.}$ (n=number of C-terminal truncated aa)	this work
pHSG_TatB$_{X3}$	epTatB$_{C.g.}$ (mutations: E61D, K64E, A121V)	this work
pHSG_TatB$_{Z3}$	epTatB$_{E.c.21C.g.139}$ (mutation: E58K)	this work

Name	Description	Reference
pHSG_TatB$_{Z4}$	epTatB$_{E.c.21C.g.139}$ (mutations: V18A, G105STOP)	this work
pHSG_TatC$_{E.c.}$	expression of *E.c. MC4100* TatC	this work
pHSG_TatC$_{C.g.}$	expression of *C.g.* TatC (Cg1684)	this work
pTrc99A	*tcrP-vector lacI^q pUC18-type polylinker Amp^R*	(Amann et al., 1988)
pTrSp	derived from pTrc99A *Spec^R*	this work
pTrSp_GFP	expression of GFP	this work
pTrSp_TorD	expression of *E.c. MC4100* TorD	this work
pTrSp_TorD^{Strep}	expression of TorD^{Strep}	this work
pKO3	*pSC101 repliconTS M13 ori Bacillus subtilis sacB gene Cm^R*	(Link et al., 1997)
pKO3_delmalE	deletion of *E.c. malE*	(Fleckenstein, 2013)

2.2.2.2 Expression in *C. glutamicum*[5]

Name	Description	Reference
pEKEx2	*pBL1 replicon P$_{trc}$ lacI^q Km^R from pUC4K*	(Eikmanns et al., 1994)
pEKEx3	derived from pEKEx2, Spec^R	(Hoffelder et al., 2010)
pEK_TorA-GFP	expression of TorA^{SP}-GFP	(Meissner et al., 2007)
pEK_PhoD$_{C.g.}$-GFP	expression of PhoD$_{C.g.}$ ^{SP}-GFP	(Meissner et al., 2007)
pEK_qcrA	expression of *C.g.* QcrA (Cg2404)	this work
pEK_qcrA^{KK}	expression of QcrA^{KK} (R143K, R144K)	this work
pEC-XC99E	*pGA1 mini-replicon P$_{trc}$ lacI^q pGA1 per gene pTrc polylinker Cm^R*	(Kirchner and Tauch, 2003)
pEC_TatA$_{C.g.}$	expression of *C.g.* TatA (Cg1685)	this work
pEC_TatB$_{C.g.}$	expression of *C.g.* TatB (Cg1273)	this work
pEC_TatB$_{E.c.}$	expression of *E.c. MC4100* TatB	this work
pK19mobsacB	*RP4 mob Bacillus subtilis sacB gene KmR*	(Schaefer et al., 1994)
pK19_deltatA	deletion of *C.g. tatA* (*cg1685*)	this work
pK19_deltatE	deletion of *C.g. tatE* (*cg3381*)	this work

5. All vectors for expression or deletion in *C. glutamicum* also replicate in *E. coli*.

Name	Description	Reference
pK19_delqcrA	deletion of *C.g. qcrA* (*cg2404*)	this work
pCRD206	*lacZα parAB RepA*^{DK} *Bacillus subtilis sacB gene Km*^{R}	(Okibe et al., 2011)
pCRD_deltatB	deletion of *C.g. tatB* (*cg1273*)	this work

2.2.3 Oligonucleotides

Name	Sequence	Description
del_tatBup-f	GAGTCTAGAGGGATGTTTTGGATGTTCGAACAAAAAC	upstream-fragment of $tatB_{C.g.}$ for pCRD206_deltatB *XbaI*-site
del_tatBup-r	CCATCCACTAAACTTAAACAACCCACGCTAGAAAACATCAGACC	
del tatBdn-f	TGTTTAAGTTTAGTGGATGGGTACTCAGGTG-GCGTCTCTTGG	downstream-fragment of $tatB_{C.g.}$ for pCRD206_deltatB *SbfI*-site
del_tatBdn-r	GTGGGTACCCCAATTGATCCCGAATGCTGAG	
deltatB-f	GATCGTGCAGGATCTAAAGC	genomic control of $tatB_{C.g.}$-deletion
deltatB-r	TCCAGCAATTCCTCACTGAC	
del_tatAup-f	GCGCTCTAGAGACAGCAAAGCAGTGCACCC	upstream-fragment of $tatA_{C.g.}$ for pK19_deltatA *XbaI*-site
del_tatAup-r	GACAATGATTCCAATTTCCC	
del_tatAdn-f	GGGAAATTGGAATCATTGTCCGTCAGAACTACGAGGATCC	downstream-fragment of $tatA_{C.g.}$ for pK19_deltatA *EcoRI*-site
del_tatAdn-r	GCGCGAATTCGAACCATACCCACCAACGCCG	
CgDel-for	AGGCTTGATCGCATCCGAAG	genomic control of $tatA_{C.g.}$- or $tatAC_{C.g.}$ deletion
CgDel-rev	CAGGCTCAAACAGTGGCATC	
del_tatEup-f	GAGGTCGACGTTGTTAAACATGTCCTCGGCG	upstream-fragment of $tatE_{C.g.}$ for pK19_deltatE *SalI*-site
del_tatEup-r	CCCATCCACTAAACTTAAACAAATATTTCTGCATTCCACCCTAG	
del_tatEdn-f	TGTTTAAGTTTAGTGGATGGGCAGATCGAAAGCTCCGATCAG	downstream-fragment of $tatE_{C.g.}$ for pK19_deltatE *BamHI*-site
del_tatEdn-r	GTGGGATCCGAACACTACCCCAATGGCACTGATC	

Name	Sequence	Description
deltatE-f	CAATGGCGTGACTCTTGGTG	genomic control of $tatE_{C.g.}$-deletion
deltatE-r	CGCGCTGTTCTTCTTCCTGC	
SalI_RB_qcrA-f	GAGAGTCGACGAAGGAGATATACATATGAGCAATG AGGATCTTGC	construction of pEKEX2_$QcrA_{C.g.}$
qcrA_KpnI-r	GAGAGGTACCTCATGACTTACGCTCCCAGAATG	
QC:QcrARR-KK-f	CTCTTGGCAGACCTCTACTCTTGGTAAGAAGAAG CTGATCATGGGACTTGCAGGTG	QuikChange of $QcrA_{RR}$ to $QcrA_{KK}$ (R143K, R144K) on pEKEx2
QC:QcrARR-KK-r	GAGAACCGTCTGGAGATGAGAAC-CATTCTTCTTCGACTAGTACCCTGAACGTCCAC	
KpnI_tatA-f	GCGCGGTACCAAGGAGATATAGATATGTCCCTC	construction of pEC-XC99E_$Tat-A_{C.g.}$
tatA-SalI-r	GCGCGTCGACTTAAGAGGTGCGGTTTGGATC	
SacI_RB_tatB-f	GCGCGAGCTCAAGGAGATATAGATATGTTTTCTAG CGTGGGTTG	construction of pEC-XC99E_$Tat-B_{C.g.}$
tatB_BamHI-r	GCGCGGATCCCTAAATAATATCGGTCCAAGAG	
EcoRI_RB_tatA-f	GCGCGAATTCAAGGAGATATAGATATGTCCCTCGG ACCATGGG	construction of pHSG_$TatA_{C.g.}$
tatA_SalI-r	GCGCGTCGACTTAAGAGGTGCGGTTTGGATC	
EcoRI_RB_tatBEc-f	GCGCGAATTCAAGGAGATATAGATGT-GTTTGATATCGGTTTTAGCG	construction of pHSG_$TatB_{E.c.}$
EctatB_SalI-r	GCGCGTCGACTTACGGTTTATCACTCGACGAAG	
EcoRI_RB_tatB-f	GCGCGAATTCAAGGAGATATAGATATGTTTTCTAG CGTGGGTTG	construction of pHSG_$TatB_{C.g.}$
tatB_SalI-r	GCGCGTCGACCTAAATAATATCGGTCCAAGAG	
tatB-10_SalI-r	GCGCGTCGACCTAGTAATTCGGGCCGTCTTTTG	reverse primers for $TatB_{C.g.}$ truncations
tatB-20_SalI-r	GCGCGTCGACCTACGTTGGGCGTGCGGTGGAAC	
tatB-30_SalI-r	GCGCGTCGACCTAACGTTCCACCACATTCGCATTG	
tatB-40_SalI-r	GCGCGTCGACCTATGCCTGCTTGTTGCGCTGAG	
tatB-50_SalI-r	GCGCGTCGACCTATGTTCCTTCGGCCATGATCTTC	
tatB-60_SalI-r	GCGCGTCGACCTAAAAGTCATCCAGGAACGAGG	
tatB-70_SalI-r	GCGCGTCGACCTAAAATAACGCCTTAGTGATGG	
tatB-80_SalI-r	GCGCGTCGACCTAGCTCATCCGGCTGTACTGTG	
tatB-90_SalI-r	GCGCGTCGACCTATAGTGGCTTTCGGATTTCATC	
tatB-100_SalI-r	GCGCGTCGACCTAACCAAAATCACTGTCCAACG	

Name	Sequence	Description
tatB_gen-f	GAATCAAAGCTGCCGACAAC	flanking primers $TatB_{E.c./C.g.}$ hybrids
tatB_gen-r	TTATACGCAAGGCGACAAGG	
BCg_g2-f	CCGGAACGGTTGCCTCGTTTG	amplification C-terminus of $TatB_{C.g.}$ for $TatB_{E.c./C.g.}$ hybrids
BCg_g4-f	TCGGAATTTGATGAAATCCG	
BCg_g6-f	ATGAGCCCCAAGACGGCCATC	
BCg_g8-f	GATAATGATTCCTCGTTCCTG	
BEc+OL_c1-r	CAAACGAGGCAACCGTTCCGGCCCCAGAAC-GACGAGGCCGATG	
BEc+OL_c3-r	CGGATTTCATCAAATTCCGATAACTC-CTGGGTCAGTTCGTTC	amplification N-terminus of $TatB_{E.c.}$ for $TatB_{E.c./C.g.}$ hybrids
BEc+OL_c5-r	GATGGCCGTCTTGGGGCTCATAGTGAGGCTCGCCTTTTCAAC	
BEc+OL_c7-r	CAGGAACGAGGAATCATTATCGGAACGCTTCATCGACTCCG	
SPcass-f	GAGAGTCATGAACGTAACGTGACTGGCAAGAG	amplification of $Spec^R$ from pEKEx3 for pTrSp
SPcass-r	GAGAGTCATGAGTACATCGATATCATATGCAAGGG	
EcoRI_RB_torD-f	CCGGGAATTCAAGGAGATATAGATATGACCACGCTGACAGCACAAC	amplification of *torD* without and with C-terminal Strep-TagII for pTrSp_TorD
torD_HindIII-r	GACAAGCTTTTATCTGTTTTGGTGGTCGCACTCC	
torD-ST_HindIII-r	GCGCAAGCTTATTATTTTTCGAACTGCGGGTGGCTCCAAGCGCTTCTGTTTTGGTGGTCGCACTCC	
EcoRI_GFP-f	ATATGAATTCGAAGGAGATATAGATATGAGTAAAG	construction of pTrSp_GFP
GFP_HindIII-r	ATATAAGCTTTTATTTGTAGAGCTCATCCATG	
epPCR_tatB-f	GGCAGTGAGCGCAACGCAATTAATGTG	error-prone PCR of $tatB_{C.g.}$ and *tatB1-2* on pHSG575
epPCR_tatB-r	GTGCTGCAAGGCGATTAAGTTGGGTAACG	
M13-Univ	CGCCAGGGTTTTCCCAGTCACGAC	sequencing primers for pK19mobsacB
M13reverse	CAGGAAACAGCTATGAC	
M13uniCSneufor	AGGGTTTTCCCAGTCACGACGTT	sequencing primers for pBBR1, pHSG575, pCRD206
M13pucrev	TTGTGTGGAATTGTGAGCGG	

Name	Sequence	Description
pEKEx3EcoTerm	CAGACCGCTTCTGCGTTC	sequencing primers for pEKEx2, pEC-XC99E, pTrc99a, pTrSp and pMMB
pEKEx3SbfTerm	CTCGTATAATGTGTGGAATTG	

2.3. Microbiological methods

2.3.1 *E. coli* media

2.3.1.1 LB (lysogeny broth) (Bertani, 1951)

Bacto-tryptone	10 g
yeast extract	5 g
NaCl	10 g
	ad. 1 l A. bidest

LB medium was used as the general complex medium for the cultivation of *E. coli*. The medium was autoclaved for 20 min. For solid media plates 20 g of agar were added prior to autoclaving. If applicable antibiotics were added after cool down of the medium to <60°C.

2.3.1.2 MacConkey agar

Maltose-containing MacConkey agar plates were made by autoclaving 40 g MacConkey agar base (Becton Dickinson/Difco GmbH, Heidelberg) with additional 6 g agar in 980 ml A. bidest. After autoclaving for 15 min, 20 ml 50% maltose and the respective antibiotics were added.

2.3.1.3 Minimal medium (Tanaka et al., 1967)

solution A (10×)

$NaH_2PO_4 \times H_2O$	46.9 g
K_2HPO_4	111.5 g
$(NH_4)_2SO_4$	26.4 g
	ad. 1 l A. bidest

solution B (100×)

$MgSO_4 \times 7\ H_2O$	7.4 g
$CaCl_2 \times 2\ H_2O$	147 mg

$ZnCl_2$	13.6 mg
$Fe(II)SO_4 \times 7\ H_2O$	28 mg
1 M HCl	1 ml
	ad 1 l A. bidest

For minimal medium agar plates with maltose as the sole carbon source, 20 g of agar were mixed with 10 ml of solution B and 889 ml A. bidest. After autoclaving for 20 min and cool-down to <60°C, 100ml of sterile solution A as well as 20 ml 20% maltose, 1 ml thiamine (10 mg/ml) and the respective antibiotics were added.
For minimal medium agar plates for the anaerobic growth of *E. coli* with TMAO as terminal electron acceptor, 20 g of agar were mixed with 10 ml of solution B and 854 ml A. bidest. After autoclaving for 20 min and cool-down to <60°C, 100ml of sterile solution A as well as 25 ml 2 M TMAO, 20 ml 20% glycerine, 1 ml thiamine (10 mg/ml) and the respective antibiotics were added.

2.3.2 *C. glutamicum* media

2.3.2.1 BHI/ BHIS

The standard complex medium for the cultivation of *C. glutamicum* (BHI) was made by autoclaving 37 g of Brain-Heart-Infusion (Becton Dickinson/Difco GmbH, Heidelberg) in 1 l A. bidest for 15 min. For the osmotic stabilization of freshly electroporated *C. glutamicum* 81 g sorbitol were added to 1 l BHI prior to autoclaving (BHIS). For solid-media agar plates 20 g/l agar were added before autoclaving.

2.3.2.2 CgXII (Keilhauer et al., 1993)

CgXII base

$(NH_4)_2SO_4$	20 g
urea	5 g
KH_2PO_4	1 g
K_2HPO_4	1 g
$MgSO_4 \times 7\ H_2O$	250 g
MOPS	42 g
	ad 800 ml A. bidest

trace elements solution

$FeSO_4 \times 7\ H_2O$	1 g
$MnSO_4 \times H_2O$	1 g
$ZnSO_4 \times 7\ H_2O$	100 mg
$CuSO_4$	20 mg

$NiCl_2 \times 6\ H_2O$	2 mg
	ad 100 ml A. bidest, adjust pH to 1.0

Prior to autoclaving, 1 ml 0.02% biotin solution and 1 ml 1% $CaCl_2$ solution were added to 800ml CgXII base solution, the pH was adjusted to 7.0 with NaOH and the total volume filled up to 960ml. After autoclaving, 1 ml trace elements solution, 1 ml 0.3% protocatechuic acid solution and 40 ml 50% glucose were added.

2.3.3 Antibiotics

	E. coli	*C. glutamicum*
kanamycin	50 µg/ml	15/ 25 µg/ml[6]
ampicillin	100 µg/ml	-
chloramphenicol	25 µg/ml	12,5 µg/ml
spectinomycin	100 µg/ml	-
tetracycline	12.5 µg/ml	7.5 µg/ml

2.3.4 Cultivation conditions

Unless noted otherwise, *E. coli* cultures were grown at 37°C and *C. glutamicum* cultures at 30°C in sterilized glassware. In liquid media, cultures were agitated at 170 rpm. *C. glutamicum* liquid media cultures in flasks with four chicanes for improved oxygen-enrichment of the medium were agitated at 120 rpm. If applicable, the respective antibiotics were added to the medium.

2.3.5 Long-term storage of cultures

For long-term storage of bacterial cultures, glycerol stocks with an end-concentration of 10% glycerol were made. These were made with a fresh overnight culture, shock-frozen with liquid nitrogen and stored at -70°C.

2.3.6 Growth measurement

C. glutamicum growth experiments were carried out in a micro-scale BioLector® system (m2p-labs, Baesweiler). Each of 48 wells of a specialized microtiter plate (flower plate) were inoculated with 750 µl culture normalized to OD_{600nm}=0.1. Shaking conditions were set to 1100rpm at 30°C and 85% rel. hum. Measurement intervals were set to 15min.

6. A concentration of 15 µg/ml kanamycin was used for selection of transformants after electroporation. In all further cultivation steps, a concentration of 25 µg/ml was used

2.3.7 In-frame gene deletions

Gene deletions in *C. glutamicum* and *E. coli* were carried out using so-called "suicide vectors". For *C. glutamicum*, either pK19mobSacB (Schaefer et al., 1994) or the temperature-sensitive pCRD206 (Okibe et al., 2011), for *E. coli* pKO3 (Link et al., 1997) were used. These three vectors underlie the same basic principle which is depicted in figure 8.
Two PCR products of ~500 bp are generated of the up- and downstream region of the gene to be deleted. These PCR products contain the first and last 12 amino acids of the gene and conserve the open reading frame to reduce the risk of polar effects. The two PCR products are joined and cloned into the deletion vector. The relevant strain is transformed with the vector and selection is carried out for kanamycin resistance. The origin of replication of the deletion vector is either temperature sensitive (pCRD206, pKO3) or does not function in the target organism (pK19mobSacB). Thus replication of the deletion vector can be prevented and selection for kanamycin resistance must lead to genomic integration of the vector at the target site via homologous recombination. The integration of the vector into the genome was verified by colony PCR.

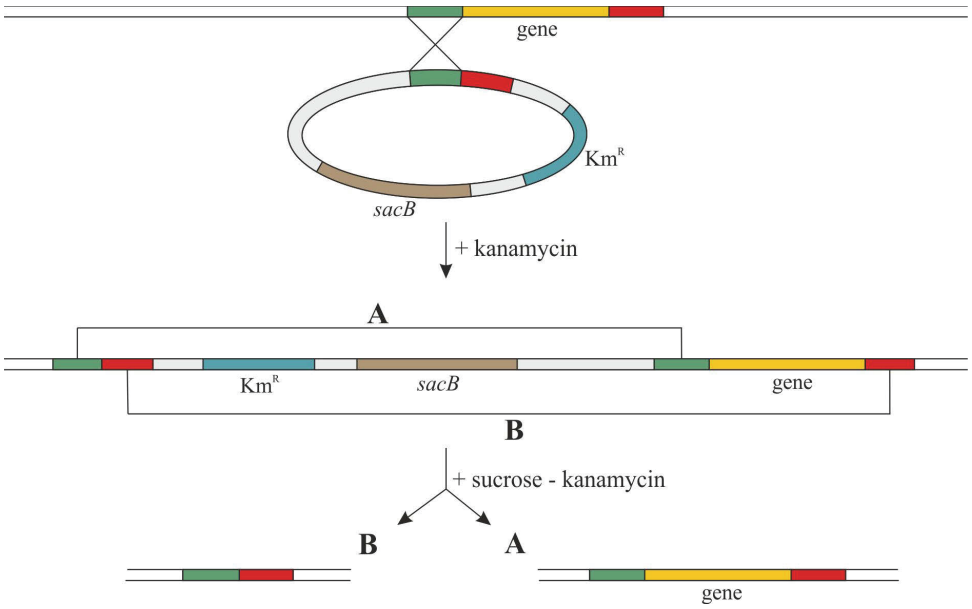

Figure 8: The general principle of the integration of a deletion vector into the genome via homologous recombination. Integration takes place via one of two homologous regions up- and downstream of the region to be deleted (green or red). A second recombination event leads again to the excision of the vector with the outcome being either the deletion of the gene (B) or the restoration of the genomic wild-type situation (A).

In the next step, the deletion vector has to removed from the genome again by plating the cells onto sucrose-containing agar plates. The deletion vector encodes for a *Bacillus subtilis* gene *sacB* which produces a levansucrase. Levansucrase produces a fructose-polymer from sucrose which is toxic in many Gram-negative bacteria (Gay et al., 1985) and also in *C. glutamicum*. By exposing the cells to solid media containing 10% sucrose, the selection pressure leads to a second recombination event in which the vector is removed from the genome. As shown in figure 8 this can lead either to the restoration of the wild-type situation or to the in-frame deletion of the gene. To verify whether the restoration of the wild-type siutation or the deletion occured colony PCR was carried out.

2.3.8 Chemically competent *E. coli*

An overnight culture of *E. coli* cells was used to inoculate a 100 ml main culture to an OD_{600nm}=0.1. This was cultivated to a mid-exponential OD_{600nm} of 0.6 - 0.8. The culture was transferred to falcon tubes and incubated on ice for 10 min. After centrifugation for 10 min at 5000 rpm at 4°C, the pellet was resuspended in 40 ml ice-cold 0.1 M $CaCl_2$ and left to stand on ice for 40 min. After a second centrifugation step, the pellet was washed once in 10 ml ice-cold 0.1 M $CaCl_2$ with 10% glycerol. The washed culture was pelleted again, resuspended in 1 ml 0.1 M $CaCl_2$ with 10% glycerol and the cells were either used directly for transformation or aliquoted into pre-chilled eppendorf tubes which were immediately shock-frozen with liquid nitrogen and stored at -70°C.

Transformation of chemically competent *E. coli*

For standard transformation of a plasmid into chemically competent *E. coli* around 100 ng of plasmid DNA were pipetted into a sterile eppendorf tube. Afterwards 50 µl of competent cells, gently thawed on ice, were mixed with the DNA and left to stand on ice for 30 min. Next a heat shock at 42°C for exactly 90 s was carried out in a heat block and then 600 µl of pre-warmed LB medium was added. The cells were regenerated by shaking at 37°C and 170 rpm for 60 min and then plated onto selective LB agar plates.

2.3.9 Electro-competent *E. coli*

An overnight culture of *E. coli* cells was used to inoculate a 50 ml main culture to an OD_{600nm}=0.1. The culture was cultivated to a mid-exponential OD_{600nm} of 0.6 - 0.8. After centrifugation (5000 rpm, 4°C) for 10 min, the pellet was washed twice in 25 ml and once in 10 ml ice-cold 10% glycerol. Afterwards, the pellet was resuspended in 500 µl 10% glycerol and the cells either used directly for transformation or aliquoted into pre-chilled eppendorf tubes which were immediately shock-frozen with liquid nitrogen and stored at -70°C.

Transformation of electro-competent *E. coli*

Electro-competent *E. coli* cells were mixed with 50-100 ng of desalted plasmid DNA (see page 30 for DNA precipitation) in a sterile eppendorf tube and then transferred to the bottom of a pre-chilled electroporation cuvette (2 mm gap, Al-electrodes, VWR). The electroporation was carried out using a Gene Pulser (Biorad, München) with the following settings: capacity: 25 µF, voltage: 2.5 kV, resistance: 200 Ω. Immediately afterwards 1 ml LB medium was added and the cells transferred to a new eppendorf tube. The cells were regenerated by shaking at 37°C and 170 rpm for 60 min and then plated onto selective agar plates. In case of direct selection on minimal medium agar plates the cells were washed twice with 0.9% NaCl prior to plating.

2.3.10 Electro-competent *C. glutamicum*

Standard method

TG-buffer	
Tris	1 mM
glycerol	10%
	adjust pH to 7.5

A BHIS overnight culture of *C. glutamicum* cells was used to inoculate a 100 ml BHIS main culture to an OD_{600nm}=0.1. At an OD_{600} of around 1.5, the culture was harvested into two 50 ml Falcon tubes. After centrifugation of 10 min at 5000 rpm and 4°C, the pellet was resuspended in 20 ml TG-buffer. This step was repeated once and then the culture was washed twice in 10% glycerol. Finally, the pellet was resuspended in 1 ml 10% glycerol and the cells either used directly for transformation or aliquoted into pre-chilled eppendorf tubes which were immediately shock-frozen with liquid nitrogen and stored at -70°C.

Transformation of electro-competent *C. glutamicum*

100 µl competent *C. glutamicum* cells were mixed with plasmid DNA in a sterile eppendorf tube and transferred to a pre-cooled electroporation cuvette (2 mm gap, Al-electrodes, VWR). The cells were then overlayed with 800 µl ice-cold 10% glycerol. The electroporation was carried out using a Gene Pulser (Biorad, München) with the following settings: capacity: 25 µF, voltage: 2.5 kV, resistance: 200 Ω. Immediately afterwards the contents of the cuvette was transferred into a 15 ml Falcon tube containing 4 ml pre-warmed BHIS which was then heat-shocked for exactly 6 min at 46°C in a water bath. The cells were regenerated for 90 min by shaking at 30°C and subsequently plated on selective BHIS agar plates.

Alternative method (van der Rest et al., 1999)

main culture medium	
isonicotinic acid hydrazide	800 mg
glycine	5 g
Tween 80	200 µl
	ad 200 ml LB medium

This method was used as an alternative for *C. glutamicum* mutant strains which showed a strong growth deficit and thus a very low transformation efficiency via the standard method described above. An Erlenmeyer flask filled with 20 ml BHIS with additional 2% glucose was inoculated with a single *C. glutamicum* colony and cultivated overnight at 30°C. This culture was used to inoculate the isonicotinic acid containing main culture to an OD_{600nm}=0.3 which was then cultivated for 28 hours at 18°C. After checking the growth of the culture to be around OD_{600}=1.0, the flask containing the culture was cooled on ice for 30 min. The cells were harvested in 50 ml Falcon tubes by centrifuging for 10 min at 5000 rpm and 4°C. The cells were washed thrice in 40 ml ice-cold 10% glycerol. Finally the pellet was resuspended in 2 ml 10% glycerol and the cells either used directly for transformation or

aliquoted into pre-chilled eppendorf tubes which were immediately shock-frozen with liquid nitrogen and stored at -70°C.

Alternative transformation of electro-competent *C. glutamicum*

100 µl competent *C. glutamicum* cells were mixed with plasmid DNA in a sterile eppendorf tube and transferred to a pre-cooled electroporation cuvette (2 mm gap, Al-electrodes, VWR). The electroporation was carried out using a Gene Pulser (Biorad, München) with the following settings: capacity: 25 µF, voltage: 2.5 kV, resistance: 600 Ω. Immediately afterwards 500 µl sterile BHIS medium were added to the cells which were then transferred to a pre-warmed 15 ml Falcon tube and heat-shocked for exactly 6 min at 46°C in a water bath. The cells were then regenerated for 90 min by shaking at 30°C and plated on selective BHIS agar plates.

2.4. Molecular Biological methods

2.4.1 Preparation of chromosomal DNA

Chromosomal DNA of *E. coli* and *C. glutamicum* was prepared using the DNeasy Tissue kit (Qiagen, Hilden) according to the manufacturers specifications.

2.4.2 Preparation of plasmid DNA

Plasmid DNA was prepared using either a kit for small volumes (GeneJetTM Plasmid Miniprep Kit, Thermo Fisher Scientific) or larger volumes (CompactPrep Plasmid Midi Kit, Qiagen) from fresh overnight cultures according to the manufacturers specifications. For preparation of plasmid DNA from *C. glutamicum,* lysozyme was added to the kits lysis buffer at a concentration of 20 mg/ml and incubated at 37°C under slight agitation for two hours.

2.4.3 Restriction of DNA

DNA	10 - 100 ng
10x buffer	2 µl
restriction enzyme(s)	0.5 - 1 µl
	ad 20 µl A. bidest

Plasmid DNA and PCR products were cut using FastDigest restriction enzymes (Thermo Fisher Scientific) according to the manufacturers specifications. The reaction time at 37°C varied from 10 min for analytical up to 30 min for preparative purposes. If more than one enzyme was utilized in the restriction these were added to the reaction simultaneously.

5'-dephosphorylation of DNA

To prevent recircularization of restricted plasmid-DNA, the 5'-ends were dephosphorylated. This was achieved by adding 1 U of FastAP Thermosensitive Alkaline Phosphatase directly to the restriction reaction and incubation at 37°C. The Fast Digest Green Buffer used for DNA-restriction is compatible with the FastAP enzyme.

2.4.4 DNA-precipitation

DNA was precipitated by adding 1 volume 4M $LiCl_2$ and 7 volumes isopropanol to 4 volumes of DNA-solution. After incubation at room temperature for one hour, the DNA was spun down, washed once in 70% ethanol, dried and then resolubilized in the desired buffer or water.

2.4.5 Ligation of DNA fragments

vector DNA	50 ng
insert DNA	200 ng
10x buffer	2 µl
T4 ligase	1 U
	ad 10 µl A. bidest

DNA was ligated using the Rapid DNA Ligation Kit (Thermo Fisher Scientific). DNA concentration was measured using a Nanodrop ND-1000 (PEQLAB Biotechnologie GmbH, Erlangen). The amount of vector DNA used varied between 20 - 50 ng but the amount of the respective insert was always in a molar ratio of 1:4 (e.g. 50 ng vector to 200 ng insert). The incubation of the ligation reaction occurred either for 20 min at room temperature or overnight at 16°C. 5µl of the ligation reaction were used to transform competent *E. coli* cells.

2.4.6 Agarose gel electrophoresis

The separation of DNA fragments was carried out using agarose gel electrophoresis. According to the size of the desired fragment(s), an agarose concentration between 0.8 and 1.5% (w/v) was chosen. After boiling the agarose in TAE-buffer and letting it cool down to around 60°C, horizontal gels were cast. DNA samples were prepared by adding one volume of 6x loading dye to five volumes of DNA solution.
The DNA separation was carried out in a horizontal gel chamber (Biometra, Göttingen) with the gel submersed in TAE buffer and, depending on the desired migration speed of the DNA and the agarose concentration of the gel, application of a constant voltage between 60 V and 90 V.

TAE buffer

Tris	40 mM
96% acetic acid	20 mM
Na_2EDTA	2.5 mM

6x loading dye

xylene cyanol	0.25% (w/v)
bromophenol blue	0.25% (w/v)
glycerine	50%
Na_2EDTA	0.25 mM

The separated DNA in the agarose gels was visualized by staining the gel for 5 - 10 min in an ethidium-bromide solution (0.25 µg/ml) (Sharp et al., 1973). After destaining in water for 5 min, a gel documentation chamber (PEQLAB Biotechnologie GmbH, Erlangen) was used to make a digital picture using UV excitation. Excision of DNA fragments was carried out on a portable UV backlight.

2.4.7 DNA purification from agarose gels

DNA fragments excised from agarose gels using a clean scalpell were purified using the QIAquick Gel Extraction Kit or (for fragments <3 kb) MinElute Gel Extraction Kit (QIAGEN, Hilden) according to the manufacturers specifications.

2.4.8 Polymerase Chain Reaction

2.4.8.1 Standard PCR

10x buffer with Mg_2SO_4	5 µl
dNTP-mix (2 mM each)	5 µl
template DNA[7]	1 ng - 1 µg
forward primer	0.1 µM
reverse primer	0.1 µM
Pfu DNA polymerase	2.5 U
	ad 50 µl A. bidest

For the amplification of DNA fragments, different PCR methods were used. For cloning purposes, either Pfu DNA-Polymerase or High Fidelity PCR Enzyme Mix (both Thermo Fisher Scientific), which both posses proofreading activity, were used. PCR reactions were prepared on ice and, after final addition of the polymerase, run in a thermocycler (Biometra, Göttingen).
Below is shown an exemplary PCR-cycler protocol for the amplification of a 1 kb fragment.

Step	**Time [s]**	**Temperature [°C]**	
initial denaturation	180	95	
denaturation	30	95	
annealing[8]	30	55	×30
extension	65	72	
final extension	600	72	

7. When plasmid DNA was used as template around, 1 ng, when genomic DNA was used up to 1 µg was employed

8. The annealing temperature was individually calculated for all primers with the help of an oligonucleotide calculator www.basic.northwestern.edu/biotools/OligoCalc.html

2.4.8.2 Colony PCR

For the verification of introduced genomic deletions, colony PCR was employed. For this purpose, a PCR master mix was prepared using DreamTaq DNA polymerase (Thermo Fisher Scientific) and the corresponding green 10x buffer according to the manufacturers specifications. Bacterial colonies were picked directly from agar plates and resuspended in 10 µl of the PCR master mix. The initial denaturation step at 95°C of the PCR program is sufficient for cell lysis and thus makes the DNA content of the cell available as PCR template. The PCR reactions were directly applied to agarose gels.

2.4.8.3 Crossover PCR

This PCR method was used to generate fusion products from two PCR products. The basic principle is shown in figure 9. For both the first and the second PCR step a proofreading polymerase such as Pfu was employed. In the crossover PCR step, equimolar concentrations of 1 ng of both fragments were used.

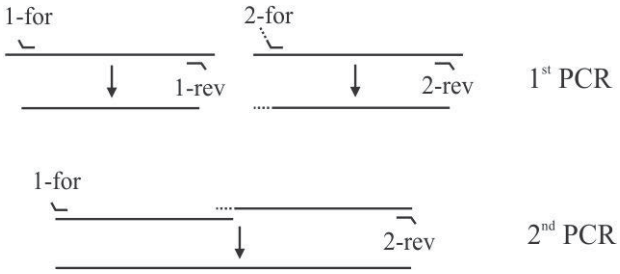

Figure 9: The basic principle of crossover PCR. Two PCR products are generated of which one has an overlapping area to the other one. These two fragments are then joined in a second PCR reaction using the outer primers.

2.4.8.4 Error prone PCR

To generate a library of TatB mutant molecules, error-prone PCR was carried out using the kit GeneMorph II (Agilent, Böblingen) according to the manufacturers specifications. A theoretical mutation frequency of 4.5 - 9 mutations per kb was achieved by using roughly 100 ng of template DNA.

2.4.9 Site-directed mutagenesis

For the insertion of point-mutations, the QuikChange kit (Agilent, Böblingen) was used according to the manufacturers specifications.

2.5. Protein biochemical methods

2.5.1 Preparation of *E. coli* membranes

2× Laemmli loading dye

1 M Tris/HCl pH 6.5	5 ml

SDS	2 g
87% glycerol	11.4 ml
DTT	1,6 g
bromophenolblue	0.25%
	ad 50 ml A. bidest

A 15 ml LB culture containing IPTG for the induction of gene expression from vectors containing an IPTG-inducible promoter was grown overnight in a 100 Erlenmeyer flask. Next, 10 ml of this culture were harvested. If several strains in one experiments were to be compared which showed a different OD_{600nm}, these were adjusted in volume to ensure that the same amount of cells was harvested. The samples were centrifuged for 10 min at 5000 rpm and 4°C. Afterwards, the pellet was washed once in 5 ml ice-cold 10 mM Tris/HCl pH 7.5. After centrifuging, the pellet was resuspended in 1 ml ice-cold 30 mM Tris/HCl and transferred to a 1.5 ml eppendorf tube. The cells were disrupted by sonication using a UP 200 S sonicator (Dr. Hielscher GmbH, Teltow) for 3 min in an ice-cold ice/saltwater solution. After pelleting the cell debris by centrifugation at 13400 rpm and 4°C for 15 min, the membrane-containing supernatant was transferred to an ultracentrifuge tube. The membranes were pelleted by centrifuging for 60 min at 50000 rpm and 4°C. The supernatant was discarded, the pellet washed once in 1 ml 1 M potassium acetate and centrifuged again for 60 min at 50000 rpm and 4°C. Finally, the pellet was resolubilized in 200 µl 10 mM Tris/HCl containing 1% Triton X-100 and the protein concentration measured by the method of (Bradford, 1976). The samples were supplemented with 2x Laemmli loading dye and denatured at 95°C. Samples designated for the detection of *E. coli* TatC were only denatured at 37°C for 5 min.

2.5.2 Fractionation of *E. coli* cells by EDTA-lysozyme spheroblasting

An overnight culture was used to inoculate 50 ml IPTG-containing LB medium in a 250 ml erlenmeyer flask to an OD_{600nm}=0.06. This main culture was grown at 37°C and 170 rpm for 4 hours. Equal amounts of cells were harvested by measuring the OD_{600} and calculating an amount of 5.5 x 10^{10} cells (an *E. coli* OD_{600}=1.0 in LB medium amounts to roughly 10^9 cells/ml). The harvested culture was pelleted for 10 min at 4800 rpm and 4°C, carefully resuspended in 2 ml ice-cold Tris/HCl pH 8.0 and transferred to a 2 ml eppendorf tube. After centrifuging again, the supernatant was discarded entirely. The pellet was very carefully resuspended in 40 µl 20% saccharose in 30 mM Tris/HCl pH 8.0 and then 20 µl of a lysozyme solution (1 mg/ml in 0.1 M EDTA pH 8.0) were added, very briefly vortexed and incubated on ice for 5 min. Next the sample was centrifuged for 15 min at 13400 rpm and 4°C. The supernatant containing the *E. coli* periplasmic fraction was transferred to a new tube. The pellet containing the spheroplasts was washed once (without centrifuging) with 80 µl 20% saccharose in 30 mM Tris/HCl pH 8.0 to prevent premature lysis and then resuspended in 1 ml 30 mM Tris/HCl pH 8.0. Next, 300 mg of glass beads (0.1 - 0.2 mm Clauss, Niederau) were added and the cells disrupted mechanically in a mixer mill (Retsch, Haan) in a pre-cooled teflon container at maximum velocity settings for 10 min. Afterwards the cell debris was pelleted by centrifugation for 15 min at 13400 rpm and 4°C and then the supernatant containing the combined cytoplasmic/membrane fraction transferred to a new tube. Of both fractions the protein concentration was measured by the method of (Bradford, 1976). The two fractions were supplemented with 2x loading dye and denatured at 95°C for 5 min.

2.5.3 Preparation of *C. glutamicum* fractions

_C.g._ lysis buffer

Tris/ HCl pH 8.0	10 mM
$MgCl_2$	25 mM
NaCl	200 mM

5× Laemmli loading dye

1 M Tris/ HCl pH 6.8	3.1 ml
SDS	100 mg
87% glycerol	5 ml
DTT	800 mg
bromophenolblue	100 mg
	ad 10 ml A. bidest

An overnight culture of *C. glutamicum* cells was used to inoculate a main culture either in 5 ml BHI in a glass test tube or in a 4 chicane 100 ml erlenmeyer flask containing 20 ml BHI to an OD_{600nm}=0.1. This main culture was grown at 30°C and 170 rpm (120 rpm when cultivated in a 4-chicane erlenmeyer flask) for 6 hours. After measuring the OD_{600} of the culture, 2 ml were harvested in a 2 ml eppendorf tube and the cells were pelleted for 15 min at 13400 rpm and 4°C. 1.8 ml of the supernatant were transferred to a new tube and another 2 ml of the culture were pelleted on top of the first pellet, resulting in a total of 4 ml culture per pellet. Again, 1.8 ml of the supernatant were transferred to a new tube.
The two 1.8 ml samples of the culture supernatant were supplemented with 200 µl 100% TCA to precipitate the containing protein overnight at 4°C. The supernatant was then centrifuged for 30 min at 13400 rpm and 4°C and then washed once in 100% acetone and once in 80% acetone. After discarding any residual fluid, the precipitated protein was dried in a SpeedVac (Eppendorf, Wesseling), then resolubilized in 80 µl 50 mM Tris/HCl pH 7.5 and supplemented with 20 µl 5x Laemmli loading dye.
The cell pellets were resuspended in 200 µl lysis buffer, 300 mg glass beads (0.1 - 0.2 mm Clauss, Niederau) were added and the cells disrupted mechanically in a mixer mill (Retsch, Haan) in a precooled teflon container at maximum velocity settings for 15 min. The cell debris was pellet by centrifuging for 15 min at 13400 rpm and 4°C. The supernatant was transferred to a new tube and supplemented with 5x Laemmli loading dye. The samples of both fractions were denatured at 95°C for 5 min and the gels loaded according to calculated cell amounts by OD_{600}.

2.5.4 *in vivo* DSS-Crosslinking

An *E.coli* LB overnight culture was used to inoculate a 50ml LB main culture to an OD_{600nm} of 0.1. The cells were induced for four hours and then two volumes of 10 ml each were harvested, washed once in cold PBS pH 8.0 and resuspended in 10 ml PBS pH 8.0. One harvested sample served as negative control to which 250 µl pure DMSO were added. To the cross-linking sample 250 µl of 100 mM DSS (disuccinimidyl suberate, Thermo Fisher) in pure DMSO were added to a final cross-linker concentration of 2.5 mM.

The reaction mixture was incubated at room temperature for 30 min. Afterwards, the reaction was quenched by adding 1 M Tris/HCl pH 7.5 to a final concentration of 50 mM. After incubating another 15 min at room temperature, the samples were washed once in PBS pH 8.0 and it was proceeded with the preparation of the membranes (see page 32).

2.5.5 Purification of *Strep*-tagged TorD

The small-scale purification of $TorD^{Strep}$ was carried out using *Strep*-Tactin coated magnetic beads. *Strep*-Tactin is an engineered streptavidin. Samples to be crosslinked of either isolated *E. coli* membrane fractions or cytoplasmic fractions were adjusted to a volume of 1 ml. Next, 200 µl of 10% *Strep*-Tactin Magnetic Beads (QIAGEN, Hilden) were added and incubated for 60 min at 4°C in an end-over-end shaker. For all following steps, a magnetic separator for 1.5 ml Eppendorf tubes (QIAGEN, Hilden) was used. The tube containing the sample was set into the separator and after 1 min the liquid was removed from the tube using a pipette.
The samples were washed two times in NP-T buffer (50 mM NaH_2PO_4, 300 mM NaCl, 0.05% Tween 20, pH adjusted to 8.0) with gently vortexing after each addition of fresh buffer. Finally the samples were eluted using NP-T buffer containing 10 mM biotin which is the natural ligand of streptavidin. This step was repeated twice so a total of three elution fractions was collected. These fractions were gently concentrated about 10-fold using a vacuum centrifuge without heating and subjected to SDS-PAGE.

2.5.6 SDS-Polyacrylamide Gel Electrophoresis (Laemmli, 1970)

	running gel		**stacking gel**
	12,5%	15%	
acrylamide/bisacrylamide 35:1	6.25 ml	7.5 ml	1.25 ml
1.5 M Tris/ HCl pH 8,8	3.75 ml	3.75 ml	-
0.5 M Tris/ HCl pH 6,8	-	-	1.875 ml
10% SDS	150 µl	150 µl	75 µl
87% glycerol	1.6 ml	1.6 ml	-
H_2O	3.09 ml	1.84 ml	4.22 ml
10% APS	150 µl	150 µl	75 µl
TEMED	10 µl	10 µl	5 µl

running buffer

Tris	25 mM
glycine	192 mM
SDS	0.1% (w/v)

The separation of proteins in SDS-Polyacrylamide Gel Electrophoresis (SDS-PAGE) was carried out by the modified method of Laemmli (1970). First, roughly 6 cm high running gels (the recipes shown

above are for two gels) were cast in a 8 x 10 cm setup (mini-gel) with glass front- and ceramic-coated back-plates (Hoefer, US-Holliston, MA) and overlayed with A. bidest. After polymerization, the water was removed, a teflon comb with the desired number of pockets was inserted and a roughly 2 cm high stacking gel was cast on top of the running gel. After polymerization, the gel was installed in the running chamber (Hoefer, US-Holliston, MA) and both buffer reservoirs were filled with SDS-gel running buffer. After loading of the samples, the gels were run at constant 16 mA per gel using Biorad power supplies.

Staining of SDS-Polyacrylamide gels

Coomassie G-250	0.02% (w/v)
$Al_2O_{12}S_3 \times H_2O$	5% (w/v)
96% ethanol	10% (v/v)
100% *ortho*-phosphoric acid	2% (v/v)

Visualization of proteins in SDS gels was done by Coomassie staining with the highly sensitive method of (Kang et al., 2002). After the gel run, the gels were washed twice for 10 min in water and then covered with Coomassie solution. After overnight staining the gels were destained with A. bidest.

2.5.7 Western Blotting

Running buffer

Tris	25 mM
glycine	192 mM

TBS-T

NaCl	8 g
1 M Tris/ HCl pH 7,5	20 ml
Tween 20	1 ml
	ad 1 l A. bidest

The transfer of proteins from SDS polyacrylamide gels to a nitrocellulose membrane by western blotting was carried out using a tank-blot setup (Biorad, München). The gel was pressed against a piece of nitrocellulose membrane between a piece of thick Whatman paper and a sponge on each side held together by a plastic frame. This frame was inserted into the blotting chamber together with a cooling pack and submerged with running buffer. The blotting took place for exactly 50 min at constant 350 mA.

After blotting and disassembly of the chamber, the blotted membrane was blocked for one hour in 5% (w/v) skim-milk in TBS-T buffer. After washing the membrane once in TBS-T, it was incubated overnight at 4°C in TBS-T containing the desired primary antibody at the appropriate dilution (see below).

2.5.7.1 Primary antibodies (anti-rabbit)

name	dilution	source
α-MalE *E. coli*	1:1000	Schimz, FZ Jülich
α-GroEL *E. coli*	1:1000	Schimz, FZ Jülich
α-GFP *E. coli*	1:1000	Roche, Mannheim
α-Bla *E. coli*	1:5000	Pineda AK Services, Berlin
α-TalB *E. coli*	1:1000	Schimz, FZ Jülich
α-TatA *E. coli*	1:1000	(Kreutzenbeck, 2005)
α-TatB *E. coli*	1:1000	(Kreutzenbeck, 2005)
α-TatC *E. coli*	1:1000	(Kreutzenbeck, 2005)

2.5.7.2 Secondary antibodies

name	dilution	source
α-rabbit, horseradish peroxidase coupled	1:10000	GE Healthcare, München
α-rabbit, alkaline phosphatase coupled	1:15000	Sigma-Aldrich, Taufkirchen
Strep-Tactin, alkaline phosphatase-conjugate	1:5000	IBA, Göttingen

After overnight incubation with the primary antibody, the blot was washed three times for 10 min at room temperature using TBS-T. Afterwards, the blot was incubated at room temperature for 90 min with TBS-T containing the secondary antibody at the appropriate dilution. Then the blot was again washed three times for 10 min with TBS-T.

2.5.7.3 Development

When the alkaline phosphatase coupled secondary antibody was used, the development of the western blot was carried with the NBT/BCIP method. After washing the blot it was transferred into development buffer and incubated for 5 min. Next, an equal amount of development buffer containing both 66 µl/ 10 ml BCIP (50 mg/ml 5-bromo-4-chloro-3-indoxylphosphate in 100% DMF) and 66 µl/ 10 ml NBT (50 mg/ml nitroblue-tetrazoliumchloride in 70% DMF) was added. When the color reaction had progressed sufficiently, the reaction was stopped by washing the blot first in 3% TCA and then in A. bidest. The alkaline phosphatase coupled *Strep*-Tactin was detected analogously.
As a more sensitive detection method, the horseradish peroxidase coupled secondary antibody was used and the development was carried out by chemiluminescence. After the final washing of the blot, it was left to air-dry for a few minutes and then sealed bubble-free between two plastic foils containing 750 µl each of two proprietary Amersham ECL™ Western Blotting System development solutions (GE Healthcare, München). The detection of the chemilumiscent signal was carried out with a LAS-3000 Mini CCD-camera (GE Healthcare, München). The analysis of the resulting pictures used the software AIDA image analyzer (Raytest GmbH, Straubenhardt).

2.5.8 Mass spectrometric protein identification

The identification of proteins out of Coomassie stained SDS polyacrylamide-gels was carried out by MALDI-TOF mass spectrometry. The stained protein bands were cut out of the polyacrylamide-gel using a clean scalpel and washed twice with 750 µl 0,1 M NH_4HCO_3 in 30% (v/v) acetonitrile to remove the blue dye. Afterwards, the gel fragments were dried in a vacuum centrifuge for 20 min and then rehydrated in 6 µl 3 mM Tris/HCl (pH 8.8) containing 10 ng/µl trypsine. After incubation at room temperature for 30 min, further 6 µl 3 mM Tris/HCl (pH 8.8) were added and the sample was digested over night at room temperature.
Next, 10 µl A. bidest were added, incubated at room temperature for 10 min and then 10 µl 0,2% (v/v) trifluoroacetic acid in 30% acetonitrile were added and again incubated for 10 min at room temperature to elute the peptides from the acrylamide residues. The peptides were purified and concentrated using a microchromatography-column "ZipTip® C18 standard bed" (Millipore, Schwalbach) according to the manufacturers specifications. Next, the peptides were eluted from the column with 3 µl saturated matrix solution (α-cyano-hydroxycinnamic acid in 50% (v/v) acetonitrile and 0.25% (v/v) trifluoroacetic acid) and applied to a sample plate "Prespotted AnchorChip" (Bruker Daltonics, Bremen).
The measurement was carried out in an Ultraflex III MALDI-TOF/TOF mass spectrometer (Bruker Daltonics, Bremen) in positive reflector mode. The instrument software used was Flexcontrol. The obtained peptide masses were analyzed using the program Biotools 3.1, the MASCOT servers (Matrix Science, London UK) and the MASCOT software (Perkins et al., 1999) and compared to a local database. The peptide mass comparison allowed "missed cleavage" during trypsin digestion, carbamidomethylsubstitution at L-cystein positions, oxidation of L-methionin, phosphorylations of L-serine and L-threonine as variable modifications as well as a discrepancy of 200 ppm. A protein was considered to be surely identified when a MOWSE-score (molecular weight search) of ≥ 50 was obtained (Pappin et al., 1993).

3. Results

3.1. TatB involvement in *C. glutamicum* Tat translocation

3.1.1 Construction of *C. glutamicum tatA/E* and *tatB*-mutants

The composition of Tat-translocases can generally be divided into two different classes. In Gram-negative organisms such as *E. coli* and in plant thylakoids, the translocase is composed of three essential components TatABC. In low G/C Gram-positive prokaryotes like *B. subtilis* on the other hand, the function of TatB seems to be obsolete. A bifunctional TatA molecule can fulfill the mechanistic role of TatB resulting in a TatAC translocase, sometimes referred to as "minimal-translocase".
The findings of Kikuchi et al. (2006) in the high G/C Gram-positive bacterium *Corynebacterium glutamicum* ATCC 13869 imply the presence of a Gram-positive style TatAC translocase. Noticeably however, the genome of *C. glutamicum* also encodes a putative *tatB* gene (*cg1273*). Assuming the annotation of *cg1273* as *tatB* is correct, it has to be tested whether *C. glutamicum* employs a TatABC-type translocase. Should the annotation of *cg1273* as *tatB* be incorrect, then the gene product belonging to the TatA/B-family has to be tested for possible bifunctionality to investigate the possibility of a "TatBC"-translocase which could operate in parallel to the TatAC-translocase.
To determine the actual Tat translocase composition and to define the role of *C. glutamicum* TatB, genomic deletions of the genes encoding the Tat components TatB and TatA/E were made in *C. glutamicum* ATCC 13032. The deletion of *tatB* was made using the temperature sensitive deletion vector pCRD_deltatB. The deletions of *tatA* and *tatE* to obtain a *tatA/E* double deletion mutant were carried out using the vectors pK19_deltatA and pK19_deltatE. Both the pCRD and the pK19 vectors are integration vectors with kanamycin resistance and *sacB* genes. The mechanism of these "suicide vectors" is explained in detail on page 26.

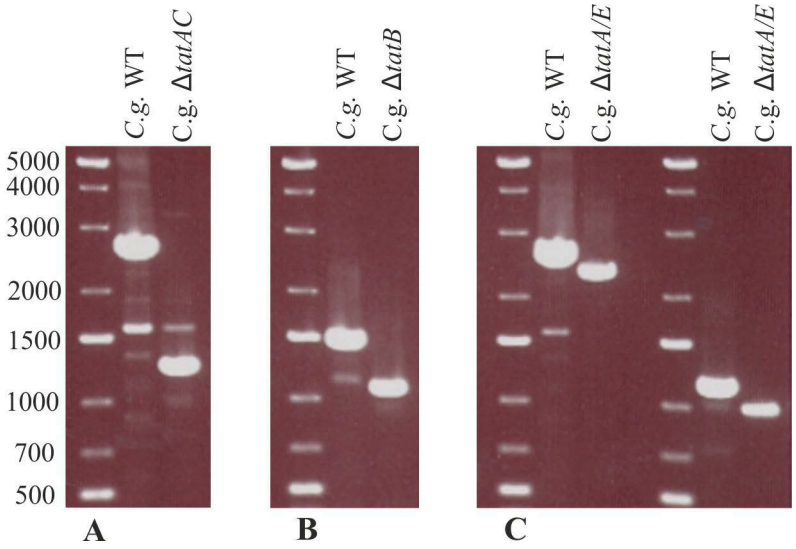

Figure 10: Agarose gels showing genomic deletions of *C. glutamicum tat*-mutants. The difference in size of the PCR product when comparing wild-type with *tat*-mutant depicts the size of the deleted region. (A) shows *C. glutamicum* Δ*tatAC* (Δ 1401 bp), (B) shows *C. glutamicum* Δ*tatB* (Δ 417 bp) and (C) shows in the left half the deletion of *tatA* (Δ 249 bp) and in the right half the deletion of *tatE* (Δ 162 bp) in *C. glutamicum* Δ*tatA/E*.

Both the newly constructed mutant strains *C. glutamicum* Δ*tatB* and Δ*tatA/E* as well as the already existing strain *C. glutamicum* Δ*tatAC* (Meissner, 2005) were verified by colony PCR for their genomic deletions. In figure 10 the deletion of the single gene loci can be seen. The size difference between the PCR product band of the wild-type and the band of the *tat*-mutant strain for each of the respective PCR products is the size of the deleted region. The deletion of the *tatAC* operon removes 1401 bp (figure 10, A), *tatB* deletion removes 417 bp (B) and the deletion of *tatA* and *tatE* removes 249 and 162 bp, respectively (C).

3.1.1.1 *C. glutamicum tat*-mutant growth phenotypes

A first characterization of the strains *C. glutamicum* Δ*tatB* and Δ*tatA/E* was carried out by comparing their growth phenotypes to the wild-type strain *C. glutamicum* ATCC 13032 as well as the strain *C. glutamicum* Δ*tatAC* (Meissner, 2005). The cultivations were carried out in complex medium in a micro fermentation system called BioLector® by m2p-labs. All cultivations with *C glutamicum* were carried out in 750 µl volume at 30ºC.

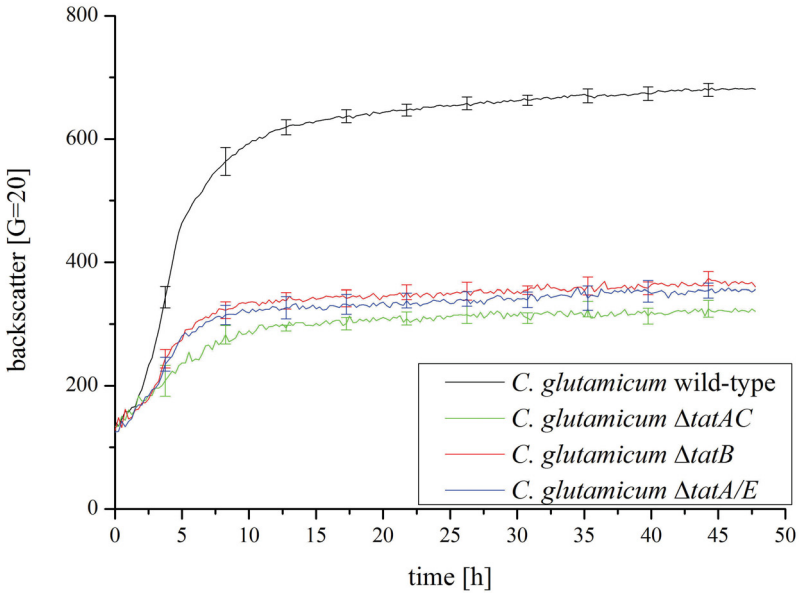

Figure 11: *C. glutamicum tat*-mutants exhibit a strong growth defect in comparison to the wild-type strain. Cultivation in BHIS medium, the optical density of cultures was measured in a BioLector micro reactor system in a volume of 750 µl at 1100 rpm, 30°C and 85% relative humidity. *C. glutamicum* wild-type (black), Δ*tatAC* (green), Δ*tatB* (red) and Δ*tatA/E* (blue). The experiment was carried out in triplicate.

As can be seen in figure 11, the deletion of *tatAC, tatB* or *tatA/E* has a detrimental effect on the growth of *C. glutamicum*. Compared to the wild-type, all three mutant strains exhibit a delayed growth during exponential growth phase and reach about half of the cell density of the wild-type strain at the end of stationary phase. Of the three investigated *tat*-mutants, all strains grow comparably bad but the deletion of the *tatAC* operon shows the most severe effect.
The growth behavior of the *C. glutamicum tatB*-mutant which was constructed in this work stands in stark contrast to the growth phenotype of the *tatB*-mutant constructed and investigated by Kikuchi et

al. (2006) which showed growth comparable to the wild-type *C. glutamicum* ATCC 13869 used in their study.

Next, the possibility of a polar effect due to the deletions of *tatB* and *tatA/E* had to be ruled out. This would, for example, be the case if *tat* gene deletion resulted in the disruption of a genetic control region of a *downstream* gene. To show that the observed growth phenotype is in fact dependent on the deletion of the *tat*-genes, the mutant strains were back-complemented with the according *tat* genes *in trans*. For this purpose, two IPTG-inducible expression vectors based on pEC-XC99E (Kirchner and Tauch, 2003) carrying *tatB* and *tatA* were constructed

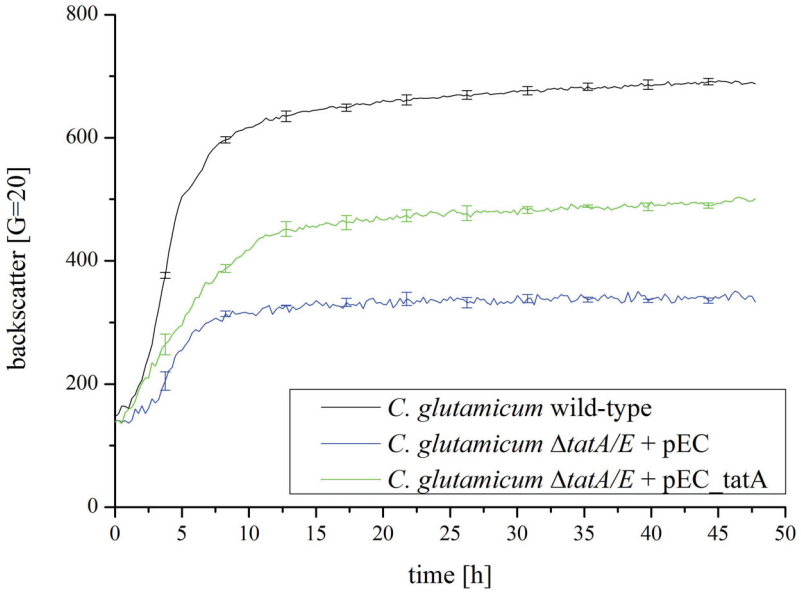

Figure 12: A *C. glutamicum tatA/E*-mutant can be partially complemented with *tatA in trans.* Cultivation in BHIS medium containing 1mM IPTG for induction of gene expression. The growth was measured in a BioLector micro reactor system in a volume of 750 µl at 1100 rpm, 30°C and 85% relative humidity. *C. glutamicum* wild-type (black), Δ*tatA/E* with pEC-XC99E empty vector (blue) Δ*tatA/E* with pEC-XC99E_TatA (green). The experiment was carried out in triplicate.

The complementation of *C. glutamicum* Δ*tatA/E* is shown in figure 12. When comparing the growth of the *tatA/E*-mutant transformed with the empty vector (blue growth curve) with the wild-type (black) the growth deficit of the mutant strain is clearly visible. Upon expression of TatA *in trans* in the *tatA/E*-mutant (green) the growth phenotype of the mutant strain can be partly reverted to the wild-type situation. Why a complete complementation is not possible is unclear at this point. Possibly the amount of expressed TatA is not ideal from the chosen pEC expression system. This could lead to a suboptimal amount of TatA within in the membrane and thus to either too few or less functional translocase complexes. A polar effect leading to complete impairment of *tatC* gene expression, which is located in an operon *downstream* of *tatA*, during the deletion process of *tatA* (see page 39) can be excluded. This would not allow for a (partial) reversion of the growth phenotype. Nonetheless, the effect on the expression level of *tatC* when *upstream tatA* is deleted is not known either and could also influence overall Tat translocase activity. If this was the case, a slight polar effect effecting the expression level of *tatC* due to the deletion of *tatA* could alternatively be the reason why a full complemen-

tation of the growth phenotype of the *C. glutamicum tatA/E* mutant is not possible.
The complementation of *C. glutamicum* Δ*tatB* is shown in figure 13. When comparing the growth of the *tatB*-mutant transformed with the empty vector (blue growth curve) with the *C. glutamicum* wild-type strain (black), the growth deficit of the mutant strain is clearly visible. Upon expression of TatB *in trans* in the *tatB*-mutant strain (green), the growth phenotype can completely be reverted to growth of the wild-type strain. A polar effect on downstream genes due to the deletion of *tatB* can therefore be excluded.

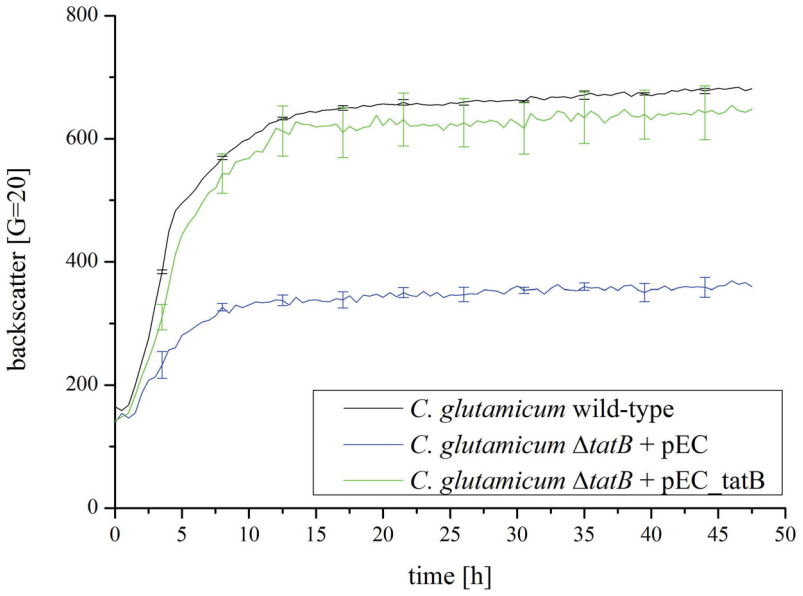

Figure 13: A *C. glutamicum tatB*-mutant can be fully complemented by plasmid-expressed TatB. Cultivation in BHIS medium containing 10µM IPTG for induction of gene expression. The growth was measured in a BioLector micro reactor system in a volume of 750 µl at 1100 rpm, 30°C and 85% relative humidity. *C. glutamicum* wild-type (black), Δ*tatB* with pEC-XC99E empty vector (blue) Δ*tatB* with pEC-XC99E_TatB (green). The experiment was carried out in triplicate.

3.1.1.2 All *C. glutamicum tat*-mutants are unable to secrete GFP Tat-dependently

The growth phenotype of the *C. glutamicum tat*-mutants obviously leads to the assumption that a physiologically very important but not absolutely essential substrate is translocated Tat dependently. The translocation of this substrate is necessary for wild-type-like growth.
To assess the Tat-dependent secretion capabilities of the *tatAC*-, *tatB*- and *tatA/E*-mutants, they were tested for the translocation of a heterologous model protein. For this purpose, two different fusions of signal peptides to the green fluorescent protein GFP from the jellyfish *Aequorea victoria* (Shimomura et al., 1962; Heim et al., 1995) were chosen. Firstly, the *E. coli* signal peptide of the trimethylamine N-oxide reductase TorA. Secondly, the *C. glutamicum* signal peptide from the alkaline phosphatase D. The two different signal peptides were chosen to verify GFP secretion using both a heterologous and an a homologous signal peptide. Both artificial substrates $TorA^{SP}$-GFP and $PhoD_{C.g.}{}^{SP}$-GFP have been shown to be efficiently secreted by *C. glutamicum* wild-type in a Tat-dependent manner (Meissner et

al., 2007). Expression occured from the IPTG-inducible expression vector pEKEx2 (Eikmanns et al., 1994).

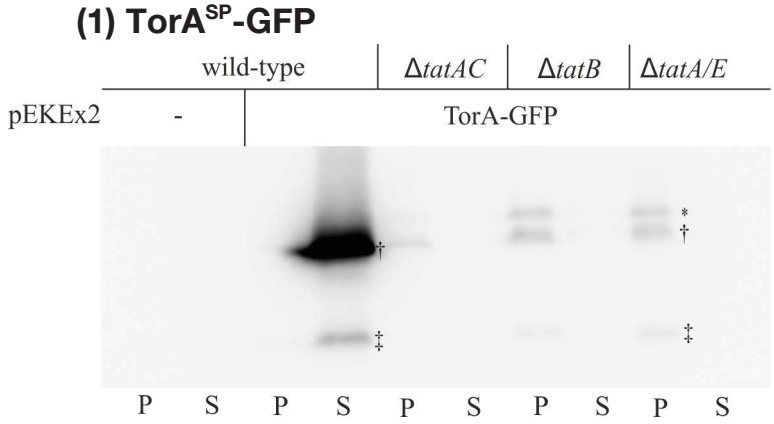

Figure 14: Western Blot showing amounts of GFP in pellet (P) and supernatant (S) fractions of *C. glutamicum* wild-type, *tatAC*-, *tatB*- and *tatA/E*-mutants. The strains expressed TorA^{SP}-GFP in a six hour induction culture containing 0.1 mM IPTG for induction of gene expression. An OD of 1.0 for the pellet fraction and an OD of 2.0 for the supernatant fraction was applied to SDS-PAGE, subsequently Western blotted and the substrate detected using a polyclonal α-GFP antibody. An asterisk (*) denotes TorA^{SP}-GFP, an obelisk (†) GFP without signal peptide and a diesis (‡) a degradation product of GFP.

The amounts of expressed and secreted TorA^{SP}-GFP in *C. glutamicum* wild-type and the three *tat*-mutant strains can be seen in figure 14. The Western-Blot shows two fractions for each strain. The supernatant fraction equals the protein outside of the cytoplasmic membrane secreted into the culture medium. The wild-type strain shows high amounts of secreted GFP in the supernatant fraction as well as an additional smaller band which is probably a degradation product of GFP. The fact that no unsecreted precursor can be seen in the pellet fraction exemplifies how efficient Tat-dependent translocation of TorA^{SP}-GFP takes place in *C. glutamicum*.

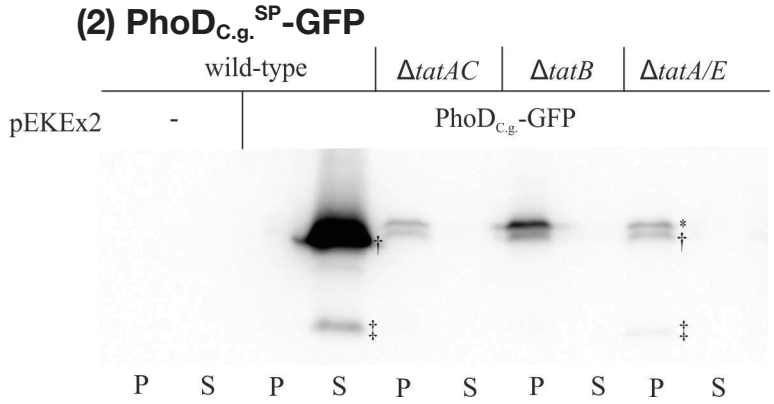

Figure 15: Western Blot showing amounts of GFP in pellet (P) and supernatant (S) fractions of *C. glutamicum* wild-type, *tatAC*-, *tatB*- and *tatA/E*-mutants. The strains expressed PhoD$_{C.g.}$^{SP}-GFP in a six hour induction culture containing 0.1 mM IPTG for induction of gene expression. An OD of 1.0 for the pellet fraction and an OD of 2.0 for the supernatant fraction was applied to SDS-PAGE, subsequently Western blotted and the substrate detected using a polyclonal α-GFP antibody. An asterisk (*) denotes PhoD$_{C.g.}$^{SP}-GFP, an obelisk (†) GFP without signal peptide and a diesis (‡) a degradation product of GFP.

The three investigated *tat*-mutants show no secreted GFP in their supernatant fractions. Rather, three different weak bands are visible in the pellet fractions. The one running highest is the accumulated precursor TorA^{SP}-GFP with the signal peptide still attached. The two lower bands are probably intracellular degradation products of TorA^{SP}-GFP.
The amounts of expressed and secreted PhoD$_{C.g.}^{SP}$-GFP in *C. glutamicum* wild-type and *tat*-mutants strains can be seen in figure 15. The wild-type strain again shows high amounts of secreted GFP in the supernatant fraction as well as a weak additional smaller band which is probably a degradation product of GFP.
The three investigated *tat*-mutant strains show no secreted GFP in their supernatant fractions. Rather, two, and in the case of the *tatA/E*-mutant strain three, different bands are visible in the pellet fractions. The one running highest is the accumulated precursor PhoD$_{C.g.}^{SP}$-GFP with the signal peptide still attached. The two lower bands are probably intracellular degradation products of PhoD$_{C.g.}^{SP}$-GFP.
All three *C. glutamicum tat*-mutant strains Δ*tatAC*, Δ*tatB* and Δ*tatA/E* are incapable of secreting TorA^{SP}-GFP or PhoD$_{C.g.}^{SP}$-GFP. This shows that in *C. glutamicum* all Tat-components TatA, TatB and TatC are vital for Tat-dependent secretion of these model substrates. In the case of the strains Δ*tatAC* and Δ*tatA/E* this is not surprising and in-line with the literature, but the inability of a *tatB*-mutant to secrete TorA^{SP}-GFP again stands in stark contrast to the findings of Kikuchi et al. (2006).
This finding firstly suggests that TatB is absolutely necessary for the Tat-dependent secretion of these two model substrates. Secondly, it is strong evidence against the substrates TorA^{SP}-GFP or PhoD$_{C.g.}^{SP}$-GFP being translocated by translocases composed of either TatAC or TatBC in the wild-type strain. If either of these "minimal translocases" were functional for these substrates in *C. glutamicum,* translocation in absence of TatB or TatA/E respectively would occur. As this is not the case, it can be concluded that translocation of TorA^{SP}-GFP and PhoD$_{C.g.}^{SP}$-GFP happens via a TatABC-type translocase.

3.1.2 The Rieske protein QcrA is an important Tat-substrate for *C. glutamicum*

As shown above, the deletion of any of the *tat* genes has a serious effect on the growth of *C. glutamicum*. Unarguably, the reason for this is that a physiologically important substrate has to be transported Tat-dependently.
By analysis of common signal peptides, Berks (1996) firstly proposed the, then still uncharacterized, twin-arginine pathway to transport complex co-factor associated proteins. It could be demonstrated that the the consensus Tat-motiv (S/T)-R-R-x-F is frequently found within signal peptides of periplasmic and membrane-associated proteins containing iron-sulfur, molybtopterin, FAD and other co-factors. Numerous co-factor-containing secreted and membrane-bound enzymes dependent on the Tat-pathway have been identified since then. One common substrate translocated by the Tat-pathway is the iron-sulfur-cluster-containing Rieske protein which is a subunit of cytochrome bc_1 complexes and necessary for oxidative phosphorylation. Amongst others, it could be shown that the Rieske protein of plant chloroplasts (Molik et al., 2001), *Paracoccus denitrificans* (Bachmann et al., 2006) and *Legionella pneumophila* (De Buck et al., 2007) depend on the Tat-pathway for correct membrane insertion into the membrane. Finally, Keller et al., 2012 could show that the Fe/S-cluster containing Rieske protein of *Streptomyces coelicolor,* albeit not possessing an N-terminal signal peptide, needs a functional Tat-pathway for correct insertion. A two-step process involving both the Sec- and the Tat-pathway in the membrane insertion of the Rieske protein could be described that seems to be unique for *Actinobacteria.* The Fe/S Rieske protein of *S. coelicolor* possesses three transmembrane domains, the first two of which are integrated into the membrane cotranslationally by the Sec pathway. When the Rieske

protein is thus attached to the cytoplasmic membrane, the complexation with the iron-sulfur-cluster takes place and an internal Tat signal peptide corresponding to the third transmembrane domain is recognized by the Tat-translocase and the protein is integrated into the membrane into its active form. This final integration step is Tat-dependent because the integration of the Fe/S-cluster has to take place in the reductive intracellular environment and after co-factor association and completed folding the translocation substrate is too large for export via the general Sec pathway.
This finding ultimately led to the identification of the *C. glutamicum* Tat-substrate responsible for the strong growth defect upon deletion of *tat* genes. The Rieske protein of *C. glutamicum* is called QcrA and a component of the cytochrome bc_1 complex of the respiratory chain (Niebisch and Bott, 2003). A comparison of the growth phenotypes of a *qcrA*-mutant strain (Chattopadhyay, 2013) with a *tatB*-mutant strain reveals that these strains show a comparable growth defect in comparison to the wild-type (see figure 16). The similarity of the growth defect of these two mutant strains was therefore a good first indicator for not only Tat-dependency of QcrA membrane insertion, but also for TatB involvement in this process in *C. glutamicum*.

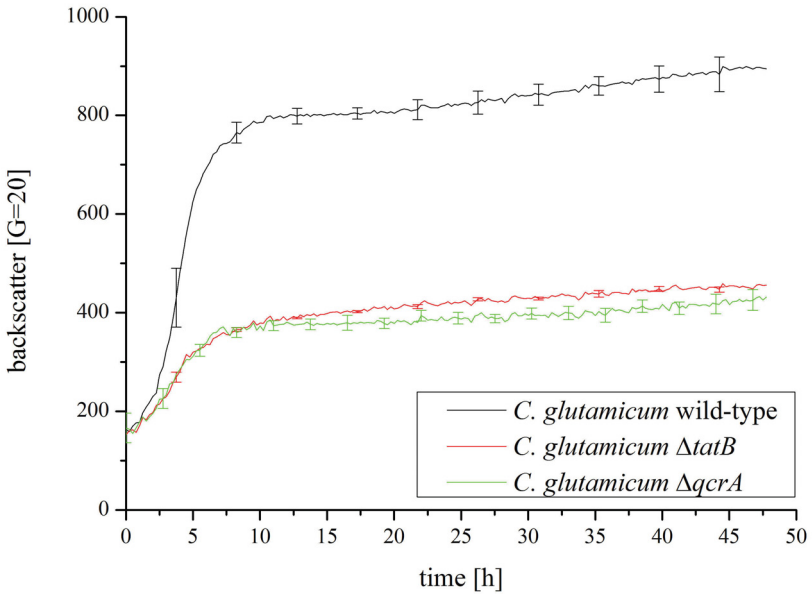

Figure 16: *C. glutamicum tatB*- and *qcrA*-mutants exhibit a similar growth defect in comparison to the wild-type strain. Cultivation in BHIS medium, the optical density of the cultures was measured in a BioLector micro reactor system in a volume of 750 µl at 1100 rpm, 30°C and 85% relative humidity. *C. glutamicum* wild-type (black), Δ*tatB* (red) and Δ*qcrA* (green). The experiment was carried out in triplicate

3.1.2.1 QcrA is integrated into the membrane in a Tat-dependent manner

Next, it was verified that, analogous to the situation in *Streptomyces coelicolor*, the membrane integration of the Fe/S-cluster containing Rieske protein QcrA is in fact dependent on the Tat-pathway. As can be seen in figure 17, the *C. glutamicum* QcrA also possesses three transmembrane domains (highlighted in orange) and, directly in front of the third transmembrane domain, an internal twin-arginine motiv is found (red box). Obviously, this internal signal peptide does not contain a cleavage site due

to the nature of the substrate. This also explains why in earlier studies QcrA was not identified as a putative Tat substrate (Watanabe et al., 2009); unpublished results R. Freudl), as bioinformatic tools for the prediction of signal peptides such as Tatfind (Rose et al., 2002) or TatP (Bendtsen et al., 2005), rely heavily on the presence of signal peptide cleavage sites for their algorithms.
To verify the Tat-dependency of QcrA membrane insertion in *C. glutamicum,* complementation experiments were carried out. Two expression vectors based on the pEKEx2 backbone were constructed. The first one for expression of wild-type QcrA and the second one for a mutated version of QcrA, wherein the two arginines of the internal signal peptide were exchanged for two lysine residues. The presence of two lysine-residues at this position is known to render Tat substrates incapable of being transported via the Tat-pathway (Berks et al., 2003).

Figure 17: QcrA (Cg2404), the Rieske protein of *C. glutamicum*. The internal Tat consensus motiv is highlighted with a red box. The three transmembrane domains are shown in orange. The Rieske domain is shown in grey. The two conserved boxes which coordinate the 2Fe-2S cluster in the mature protein are underlined and the four cysteine residues responsible for complexation are highlighted.

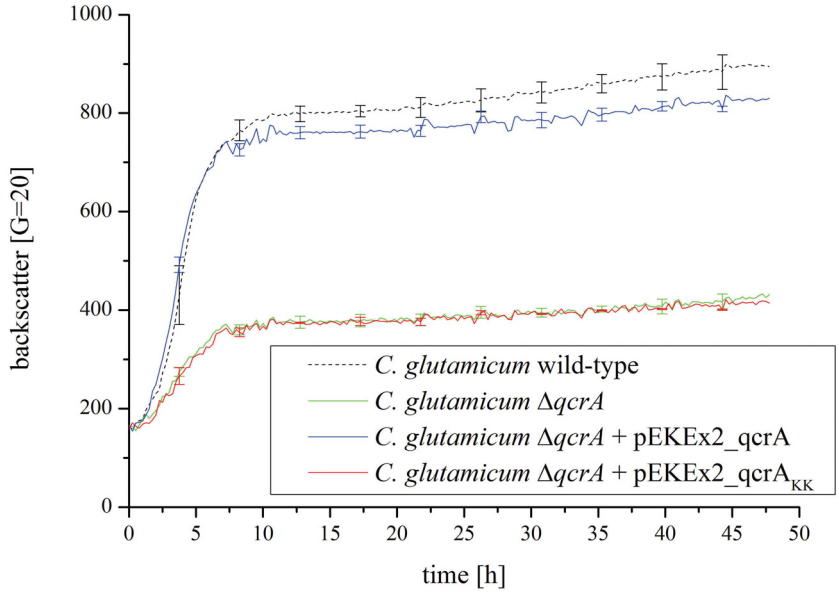

Figure 18: The *C. glutamicum* Rieske protein QcrA is integrated into the membrane in a Tat-dependent manner. A *C. glutamicum qcrA*-mutant can be complemented with wild-type *qcrA in trans* but not with $qcrA_{KK}$. Cultivation in BHIS medium, the optical density of the cultures was measured in a BioLector micro reactor system in a volume of 750 µl at 1100 rpm, 30°C and 85% relative humidity. *C. glutamicum* wild-type (black), Δ*qcrA* (green), Δ*qcrA* with wild-type QcrA in trans (blue) and Δ*qcrA* with $QcrA^{KK}$(red). The experiment was carried out in triplicate.

As can be seen in figure 18, a *C. glutamicum qcrA*-mutant strain (green growth curve) shows a growth defect in comparison to the wild-type strain (black). The *in trans* expression of wild-type QcrA (blue) in the *qcrA*-mutant leads to a near full reversion of this growth phenotype. If, on the other hand, $QcrA^{KK}$ with a mutated internal Tat signal peptide with an exchange of the two arginines to two lysines is expressed in the *qcrA*-mutant (red growth curve), a reversion does not take place.
These results are a first clear evidence for a situation that, just like *Streptomyces coelicolor*, *C. glutamicum* relies on the Tat pathway to correctly insert its iron-sulfur-cluster containing Rieske protein into the membrane after full maturation of the protein has been achieved.

3.1.2.2 TatB is necessary for the membrane integration of QcrA

To show that *C. glutamicum* TatB is in fact involved and necessary for the membrane integration of QcrA, a Δ*qcrA* Δ*tatB* double mutant was constructed by deleting *tatB* in *C. glutamicum* Δ*qcrA* using the deletion vector pCRD_deltatB. This Δ*qcrA* Δ*tatB* double mutant shows the same growth phenotype as a Δ*qcrA* single mutant (see figure 19). This indicates that the two mutations do not lead to an additive effect and that the reason for the growth defect in the two single mutant strains Δ*tatB* and Δ*qcrA* is the same as in the double mutant strain, namely the mislocalization of QcrA.
Next, QcrA complementation experiments were carried out under the assumption that only if TatB is involved in the Tat-dependent membrane integration of QcrA, a double mutant Δ*qcrA* Δ*tatB* could not be reverted in its growth phenotype. If, as the growth phenotype of the *tatB*-mutant of Kikuchi et al. (2006) suggests, TatB is not involved in this process, then a double mutant Δ*qcrA* Δ*tatB* should show

wild-type like growth when plasmid-borne QcrA is expressed. Figure 19 clearly shows that is is not the case as the double mutant strain cannot be complemented by QcrA. Whereas a *qcrA* single mutant upon *in trans* expression of QcrA reverts its growth phenotype to that of the wild-type strain (blue growth curve), the *qcrA/tatB*-double mutant is not complementable by *qcrA in trans*. After having shown that the membrane integration of QcrA is dependent on the Tat-pathway (see page 45ff.), this experiment additionally demonstrates that TatB is explicitly necessary for functionality of the *C. glutamicum* Rieske protein. This finding therefore adds further strong evidence that a translocase of the ABC-type is active in *C. glutamicum*.

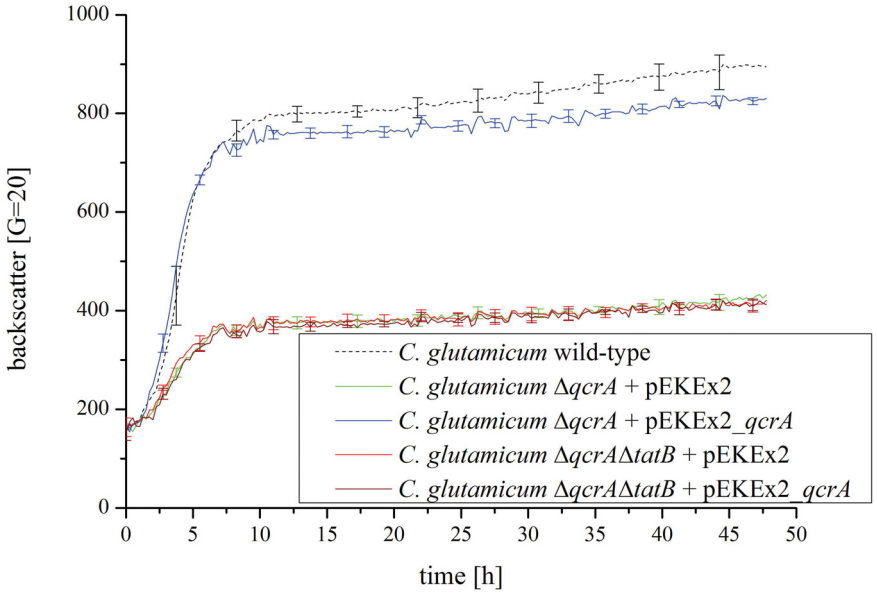

Figure 19: A *C. glutamicum* Δ*qcrA*Δ*tatB* strain is not complementable by *qcrA in trans.* Cultivation in BHIS medium, the optical density of the cultures was measured in a BioLector micro reactor system in a volume of 750 µl at 1100 rpm, 30°C and 85% relative humidity. *C. glutamicum* wild-type (black), Δ*qcrA* with empty vector (green), Δ*qcrA* with wild-type *qcrA* in trans (blue), Δ*qcrA* Δ*tatB* double-mutant with empty vector (red) and Δ*qcrA* Δ*tatB* with wild-type *qcrA* (magenta). The experiment was carried out in triplicate.

3.1.3 $TatB_{C.g.}$ is a *bona fide* TatB protein

In the previous sections it could be shown that *C. glutamicum* TatB is essential for the secretion of $TorA^{SP}$-GFP and $PhoD_{C.g.}{}^{SP}$-GFP as well as for the translocation of the Rieske protein QcrA. To further clarify the role of *C. glutamicum* TatB regarding its function within the translocation process itself, it was tested whether $TatB_{C.g.}$ could fulfill the role of *E. coli* TatB in an *E. coli tatB*-mutant strain BØD (Sargent et al., 1999). It is known that in *E. coli* TatB fulfills a distinct role that distinguishes itself clearly from a "TatA-role". TatB acts together with TatC in a TatBC receptor complex which is responsible for initially binding the signal peptide of the substrate (Cline and Mori, 2001) and only then the complete translocase is assembled by recruiting TatA multimers (Dabney-Smith et al., 2006). In *E. coli*, the presence of TatB is mandatory for the functioning of Tat-dependent translocation under native conditions (Sargent et al., 1999). TatA on the other hand is, in ABC-type translocases such as in *E. coli*, not involved in substrate recognition and signal peptide binding. Here, the function of TatA is

solely to form the protein conducting channel through which the export of the substrate takes place (Gohlke et al., 2005). In Gram-positive AC-type Tat translocases on the other hand, these two mechanistically different functions are not carried out by two different proteins but by "bifunctional" TatA molecules which are capable of both acting within a TatAC receptor complex for signal peptide binding as well as forming the TatA-multimer protein conducting channel.

The *C. glutamicum tatB*-mutant strain of Kikuchi et al. (2006) allowed for significant translocation of the strictly Tat-dependent substrate $TorA^{SP}$-GFP. This suggests that in their *C. glutamicum* strain a TatAC translocase is capable of secreting $TorA^{SP}$-GFP which would mean that the TatA molecule is bifunctional. As could be shown above (see page 39), this stands in contrast to the findings of this work where TatB presence was found to be necessary for translocation of $TorA^{SP}$-GFP. To present further evidence for or against a possible bifunctionality, it was tested whether the Tat-components TatA and TatB of *C. glutamicum* could fulfill the clearly defined roles of *E. coli* TatA and TatB.

The following complementation tests were carried out using a simple agar plate assay. Two natural Tat-substrates of *E. coli* are the amidases AmiA and AmiC. These N-acetylmuramoyl-l-alanine amidases are necessary for maintaining cell wall integrity during growth. Ami^- or Tat-pathway deficient *E. coli* cells tend to form long cell-chains and are highly susceptible to strong surfactants (Bernhardt and de Boer, 2003). The addition of 4% SDS to LB-agar plates renders these cells unable to grow and thus presents an easy assay to test for functionality of the Tat-pathway. This assay has been used multiple times for testing the functionality of the Tat pathway (Hicks et al., 2006; Kikuchi et al., 2006; Barnett et al., 2008).

To express the homologous $TatB_{E.c.}$ and the heterologous $TatB_{C.g.}$ and $TatA_{C.g.}$ in *E. coli* Δ*tatB,* three IPTG-inducible expression vectors based on pHSG575 (Takeshita et al., 1987) were constructed, resulting in pHSG_$TatB_{E.c.}$, pHSG_$TatB_{C.g.}$ and pHSG_$TatA_{C.g.}$. Overnight cultures of an *E. coli tatB*-mutant BØD expressing either of these three Tat-components were grown and spotted in dilution series onto LB agar plates containing either no or 4% SDS.

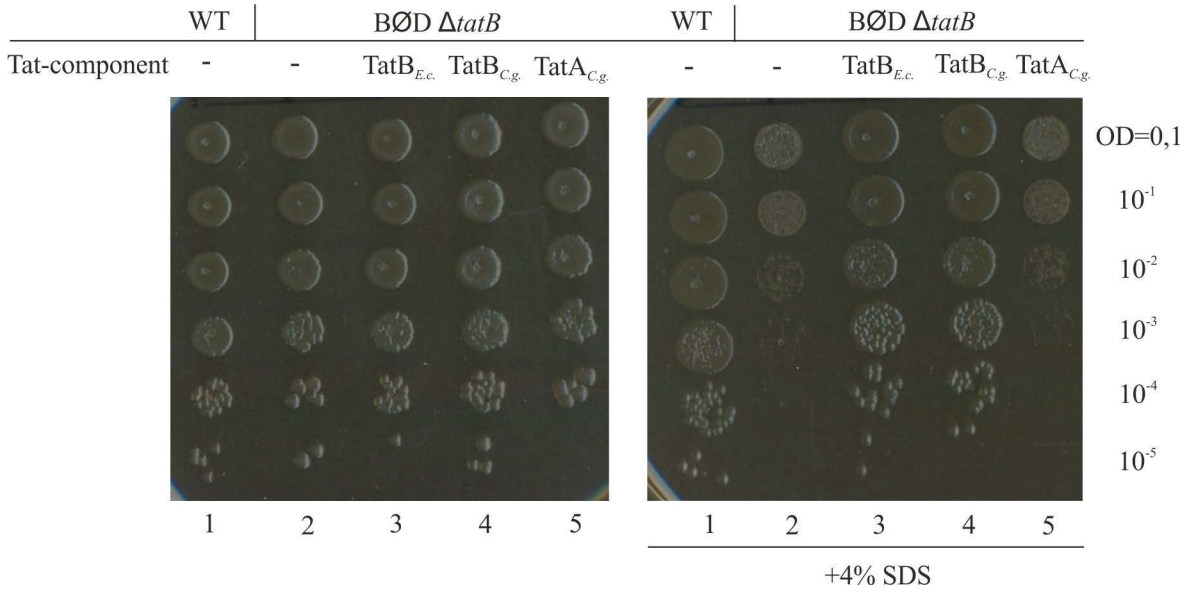

Figure 20: *C. glutamicum* TatB is able to fulfill the role of $TatB_{E.c.}$ in an *E. coli tatB*-mutant. Test for viability on SDS-containing agar plates. Dilution series from OD600nm 0,1 of *E. coli* cells were spotted in a volume of 3 µl on LB-plates containing either no (left) or 4% SDS (right). The agar plates were incubated overnight at 37°C. Lane 1 is the wild-type control MC4100 with empty vector, lane 2 is the *tatB*-mutant BØD with empty vector, lane 3 is BØD expressing $TatB_{E.c.}$, lane 4 is BØD expressing $TatB_{C.g.}$ and lane 5 is BØD expressing $TatA_{C.g.}$.

In the absence of SDS (left plate, figure 20), the three *E. coli* Δ*tatB* strains expressing either homologous $TatB_{E.c.}$, heterologous $TatB_{C.g.}$, or $TatA_{C.g.}$ grow comparable to the positive control wild-type strain MC4100 and the negative control *E. coli* Δ*tatB* with the empty vector. When spotted onto LB agar plates containing 4% SDS (right plate), the growth of wild-type strain MC4100 is unaffected, whereas the *tatB*-mutant *E. coli* BØD carrying the empty vector is unable to grow save a very thin and opaque cell layer at high applied cell density.
Both the complementation with homologous $TatB_{E.c.}$ and heterologous $TatB_{C.g.}$ of the *E. coli tatB*-mutant led to growth comparable to the positive control. In contrast, the *tatB*-mutant strain expressing $TatA_{C.g.}$ is not able to grow. This is a clear indication for $TatB_{C.g.}$ being able to fully substitute for $TatB_{E.c.}$ and thus fulfilling the TatB role in the TatBC-substrate receptor complex. The inability of $TatA_{C.g.}$ to substitute for $TatB_{E.c.}$ shows that *C. glutamicum* TatA cannot fulfill this role. This means that $TatA_{C.g.}$ cannot act together with *E. coli* TatC to form a receptor complex for initial binding of the signal peptide of the substrate. This is evidence for *C. glutamicum* TatA also being responsible for forming the protein conducting channel in *C. glutamicum*, just like in *E. coli*.

3.1.3.1 $TatB_{C.g.}$ is unable to substitute for *E. coli* TatA function

In a next step, it was tested whether $TatB_{C.g.}$ would be able to fulfill the role of *E. coli* TatA. If $TatB_{C.g.}$ is of a bifunctional nature, this might be the case. Next to investigating a possible bifunctionality of $TatB_{C.g.}$, it was tested whether $TatA_{C.g.}$ (which was unable to complement an *E. coli tatB*-mutant, see above) could complement for *E. coli* TatA in a *tatA/E*-mutant strain.
For these complementation experiments, the same assay using SDS-containing LB agar plates was used. For expression of homologous $TatA_{E.c.}$ and heterologous $TatA_{C.g.}$, two IPTG-inducible expression vectors based on pHSG575 were constructed, resulting in pHSG_$TatA_{E.c.}$ and pHSG_$TatA_{C.g.}$. Dilution series of overnight cultures of an *E. coli tatA/E*-mutant strain JARV15 (Sargent et al., 1999) expressing the three Tat-components were spotted on plates containing no or 4% SDS. This experiment was carried out in an *E. coli tatA/E* double mutant strain as it is known that *E. coli tatE* is probably a cryptic gene duplication of *tatA* and TatE can substitute for TatA function although leading to a limited efficiency of the resulting TatEBC translocase (Sargent et al., 1998).
In the absence of SDS (left plate, figure 21) the three *E. coli* Δ*tatA/E* strains expressing either homologous $TatA_{E.c.}$, heterologous $TatA_{C.g.}$ or $TatB_{C.g.}$ grow comparable to the positive control wild-type strain MC4100 and the negative control *E. coli* Δ*tatA/E* with empty vector. When spotted onto LB agar plates containing 4% SDS (right plate), the growth of wild-type strain MC4100 is unaffected whereas the *tatA/E*-mutant *E. coli* JARV15 carrying the empty vector is unable to grow save a very thin and opaque cell layer at high applied cell density.
The homologous complementation of the *E. coli tatA/E*-mutant with $TatA_{E.c.}$ grows comparable to the wild-type control. In contrast, both the expression of $TatA_{C.g.}$ or $TatB_{C.g.}$ does not lead to growth. Under given conditions, neither of these Tat-components can substitute for $TatA_{E.c.}$.
The finding that $TatB_{C.g.}$ is not able to complement an *E. coli tatA/E*-mutant strengthens the theory of *C. glutamicum* TatB not being of a bifunctional nature. The finding that $TatA_{C.g.}$ is not able to complement an *E. coli tatA*-mutant is more surprising. To be able to interpret this result, it had to be checked whether $TatA_{C.g.}$ expression in fact occurs from pHSG_$TatA_{C.g.}$. For this reason, an LB induction culture of *E. coli* JARV 15 (Δ*tatA/E*) cells expressing pHSG_$TatA_{C.g.}$ was grown and, after harvest and cell-lysis, the cytoplasmic/membrane fraction applied to a SDS-gel. The gel was stained with Coomassie brilliant blue. Although a band with the expected theoretical size of $TatA_{C.g.}$ of around 12,0 kDa could not be detected, a single prominent band with an approximate size of 20-25 kDa which was

not present in the negative control with empty vector was seen (data not shown). This band was excised, digested and identified by mass spectrometric analysis. With a coverage of 52% this band was identified as the *E. coli* phage shock protein PspA. It has been shown that elevated levels of *E. coli* TatA lead to an increased production of the membrane stress protein PspA and that these two proteins can be co-purified (Mehner et al., 2012). For this reason, it seems likely that $TatA_{C.g.}$ in fact was expressed and that the expression leads to an activation of the membrane stress response which results in a PspA up-regulation but is not able to build up a functioning translocase together with *E. coli* TatBC. Most likely, *C. glutamicum* TatA is not able to build up a functional translocase in conjunction with *E. coli* TatBC because either the resulting stochiometry of Tat components is faulty or the interaction of $TatA_{C.g.}$ with $TatBC_{E.c.}$ does not work. This finding of course slightly weakens the conclusion that $TatB_{C.g.}$ is not bifunctional because if it was bifunctional after all the complementation of the *E. coli tatA/E* could possibly not take place for the same reason that $TatA_{C.g.}$ does not complement this strain, i.e. false stochiometry or mis-interaction of Tat-components.

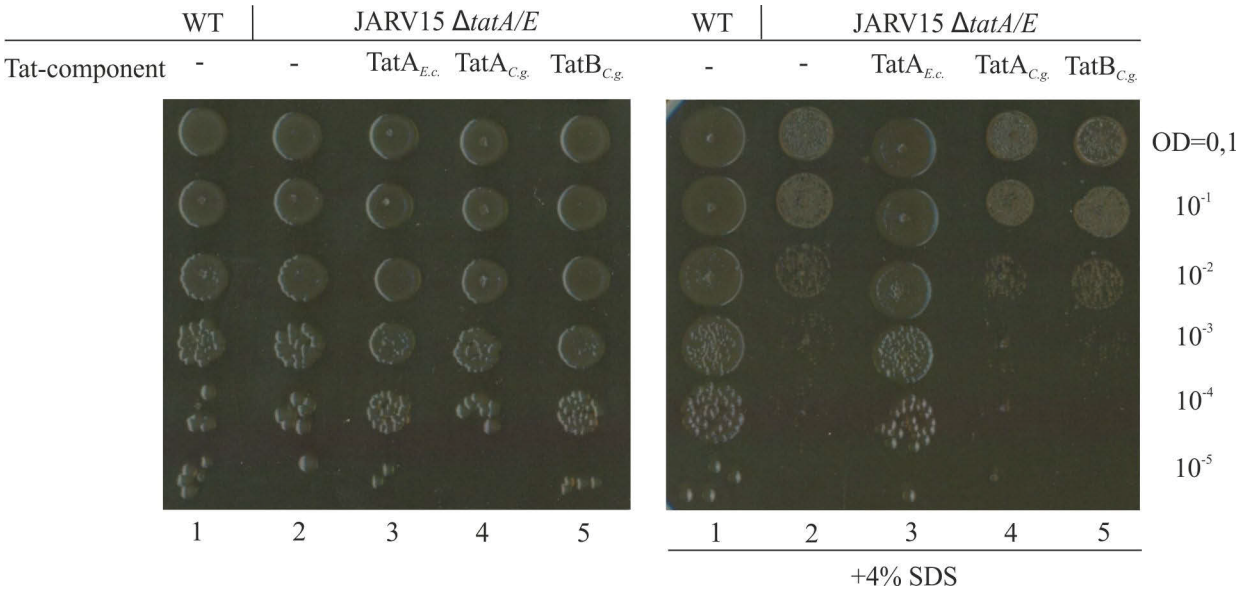

Figure 21: *C. glutamicum* TatB is unable to substitute for *E. coli* TatA function. Test for viability on SDS-containing agar plates. Dilution series from OD600nm 0,1 of *E. coli* cells were spotted in a volume of 3 µl on LB-plates containing either no (left) or 4% SDS (right). The agar plates were incubated overnight at 37°C. Lane 1 is the wild-type control MC4100 with empty vector, lane 2 is the *tatA/E*-mutant JARV15 with empty vector, lane 3 is JARV15 expressing $TatA_{E.c.}$, lane 4 is JARV15 expressing $TatA_{C.g.}$ and lane 5 is JARV15 expressing $TatB_{C.g.}$.

3.1.4 Conclusion I: *C. glutamicum* possesses an ABC-type Tat-translocase

In summary, it can be stated that all presented evidence demonstrates that *Corynebacterium glutamicum* utilizes a Tat-translocase that is composed of the components TatA, TatB and TatC. All three components are necessary for translocation of the artificial model substrates $TorA^{SP}$-GFP and $PhoD_{C.g.}{}^{SP}$-GFP. Furthermore, all three components are necessary for the membrane integration of the physiologically important iron-sulfur cluster containing Rieske protein QcrA which could be shown to be translocated in a Tat-dependent manner. The genomic deletion of any of the *tat*-genes results in a heavily impaired growth phenotype caused by a defective respiratory chain because of a mislocalized Rieske protein QcrA.

Furthermore, it could be demonstrated that the presence of *C. glutamicum* TatB is not only essential for functionality of the translocase, which stands in contrast to what the results of Kikuchi et al. (2006) suggest, but also that $TatB_{C.g.}$ is able to fully substitute for the missing TatB-function in an *E. coli tatB*-mutant, but not for the missing TatA-function in an *E. coli tatA/E*-mutant. This ability of $TatB_{C.g.}$ to form a receptor complex together with *E. coli* TatC indicates that *C. glutamicum,* as a prototypical representative for the class of *Actinobacteria,* utilizes a Tat-translocase more closely related to the one of Gram-negative bacteria and plant chloroplasts than to the TatAC-type translocase of the majority of low-G/C Gram-positive bacteria.

3.2. The effect of TorD coexpression

The following work is based on an effect observed by Henrieke Brundiek in the course of her doctoral studies (Brundiek, 2008). With the aim of improving the quality and quantity of secreted heterologous proteins in *Corynebacterium glutamicum,* the intracellular *E. coli* REMP (redox enzyme maturation protein) TorD was coexpressed together with $TorA^{SP}$-GFP as substrate. TorD participates in the maturation of the trimethylamine-N-oxide reductase TorA from *E. coli* and is specific for the TorA signal peptide (Pommier et al., 1998). The coexpression of the chaperone TorD together with $TorA^{SP}$-GFP in *E. coli* has been suggested to lead to an at least three-fold improved export of the substrate (Li et al., 2006).
Surprisingly, the coexpression of TorD and $TorA^{SP}$-GFP in *C. glutamicum* did not lead to an enhanced export but rather to a complete block of the export of $TorA^{SP}$-GFP. This resulted in the theory that possibly the intracellular event of release of the TorA signal peptide from the chaperone TorD is not taking place due to a missing interaction between the homologous *C. glutamicum* Tat-translocase and the heterologous *E. coli* chaperone TorD.
Trying to identify the Tat-component responsible for this effect, H. Brundiek tried several approaches but the only circumstance in which this export block could be reversed to some degree was when the *E. coli* Tat translocase TatABC was additionally expressed together with TorD and $TorA^{SP}$-GFP in the *C. glutamicum* wild-type strain (for more details see page 13ff. and Brundiek, 2008). Neither coexpression of *E.coli* TatC nor *E. coli* TatAC alone cancelled the export block.
Since "mix-translocases", referring to Tat-translocases which are composed of a mixture of homologous and heterologous translocase components, are problematic in *C. glutamicum* (Brundiek, 2008), it was considered advantageous to shift the situation to a clean genomic background for this work. Especially the simultaneous presence of two TatB species (in *C. glutamicum:* homologous $TatB_{C.g.}$ and heterologous $TatB_{E.c.}$) could be critical for functional Tat-dependent transport (for more details also see page 13ff. and Brundiek, 2008).

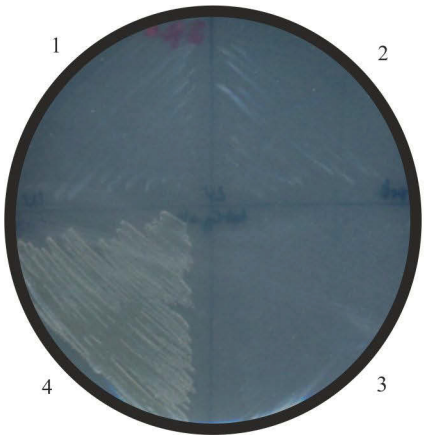

		pBBR	pTrc	pMMB	growth on MM
1	DADE Δ*tat* Δ*malE*	TorA^{SP}-MalE	-	-	-
2			-	TorD	-
3			*C. glutamicum* TatACBE ΔIG	TorD	-
4				-	+

Figure 22: The additional expression of TorD in an *E. coli tatACBE*-mutant DADE complemented with a modified *C. glutamicum* Tat translocase TatACBE ΔIG results in an export block of TorA^{SP}-MalE. Screening for MalE export on maltose minimal medium agar plates incubated at 37ºC for ~72 hours. (- no growth + growth)

First, a modified *C. glutamicum* Tat-translocase operon TatACBE ΔIG was constructed in which the intergenic region between TatA and TatC has been deleted. When expressed in *E. coli* DADE (*tat*$^-$) from the IPTG-inducible expression vector pTrc99A (Amann et al., 1988), this translocase complemented for Tat-dependent translocation. *E. coli* DADE transformed with a plasmid encoding the substrate TorA^{SP}-MalE, the periplasmic *E. coli* maltose binding protein fused to the aforementioned TorA signal peptide and a plasmid encoding the *C. glutamicum* Tat-translocase TatACBE ΔIG led to growth on minimal medium containing maltose as the sole carbon source, albeit only after ~72 hours of incubation at 37ºC. An additional expression of TorD from the expression vector pMMB again led to an export block of the TorA substrate TorA^{SP}-MalE resulting in no growth on maltose minimal medium (see figure 22).
As the expression of *C. glutamicum* TatACBE ΔIG resulted in a very slow growth phenotype when expressed in *E. coli* DADE (*tat*$^-$), the focus was shifted from whole translocase expression to single Tat components. Also, the results of H. Brundiek had suggested that the presence of *E. coli* TatB could stand in relation to the reversion of the TorD-induced export block of TorA^{SP}-GFP in *C. glutamicum*. Under all conditions where a TorD-induced export block had been observed, the homologous TatB$_{C.g.}$ had been present and cancelation of the export block only took place when heterologous TatB$_{E.c.}$ was present. For this reason, it was decided to investigate the effect of TorD coexpression in the *E. coli tatB*-mutant strain BØD in more detail which was already shown to be complementable with either homologous TatB$_{E.c.}$ or heterologous TatB$_{C.g.}$ (see page 48).

3.2.1 Coexpression of TorD in complemented *E. coli* Δ*tatB* leads to an export block

Coexpression of TorD in *E. coli* was carried out in a three vector system. One for the substrate to be exported based on pBBR1MCS2 (Kovach et al., 1995), one for the Tat-component based on pHSG575 (Takeshita et al., 1987) and TorD on pTrSp. The vector pTrSp was newly constructed for this work and is based on the backbone of pTrc99A (Amann et al., 1988) out of which the ampicillin resistance gene was excised using *BspHI*. Next, the spectinmoycin resistance gene of pEKEx3 (Hoffelder et al., 2010) was PCR-amplified and ligated into the *BspHI* site in pTrc99A resulting in pTrSp.

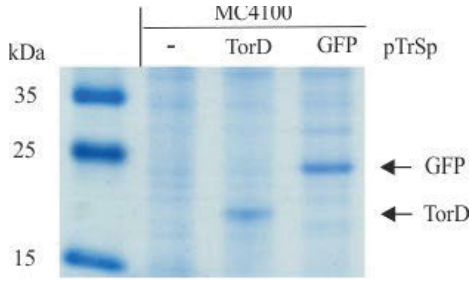

Figure 23: Coomassie-stained SDS-gel of whole cell protein fraction of *E. coli* MC4100 induction cultures containing pTrSp empty vector , pTrSp_TorD and pTrSp_GFP. A protein amount equal to an OD_{600} of 0,5 was applied to SDS-PAGE.

The *torD* gene was amplified using PCR and cloned into pTrSp under the control of an IPTG-inducible promoter. To account for the additional overexpression of a third *in trans* product, a control vector based on pTrSp was constructed. On this vector the gene for GFP (26,9 kDa) was cloned which is similar in size to TorD (22,6 kDa). Strains transformed with this vector are of green color at visible light and fluoresce upon UV-exposure. To check for expression of TorD and GFP from pTrSp, *E. coli* MC4100 was transformed with these two vectors, a four hour induction culture was grown, the cells disrupted and the whole cell fraction applied to SDS-PAGE. The Coomassie-blue stained gel can be seen in figure 23. Both TorD and GFP are expressed in substantial and comparable amounts.

3.2.1.1 The export of $TorA^{SP}$-Bla can be blocked by TorD

The results of Brundiek (2008) pointed towards a possible involvement of the nature of TatB in the observed TorD-induced export block of $TorA^{SP}$-GFP. For this reason, TorD coexpression was carried out in an *E. coli tatB*-mutant strain complemented with either $TatB_{E.c.}$ or $TatB_{C.g.}$. The first substrate tested was $TorA^{SP}$-Bla. This substrate has been shown to be usable as a selection system for functional Tat-dependent translocation as only cells exporting the β-lactamase into the periplasm are able to grow on ampicillin-containing solid growth media (Fisher et al., 2006). For this purpose, the *E. coli* β-lactamase TEM1 fused to the TorA signal peptide was transferred from pTMB (Fisher et al., 2006) to the IPTG-inducible pBBR expression vector (unpublished results, F. Lausberg).
E. coli strain BØD (Δ*tatB*) was transformed with the three vectors pBBR_TorA-Bla for expression of the substrate, pHSG_$TatB_{E.c.}$ or pHSG_$TatB_{C.g.}$ for expression of $TatB_{E.c.}$ and $TatB_{C.g.}$ respectively and pTrSp_TorD or pTrSP_GFP for expression of either TorD or GFP. The *E. coli* wild-type strain MC4100 was transformed with the three vectors expressing the substrate pBBR_TorA-Bla, the pHSG empty vector and either pTrSp_TorD or pTrSp_GFP. The resulting strains were cultivated overnight in complex medium and then spotted in dilution series on LB agar plates containing either no or 100 µg/ml ampicillin.
Figure 24 shows the LB agar plates with cells expressing the Tat-dependent substrate $TorA^{SP}$-Bla. As can be seen in the top part of the figure, all strains grow comparable in the absence of ampicillin. Also, in the respective strains expressing GFP from pTrSp the distinct green color of the colonies can be seen. When the plates contain 100µg/ml ampicillin, only cells exporting sufficient amounts of β-lactamase are able to grow. In the absence of TorD, the wild-type strain MC4100 (lane 3) and the *tatB*-mutant strain BØD complemented with homologous $TatB_{E.c.}$ (lane 7) and $TatB_{C.g.}$ (lane 10) are unaffected by the presence of ampicillin, indicative of good export of $TorA^{SP}$-Bla. The *tatB*-mutant strain expressing

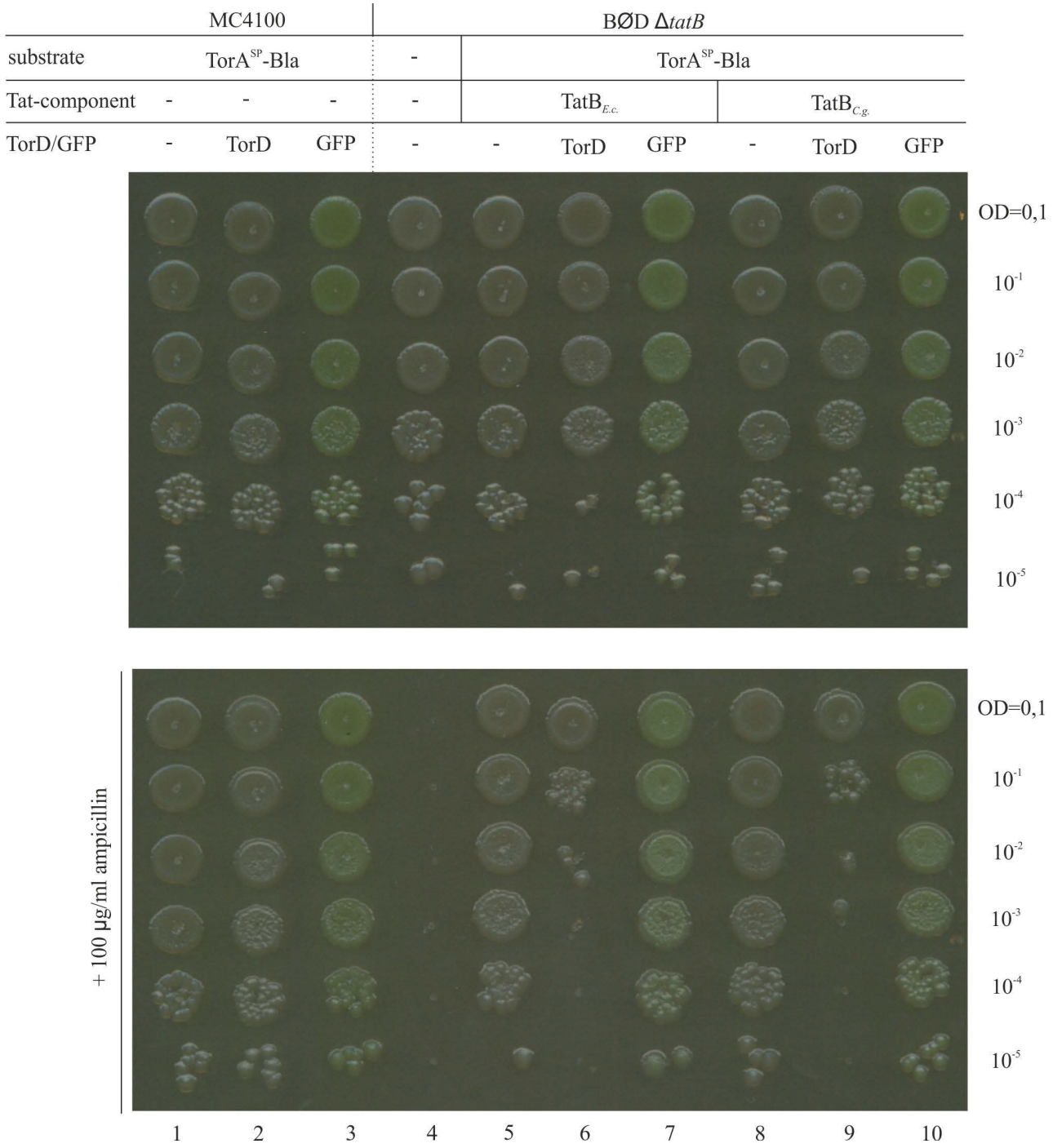

Figure 24: The export of TorA^{SP}-Bla is blocked in presence of TorD in an *E. coli tatB*-mutant complemented with either TatB$_{E.c.}$ or TatB$_{C.g.}$. Only cells expressing and translocating the substrate TorA^{SP}-Bla are able to grow on ampicillin-containing plates (bottom). The cells were grown overnight, spotted in dilution series on both LB agar plates without (top) and with 100 µg/ml ampicillin (bottom) and cultivated overnight at 37ºC. *E. coli* wild-type strain MC4100 (lanes 1-3) and *tatB*-mutant strain BØD (lanes 4-10) are transformed with the three plasmids pBBR, PHSG and pTrSp according to the top of the figure.

neither the substrate TorA^{SP}-Bla nor a TatB component (lane 4) is unable to grow.
In presence of TorD, the wild-type strain (lane 2) grows comparable to the situation without TorD (lane 3). In contrast, both *tatB*-mutant strains complemented with TatB$_{E.c.}$ (lane 6) or TatB$_{C.g.}$ (lane 9) show significantly reduced growth in the presence of TorD. From comparing several experiments it

seems that the heterologously complemented strain grows slightly less well than the strain complemented with $TatB_{E.c.}$. This indicates that upon presence of TorD the export of the β-lactamase in these two strains is either blocked completely or reduced to a very low level

In a next step, the export of $TorA^{SP}$-Bla was examined on protein level. For this purpose, EDTA lysozyme spheroblasts of *E. coli* cells were made. This method - a cold osmotic shock - allows, through lysozyme-treatment of the bacterial cell wall, to access the content of the periplasm and thus fractionate the cells into a periplasmic and a combined cytoplasmic/membrane fraction. These fractions are then subjected to SDS-PAGE, Western blotted and then incubated with the desired antibody. Due to the nature of the method a limited amount of cell lysis is inevitable. For this reason, an identical set of Western blots of the two fractions is always assayed in parallel with an antibody against an intracellular protein (in this work, either α-TalB or α-GroEL were used). The occurred lysis, i.e. the amount of intracellular protein in the periplasmic fraction, always has to be taken into consideration when interpreting these fractionation experiments.

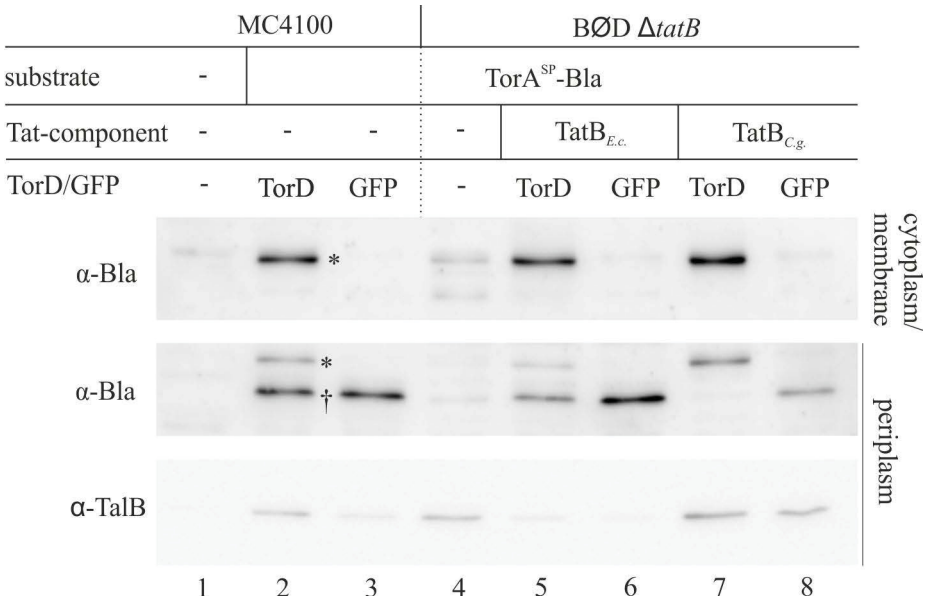

Figure 25: TorD coexpression in an *E. coli tatB*-mutant complemented with $TatB_{C.g.}$ leads to a complete block of $TorA^{SP}$-Bla export. EDTA-lysozyme spheroblasts of *E. coli* cells expressing $TorA^{SP}$-Bla for the preparation of periplasmic and cytoplasmic/membrane fractions. Isolated fractions were subjected to SDS-PAGE and subsequently Western blotted. The top Western blot depicts the cytoplasm/membrane fractions, the two lower blots the periplasmic fractions. The top and middle blots were incubated with an antibody against TEM1 beta-lactamase and the bottom blot with an antibody against TalB (to evaluate cell lysis occurring during the preparation). Lanes 1 to 3 show the wild-type strain *E. coli* MC4100 and lanes 4 to 8 the *tatB*-mutant BØD. All strains have been transformed with three plasmids as indicated at the top of the figure. Of the cytoplasmic/membrane fractions 10 µg and of the periplasmic fraction 2 µg of protein were applied to the SDS-gel. The asterisk (*) denotes the precursor $TorA^{SP}$-Bla and the obelisk (†) the mature Bla.

The fractionation of *E. coli* cells expressing $TorA^{SP}$-Bla is shown in figure 25. The top blot shows the cytoplasmic/membrane fraction, the middle blot the exported periplasmic fraction and the bottom blot is the lysis control of the periplasmic fraction developed with an antibody against (intracellular) *E. coli* transaldolase TalB.

In absence of TorD, the wild-type strain MC4100 (lane 3) shows good export of $TorA^{SP}$-Bla into the periplasm (middle pane). The *tatB*-mutant strain BØD not expressing a TatB molecule shows no ex-

port of Bla (lane 4). When complemented with homologous $TatB_{E.c.}$, the *tatB*-mutant strain shows good export (lane 6), even slightly more than the wild-type strain. The *tatB*-mutant strain complemented with heterologous $TatB_{C.g.}$ (lane 8) shows a somewhat reduced export in comparison to the aforementioned strain, indicating that a $TatB_{C.g.}$-containing translocase is not quite as efficient as the endogenous one in translocating $TorA^{SP}$-Bla.
In presence of TorD, the wild-type strain shows about the same amount of exported Bla (lane 2) as without TorD. Additionally, a significant accumulation of precursor $TorA^{SP}$-Bla is found within the cytoplasm/ membrane fraction and a smaller amount of precursor is found in the periplasm. In the *tatB*-mutant strain complemented with homologous $TatB_{E.c.}$ a strong reduction of exported Bla in the periplasmic fraction is found when TorD is coexpressed (lane 5). Also here, an accumulation of precursor $TorA^{SP}$-Bla in the cytoplasm/ membrane fraction takes place and a small amount of precursor is found in the periplasmic fraction. In the *tatB*-mutant strain complemented with heterologous $TatB_{C.g.}$ the presence of TorD leads to complete block of the export of $TorA^{SP}$-Bla into the periplasm (lane 7) but also to an accumulation of precursor in the cytoplasm/ membrane fraction as well as some precursor in the periplasm.
The accumulation of precursor $TorA^{SP}$-Bla within the cytoplasm, which is found in every strain upon expression of TorD, is presumably due to an intracellular protection of the substrate by TorD from proteolysis. The presence of precursor $TorA^{SP}$-Bla in the periplasmic fractions of strains expressing TorD (lanes 2, 5 and 7) is probably due to light lysis which occured during the fractionation of the cells. To evaluate this hard to avoid experimental flaw, the blot of the periplasmic fraction was always also developed with an antibody against an intracellular protein (in this case α-TalB). Regarding the strength of the TalB signal (bottom panel) reveals that a correlation between the amount of TalB and precursor $TorA^{SP}$-Bla in the periplasm exists.
Regarding the test for $TorA^{SP}$-Bla export in the plate assay (figure 24) in comparison to the EDTA-lysozyme spheroblast formation (figure 25), the behavior of the cells on ampicillin containing LB agar plates might seem contradictory to the amounts of exported Bla found in the periplasmic fractions of the fractionation experiment. The *tatB*-mutant complemented with homologous $TatB_{E.c.}$ shows more exported Bla in presence of TorD than the $TatB_{C.g.}$-complemented *tatB*-mutant in absence of TorD. Nonetheless, these two differently complemented strains only show growth restrictions on ampicillin in presence of TorD. A direct correlation between the plate assay and the fractionation experiment is therefore not possible. This is probably due to the different growth conditions of the strains on LB agar plates and the much faster growing cells in a liquid medium induction culture.

3.2.1.2 The export of $TorA^{SP}$-MalE can be blocked by TorD

The second $TorA^{SP}$ substrate tested for export in presence of TorD was $TorA^{SP}$-MalE. $TorA^{SP}$-MalE is the maltose binding protein of *E. coli* wherein the native Sec dependent signal peptide has been exchanged for the Tat-specific TorA signal peptide. This substrate allows for an effective plate assay for functional Tat-dependent translocation by screening for cells able to grow on minimal medium containing maltose as the only carbon source. The export of MalE into the bacterial periplasm is crucial for the cells to be able to bind the maltose in the periplasm which is then imported and metabolized. This assay is strictly Tat-pathway specific and has previously been used to screen for bifunctional TatA muteins and for genetic substrate-Tat-translocase interaction studies (Blaudeck et al., 2003; Blaudeck et al., 2005; Lausberg et al., 2012).
The substrate vector used in these experiments was pBBR_TorA-MalE (Blaudeck et al., 2003). As before, the $TatB_{E.c.}$ and $TatB_{C.g.}$ molecules were expressed from pHSG_$TatB_{E.c.}$ and pHSG_$TatB_{C.g.}$ re-

spectively. TorD and GFP were expressed from pTrSp_TorD and pTrSp_GFP respectively. The transformed strains were grown overnight in LB-medium, diluted and then streaked onto maltose minimal medium agar plates.

Due to the presence of a genomically encoded Sec-dependently exported copy of MalE, the *malE* gene in *E. coli* BØD had to be deleted prior to these experiments using the suicide vector pKO3. The *malE* gene in *E. coli* MC4100 has previously been deleted (Blaudeck et al., 2003). Figure 26 shows a minimal medium agar plate assay with maltose as sole carbon source for the screening of *E. coli* wild-type MC4100 (*malE*$^-$) and *E. coli tatB*-mutant BØD (*malE*$^-$) strains expressing and translocating the maltose binding protein MalE fused to the TorA signal peptide (TorA^{SP}-MalE). Export of the maltose binding protein into the periplasm is paramount for the strains to be able to access the maltose and grow. The wild-type strain cannot grow when transformed with the pBBR empty vector thus not expressing the substrate (1). Growth of the wild-type in presence or absence of TorD (2,3) is comparably good. The *E. coli tatB*-mutant strain BØD not expressing a TatB molecule (4) is unable to grow on maltose minimal medium. The *tatB*-mutant complemented with homologous $TatB_{E.c.}$ shows growth comparable to the wild-type strain in absence of TorD (6), but in presence of TorD (5) grows only very slowly and not to the density of the wild-type cell layer. The *tatB*-mutant complemented with $TatB_{C.g.}$ also grows well in absence of (8), but shows no growth in the presence of TorD (7). The overall picture of blocked export in the two complemented *tatB*-mutants expressing TorA^{SP}-MalE is thus comparable to the strains expressing TorA^{SP}-Bla on LB plates containing ampicillin (see page 54).

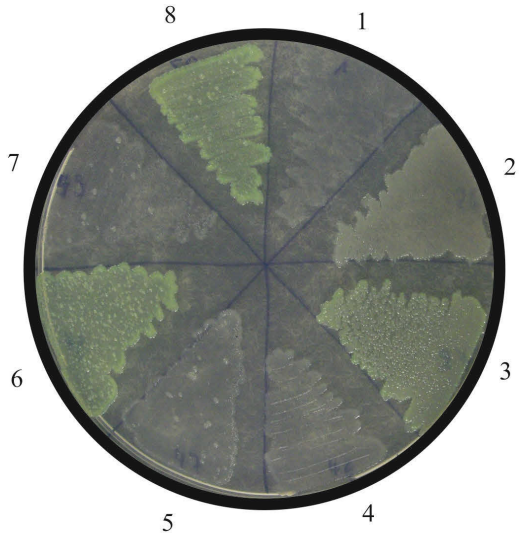

		pBBR	pHSG	pTrSp	growth on MM
1	MC4100 WT Δ*malE*	-	-	-	-
2	TorA-MalE		-	TorD	++
3			-	GFP	++
4	BØD Δ*tatB* Δ*malE*	TorA-MalE	-	-	-
5			$TatB_{E.c.}$	TorD	+
6				GFP	++
7			$TatB_{C.g.}$	TorD	-
8				GFP	++

Figure 26: In presence of TorD, the export of TorA^{SP}-MalE is blocked in an *E. coli tatB*-mutant complemented with $TatB_{C.g.}$ and strongly reduced when complemented with $TatB_{E.c.}$. Screening on maltose minimal medium agar plates. The strains were transformed according to the table in the figure, grown overnight in LB-medium, diluted to an OD=0,1 and subsequently streaked onto maltose minimal medium agar plates. Incubation occured at 37ºC for ~48 hours (++ wild-type growth, + limited growth, - no growth).

By EDTA-lysozyme spheroblast formation, the above strains expressing TorA^{SP}-MalE were probed for actually exported amounts of MalE. As with TorA^{SP}-Bla, the transformed strains were cultivated in a four hour induction culture and then separated into a combined cytoplasm/membrane and a periplas-

mic fraction.

Figure 27 shows the fractionation experiment of *E. coli* wild-type strain MC4100 (*malE*$^{-}$) and the *tatB*-mutant strain BØD (*malE*$^{-}$) expressing TorA^{SP}-MalE.

In absence of TorD, the wild-type strain *E. coli* MC4100 shows good export of TorA^{SP}-MalE into the periplasm and hardly any precursor in the cytoplasm/ membrane fraction (lane 3). The *tatB*-mutant strain BØD not expressing a TatB molecule is unable to export TorA^{SP}-MalE (lane 4). The small amount of MalE within the periplasm is due to lysis which occured during the fractionation experiment. The *tatB*-mutant strain expressing homologous TatB$_{E.c.}$ shows very good export of TorA^{SP}-MalE into the periplasm (lane 6), roughly twice as much as the wild-type strain. Also, a limited amount of mature MalE is found within the cytoplasm/ membrane fraction, probably due to intracellular cleavage of the signal peptide from TorA^{SP}-MalE. The *tatB*-mutant strain complemented with heterologous TatB$_{C.g.}$ also shows good export of TorA^{SP}-MalE into the periplasm in absence of TorD (lane 8), the amount is comparable to that of the wild-type strain. Also, a limited amount of MalE with cleaved signal peptide is found in the cytoplasm/ membrane fraction.

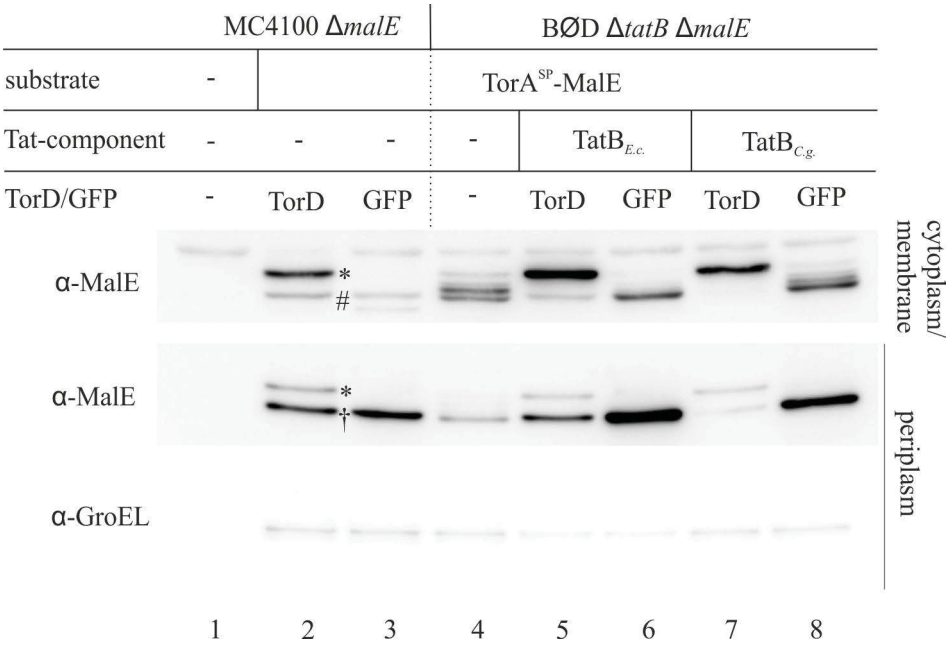

Figure 27: The coexpression of TorD leads to blocked export of TorA^{SP}-MalE when an *E. coli tatB*-mutant is complemented with TatB$_{C.g.}$ and to reduced export when complemented with TatB$_{E.c.}$. EDTA-lysozyme spheroblasts of *E. coli* cells expressing TorA^{SP}-MalE for the preparation of periplasmic and cytoplasmic/membrane fractions. Isolated fractions were subjected to SDS-PAGE and subsequently Western blotted. The top Western blot depicts the cytoplasm/ membrane fractions, the middle and bottom blots the periplasmic fractions. The two upper blots were incubated with an antibody against the maltose binding protein MalE and the bottom blot with an antibody against GroEL (to evaluate cell lysis occurring during the preparation). Lanes 1 to 3 show the wild-type strain MC4100 Δ*malE* and lanes 4 to 8 the *tatB*-mutant BØD ΔmalE. All strains have been transformed with three plasmids as indicated at the top of the figure. Of the cytoplasmic/membrane fraction 10 µg and of the periplasmic fraction 2 µg of protein were applied to SDS-PAGE. The asterisk (*) denotes the precursor TorA^{SP}-MalE, the obelisk (†) the mature MalE and the hash (#) a degradation product of TorA^{SP}-MalE.

In presence of TorD (lane 2), the amount of mature MalE found in the periplasmic fraction of the wild-type strain is slightly reduced in comparison to without TorD (lane 3). Furthermore, a significant accumulation TorA^{SP}-MalE precursor is found in the cytoplasm/ membrane fraction as well as a small

amount of TorA^{SP}-MalE precursor in the periplasmic fraction. Upon coexpression of TorD, the *tatB*-mutant strain complemented with TatB$_{E.c.}$ has a strongly reduced amount of mature MalE in the periplasm (lane 5). Also, a strong accumulation of precursor TorA^{SP}-MalE takes place in the cytoplasm/ membrane fraction and a small amount of TorA^{SP}-MalE is found within the periplasm. The export of TorA^{SP}-MalE into the periplasm is blocked completely in the *tatB*-mutant strain complemented with TatB$_{C.g.}$ when TorD is present (lane 8). Again, an accumulation of TorA^{SP}-MalE precursor is found in the cytoplasm/ membrane fraction.
Like with TorA^{SP}-Bla (see page 54ff.), TorD coexpression leads to an intracellular accumulation of TorA^{SP}-MalE precursor, pointing towards the role TorD plays in protecting its TorA^{SP}-substrate from proteolysis. Also, very small amounts of TorA^{SP}-MalE precursor are found in the periplasmic fractions of some strains which is due to light lysis which occured during the fractionation experiment.
Comparing the results of the growth phenotypes of these strains on maltose minimal medium with the obtained protein data by fractionation, a correlation regarding the export block can be seen. Surprising however is the comparibly poor growth on maltose minimal medium of the *tatB*-mutant complemented with TatB$_{E.c.}$ in presence of TorD (figure 26) when regarding the amount of MalE translocated into the periplasm (lane 5, figure 27). This is approximately half of the exported amount of TorA^{SP}-MalE of the wild-type coexpressing TorD.

3.2.1.3 The export of TorA^{SP}-GFP can be blocked by TorD

The third TorA^{SP} substrate tested for export in presence of TorD was TorA^{SP}-GFP. Apart from investigating the presence of an export block of TorA^{SP}-GFP in presence of TatB$_{C.g.}$ and TorD it was also to be verified whether the export enhancing effect of TorD as reported by Li et al., 2006 could be reproduced in the wild-type strain *E. coli* MC4100. The gene for the green fluorescent protein GFP from the jellyfish *Aequrorea victoria* (Shimomura et al., 1962; Heim et al., 1995) was fused to the sequence of the TorA signal peptide resulting in pBBR_TorA-GFP (unpublished, F. Lausberg). The expression of the TatB variants again occured from the expression vectors pHSG_TatB$_{E.c.}$ and pHSG_TatB$_{C.g.}$. The expression of TorD was from pTrSp_TorD. Other than before, instead of using pTrSp_GFP as expression control, the empty vector pTrSp was transformed to avoid GFP being expressed twice from two plasmids.
To visualize the expressed and translocated amounts of TorA^{SP}-GFP, fractionation of the *E. coli s*trains by EDTA-lysozyme spheroblastation was carried out. These can be seen in figure 28. In absence of TorD, the wild-type strain MC4100 shows good export of TorA^{SP}-GFP into the periplasm (lane2). The *tatB*-mutant strain BØD not expressing a TatB molecule is unable to export TorA^{SP}-GFP (lane 4). The *tatB*-mutant strain complemented with homologous TatB$_{E.c.}$ (lane 5) shows even better export than the wild-type strain, approximately twice as much. The *tatB*-mutant strain complemented with heterologous TatB$_{C.g.}$ also shows good export of TorA^{SP}-GFP into the periplasm in absence of TorD (lane 7), even slightly more than the wild-type strain.
In presence of TorD, the wild-type strain has a reduced amount of GFP in the periplasmic fraction (lane 3). Again, in the cytoplasmic/ membrane fraction an accumulation of TorA^{SP}-GFP precursor is found as well as some precursor in the periplasmic fraction. The *tatB*-mutant strain complemented with TatB$_{E.c.}$ also shows a drastically reduced amount of mature GFP in the periplasmic fraction and an accumulation of TorA^{SP}-GFP precursor in the cytoplasm/ membrane fraction (lane 6). The export of TorA^{SP}-MalE into the periplasm of the *tatB*-mutant strain complemented with TatB$_{C.g.}$ is again completely blocked in presence of TorD (lane 8). Also, a significant accumulation of TorA^{SP}-GFP precursor is found in the cytoplasm/ membrane fraction.

The TorD-induced export block of TorA^{SP}-GFP in an *E. coli tatB*-mutant complemented with TatB$_{C.g.}$ is comparable with the block of TorA^{SP}-Bla and TorA^{SP}-MalE. Surprisingly, the reported three-fold increase of TorA^{SP}-GFP export in the *E. coli* wild-type strain upon coexpression of TorD (Li et al., 2006) could not be reproduced. In the contrary, under given circumstances the presence of TorD in the wild-type strain led to reduced amounts of GFP in the periplasm and a significant accumulation of the precursor in the cytosol.

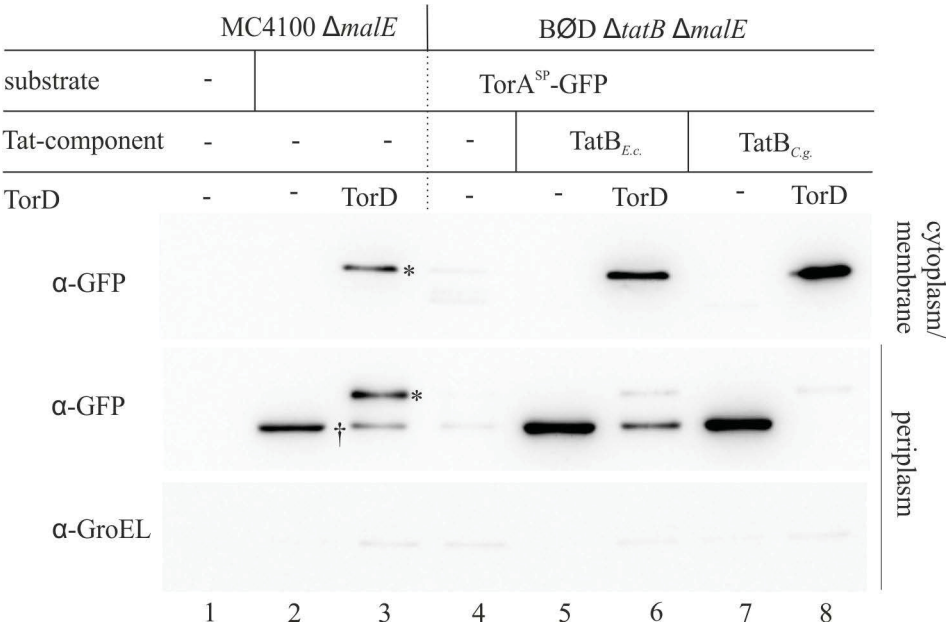

Figure 28: The coexpression of TorD leads to blocked export of TorA^{SP}-GFP when an *E. coli tatB*-mutant is complemented with TatB$_{C.g.}$ and to reduced export when complemented with TatB$_{E.c.}$. EDTA-lysozyme spheroblasts of *E. coli* cells expressing TorA^{SP}-GFP for the preparation of periplasmic and cytoplasmic/membrane fractions. Isolated fractions were subjected to SDS-PAGE and subsequently Western blotted. The top Western blot depicts the cytoplasmi/ membrane fractions, the middle and bottom blots the periplasmic fractions. The two upper blots were incubated with an antibody against GFP and the bottom blot with an antibody against GroEL (to evaluate cell lysis occurring during the preparation). Lanes 1 to 3 show the wild-type strain *E. coli* MC4100 and lanes 4 to 8 the *tatB*-mutant strain BØD. All strains have been transformed with three plasmids as indicated at the top of the figure. Of the cytoplasmic/membrane fraction 10 µg and of the periplasmic fraction 2 µg of protein were applied to SDS-PAGE. The asterisk (*) denotes the precursor TorA^{SP}-GFP and the obelisk (†) the mature GFP.

In summary, the complementation of an *E. coli tatB*-mutant with *C. glutamicum* TatB results in good export of TorA^{SP}-MalE and TorA^{SP}-GFP as well as mediocre export of TorA^{SP}-Bla. In the case of TorA^{SP}-Bla and TorA^{SP}-MalE the amount of exported β-lactamase and maltose binding protein is sufficient for growth on ampicillin-containing LB plates and maltose-minimal medium plates, respectively. Coexpression of TorD in an *E. coli tatB*-mutant strain complemented with TatB$_{C.g.}$ leads to a complete block of the export of TorA^{SP}-Bla, TorA^{SP}-MalE and TorA^{SP}-GFP. This also leads to the inability of TorA^{SP}-Bla expressing strains to grow on ampicillin containing media as well as TorA^{SP}-MalE expressing strains to grow on maltose minimal medium agar plates.
The homologous complementation of an *E. coli tatB*-mutant strain with TatB$_{E.c.}$ also leads to good export of all tested TorA^{SP}-substrates, resulting in even slightly higher amounts of exported protein than the wild-type control strain. The coexpression of TorD had a surprising effect. Even though the effect

was not as strongly pronounced as in the *tatB*-mutant strain complemented with $TatB_{C.g.}$, a significant reduction in the amount of exported $TorA^{SP}$-Bla, $TorA^{SP}$-MalE and $TorA^{SP}$-GFP could be seen on protein level. The reduction in the amount of exported $TorA^{SP}$-Bla and $TorA^{SP}$-MalE manifested itself in the inability of these cells to grow on the respective selection media.
Noticeable was the amount of protected precursor within the cytoplasm in all strains expressing TorD. This clearly shows how efficiently the chaperone TorD binds to to the TorA signal peptide of the substrates tested and protects them from intracellular proteolysis. The hypothesis of an interaction between the Tat-translocase and the $TorA^{SP}$-substrate/ TorD complex to take place in order to release TorD from the substrate remains open. Clearly, the *tatB*-mutant strains harboring a $TatB_{C.g.}$-containing Tat-translocase show a complete export block of $TorA^{SP}$-substrates, indicating that *C. glutamicum* TatB presence in the translocase could pose a problem for this proposed interaction. On the other hand, the fact that TorD coexpression also shows an effect in a *tatB*-mutant strain expressing homologous $TatB_{E.c.}$ from a plasmid *in trans* indicates that a further circumstance, different from the nature of the TatB protein, could influence TorD release from its substrate.

3.2.2 Crosslinking of $TorD^{Strep}$ to its artificial substrate $TorA^{SP}$-MalE

The above experiments strongly suggest that an interaction between the *E. coli* chaperone TorD and the artificial substrates $TorA^{SP}$-Bla, $TorA^{SP}$-MalE and $TorA^{SP}$-GFP takes place, leading to reduced or completely blocked export in an *E. coli tatB*-mutant complemented with $TatB_{E.c.}$ or $TatB_{C.g.}$ respectively. This is most evident by the accumulation of varying amounts of protected precursor proteins which are located within the cytoplasm (figures 25, 27 and 28), when TorD is expressed in the different strains.
To directly prove this interaction, crosslinking studies were carried out. Firstly, a purifiable variant of TorD, $TorD^{Strep}$ with a C-terminal *Strep*-tag II, was constructed. The *Strep*-tag II was chosen for its gentle elution conditions from streptavidin to protect fragile protein-protein interactions (Schmidt and Skerra, 2007). *E. coli* MC4100 was transformed with the IPTG-inducible expression vector pTr-Sp_$TorD^{Strep}$. The strain was cultivated in a four-hour induction culture, the cells lysed and the whole cell protein fraction applied to SDS-PAGE and Western blotted. $TorD^{Strep}$ could be detected in the whole cell fraction using a *Strep*-Tactin alkaline phosphatase conjugate (data not shown). Next, it was verified that the addition of the tag to TorD had not altered the above described effect on $TorA^{SP}$-MalE export in the *E. coli* wild-type strain MC4100 and the with $TatB_{E.c.}$ or $TatB_{C.g.}$ complemented *tatB*-mutant strain BØD, which was not the case (data not shown).

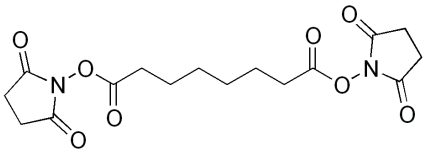

As crosslinking agent disuccinimidyl suberate (DSS) was chosen. DSS is membrane-permeable and at each end of a (medium-sized) 8 carbon-atom-long linker it carries an amine-reactive N-hydroxysuccinimide (NHS) ester. It crosslinks to primary amines: protein N-termini and amine side chains of lysine residues. The membrane permeability of DSS allows crosslinking to be carried out *in vivo*.
Three strains were investigated for possible TorD interactions. The wild-type strain *E. coli* MC4100 (*malE*$^-$) expressing $TorA^{SP}$-MalE and $TorD^{Strep}$ and the *tatB*-mutant *E. coli* BØD (*malE*$^-$) once complemented with $TatB_{E.c.}$ and once with $TatB_{C.g.}$ expressing $TorA^{SP}$-MalE and $TorD^{Strep}$. The strains were cultivated in a four hour induction culture, incubated with the crosslinker DSS, harvested and then the membrane and the cytoplasmic fractions were isolated. Out of both fractions $TorD^{Strep}$ was purified using *Strep*-Tactin coated magnetic beads. The elution fractions were subjected to SDS-PAGE. The gels were stained with Coomassie-Blue as well as Western blotted. The Western Blots were incubated with

antibodies against MalE to detect the potential interaction partner TorA^{SP}-MalE and against *Strep*-Tactin to detect the chaperone TorD. As the elution fractions turned out to have a very low protein content they were enriched around 100-fold using a SpeedVac.
The (enriched) membrane fractions were devoid of any traces of either TorD^{Strep} or MalE (data not shown). The cytoplasmic fractions showed substantial amounts of TorD (theoretical size of the monomer: 22,6 kDa) when visualized with protein-staining Coomassie blue (see figure 29, lower part) in all three strains with and without DSS crosslinking. Current literature suggests that this TorD monomer is also the form which is active as a TorA^{SP}-binding chaperone (Dow et al., 2013). TorD^{Strep} could also be visualized in all three strains with and without DSS when the Western blots were developed with alkaline phosphatase coupled *Strep*-Tactin. The amount of TorD^{Strep} in the cytoplasm did not vary significantly from strain to strain (data not shown).

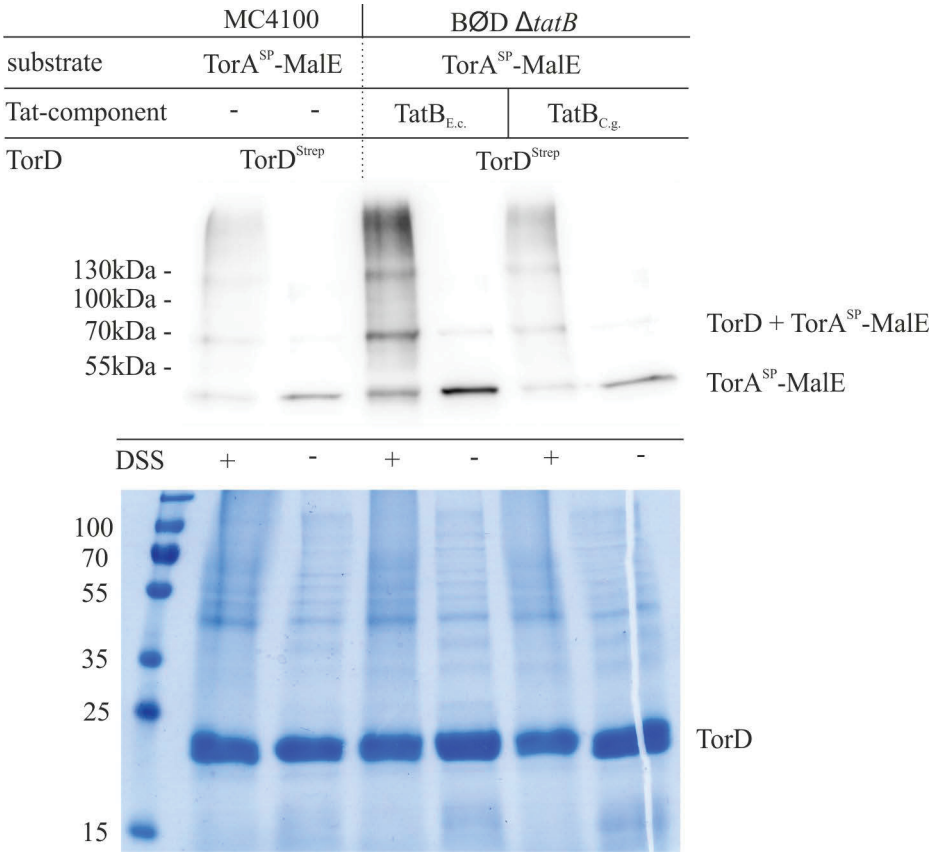

Figure 29: Crosslinks of TorD^{Strep} to the substrate TorA^{SP}-MalE using the crosslinker disuccinimidyl-suberate (DSS). After crosslinking, the cytosolic fraction was prepared from the cultures and TorD^{Strep} was subsequently purified using *Strep*-Tactin coated magnetic beads. The first elution fraction was applied to SDS-PAGE and stained with Coomassie blue (bottom) and Western blotted followed by detection of the substrate TorA^{SP}-MalE by using an α-MalE antibody (top).

In the top part of figure 29, a Western blot of the cytosolic fractions of the three tested strains is shown which has been developed with an α-MalE antibody. In absence of the crosslinker DSS, a band representing the intracellular precursor TorA^{SP}-MalE (46,0 kDa) can be seen. Very faint bands of a higher molecular weight can also be seen. In the crosslinked strains, the 46,0 kDa TorA^{SP}-MalE band can also be observed. Furthermore a second and third band with higher molecular weight can be seen. Given a theoretical size of a crosslinked TorD^{Strep}/-TorA^{SP}-MalE complex of around 68,6 kDa, it is very likely that the middle band represents this complex. The even higher-running third band is likely

a crosslinked double complex with an approximate size of 137,2 kDa.
Due to the fact that the elution fractions had to be enriched in order to get a sufficiently strong signal for these Western blots, these data are not quantifiable. This means the amount of $TorD^{Strep}$/-$TorA^{SP}$-MalE complexes of the three strains cannot really be compared with each other. Nonetheless, it can be said that complexes of TorD and substrate appear in the cells in significant amounts.

3.2.3 Comparing the TatB proteins of *C. glutamicum* and *E. coli*

The coexpression of TorD results in its binding to the TorA signal peptide of model substrates and, as could be directly shown in the previous section, results in intracellular complexes of TorD and substrate precursor. In theory, it has been suggested that these complexes might interact with the Tat-translocase, the chaperone dissociates and an export of the substrate occurs (Kostecki et al., 2010). But when coexpression of TorD and $TorA^{SP}$-substrate takes place in an *E. coli tatB*-mutant complemented with plasmid-expressed TatB, the export is blocked. This is most pronounced when an *E. coli tatB*-mutant was complemented with $TatB_{C.g.}$. But also when an *E. coli tatB*-mutant was complemented with homologous $TatB_{E.c.}$, a significant reduction in the amount of translocated substrate could be observed.
This ultimately leads to the question why a coexpression of $TorA^{SP}$-substrate and TorD in the *tatB*-mutant strain results in a significant decrease in the amount of exported protein when complemented with $TatB_{E.c.}$ and to a complete export block when complemented with $TatB_{C.g.}$.
The data presented in the previous sections (page 54ff.) points towards two different observations. Firstly, the strength of the TorD-induced export block seems to stand in relation to how well the Tat-translocase functions regardless of TorD presence, i.e. translocation efficiency determines how well TorD is released from the TorA signal peptide. This becomes obvious, when comparing the varying translocation efficiencies between the wild-type strain MC4100 and the homologously complemented *tatB*-mutant BØD - even though the TatB molecules present in these two strains are identical. This could point towards a stochiometrical issue in the membrane due to different amounts of TatB in the wild-type and complemented *tatB*-mutant strains. Secondly, $TorA^{SP}$-substrate and TorD coexpression in a *tatB*-mutant strain only leads to a reduction in the amount of exported protein when complemented with $TatB_{E.c.}$ but to a complete block of export when complemented with $TatB_{C.g.}$. This could point to, in accordance with the original hypothesis, *C. glutamicum* TatB either missing a specific residue or secondary-structure element which is necessary within the translocase to interact with the $TorA^{SP}$-substrate/ TorD complex or otherwise, possessing a specific residue which prevents this interaction. To complicate matters, it also has to be considered that a combination of these possibilities might be true.
To address the question of whether a $TatB_{C.g.}$-containing translocase could be deficient in $TorA^{SP}$-substrate/ TorD complex interaction, the structural differences to the endogenous *E. coli* TatB molecule were analyzed. Regarding the amino acid sequence of the two molecules, heterologous $TatB_{C.g.}$ is with 156 amino acids (17,0 kDa) slightly smaller than homologous $TatB_{E.c.}$ with 171 amino acids (18,4 kDa). The overall sequence identity of the two TatB molecules is at 23,57%[9]. Both molecules contain an N-terminal transmembrane domain which is connected to an amphipathic helix via a hinge region. The hinge region between the transmembrane domain and the amphipathic helix is preceded by an invariant glycine residue (G21 in *E. coli*, G22 in *C. glutamicum*) followed by a proline residue which defines the angle at which the amphipathic helix lies along the cytoplasmic membrane (P22 in *E. coli*,

9. PIM: percent identity matrix calculated using Clustal2.1

P23 in *C. glutamicum*) (Hicks et al., 2003). The amphipathic helix is followed by an unstructured C-terminus which is located in the cytoplasm (Koch et al., 2012).
A pairwise global alignment of the amino acid sequences of $TatB_{E.c.}$ and $TatB_{C.g.}$ using the bioinformatic tool EMBOSS Needle (McWilliam et al., 2013) reveals a decreasing homology of the two molecules from N- to C-terminus (see figure 30). The first 50 amino acids of the TatB molecules, contain

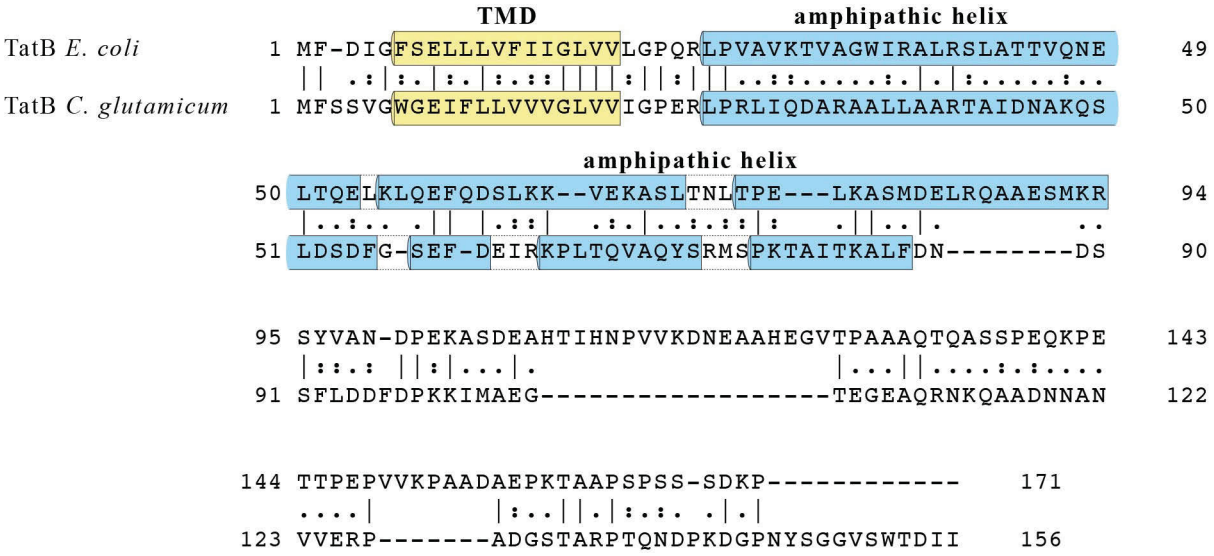

Figure 30: Alignment of *E. coli* and *C. glutamicum* TatB using EMBOSS Needle global pairwise alignment tool (http://www.ebi.ac.uk/Tools/psa/emboss_needle/). The transmembrane domains (TMD) are highlighted in yellow, the predicted α-helical segments of the amphipathic helix in blue. A | (vertical line) indicates positions which have identical residues. A : (colon) indicates conservation between groups of strongly similar properties scoring > 0.5 in the BLOSUM62 matrix. A . (period) indicates conservation between groups of weakly similar properties scoring ≤ 0.5 in the BLOSUM62 matrix. BLOSUM is a bioinformatic substitution matrix which describes the chemical properties of amino acids relative to each other.

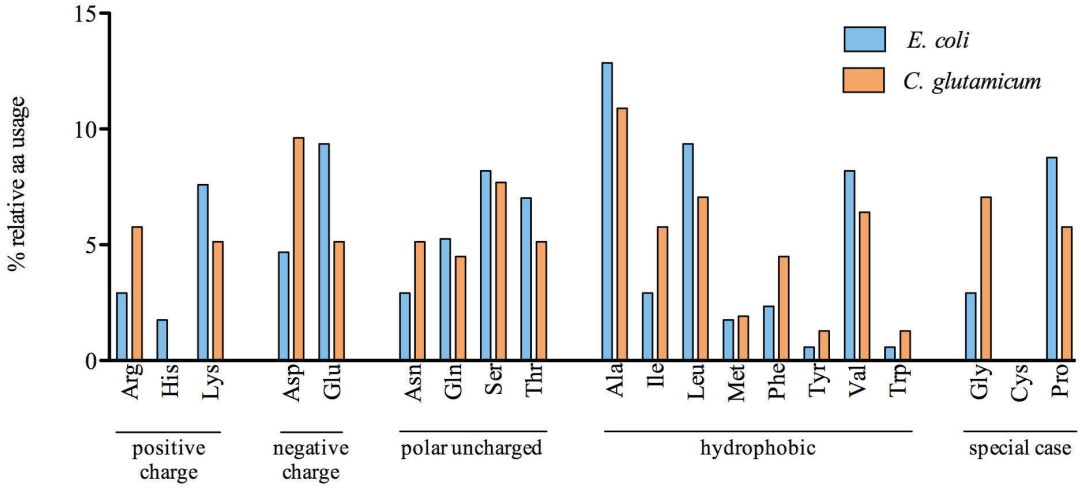

Figure 31: Relative amino acid usage (in %) of *E. coli* TatB (blue) in comparison to *C. glutamicum* TatB (orange), grouped according to side chain characteristics.

ing the transmembrane domain and the N-terminal part of the amphipathic helix, exhibit a sequence similarity of 58%[10]. The rest of the sequences towards the C-terminus is more divergent. Especially the unstructured C-terminus of $TatB_{C.g.}$, shows grave differences to the *E. coli* molecule. Another striking difference of the two TatB molecules is the relative amino acid composition which is depicted in the graph in figure 31. Especially the occurence of amino acids with electrically charged side chains is noticeable. While the overall polypeptide sequence results in $TatB_{C.g.}$ possessing a slightly lower net charge (at pH 7.0) of -7.0 in comparison to $TatB_{E.c.}$ of -6.7, the amino acids used to achieve this vary greatly. As positively charged amino acids, the *E. coli* TatB molecule contains 5 arginine, 3 histidine and 13 lysine residues and the *C. glutamicum* molecule contains 9 arginine, 8 lysine and no histidine residues. For negatively charged amino acids, *E. coli* TatB contains 8 aspartate and 16 glutamate residues and in *C. glutamicum* the values are reversed to 15 aspartate and 8 glutamate residues.
The amphipathic helix of both TatB molecules is comprised of a subset of α-helical segments. To identify these the bioinformatic tool PSIPRED 3.3 was used (Buchan et al., 2013). These α-helices are shown in blue in the TatB alignment in figure 30. The *E. coli* amphipathic helix consists of three predicted helices (L25-E53; K55-L71; P76-R94). The *C. glutamicum* amphipathic helix consists of four predicted helices (L26-F55; S57-I62, K64-S73; P77-F86). Whether all these differences have an influence on the functionality of the TatB molecule cannot be said at this point but in all respects it seems as though the *C. glutamicum* TatB molecule is a more "compact" version in comparison to *E. coli* TatB.
It was originally postulated that *C. glutamicum* TatB could either miss a specific residue or secondary structure necessary for the interaction of the translocase with the $TorA^{SP}$-substrate/ TorD complex or otherwise possess a residue which prevents this interaction from taking place. It was hypothesized that it would be most likely to identify a residue or structural element playing such a role within a part of $TatB_{C.g.}$ with low homology to *E. coli* TatB. For this reason, it was firstly investigated whether the alternatively structured extreme C-terminus of $TatB_{C.g.}$ contains a residue or region prohibiting the $TatB_{C.g.}$-containing translocase to mediate the release of TorD from the $TorA^{SP}$-substrate (see next section). Secondly, the differently structured amphipathic helices of $TatB_{C.g.}$ and $TatB_{E.c.}$ were analyzed to investigate the influence of this critical part of TatB on a possible interaction of the Tat-translocase with the $TorA^{SP}$-substrate/ TorD complex (see page 69).

3.2.3.1 Truncation analysis of $TatB_{C.g.}$

The primary aim of the following experiments was to elucidate whether the C-terminal end of $TatB_{C.g.}$ plays an inhibiting role in the interaction between the $TatB_{C.g.}$-containing translocase and a $TorA^{SP}$-substrate/ TorD complex. A truncation analysis of $TatB_{C.g.}$ was carried out with the goal of removing residues within the unstructured C-terminus which might be responsible for preventing the release of the $TorA^{SP}$-substrate from TorD . For this purpose, 12 variants of $TatB_{C.g.}$ were constructed in which 10, 20, 30,...120 amino acids of the C-terminus were deleted (see top part of figure 32). These truncated $TatB_{C.g.}$ molecules were cloned into the expression vector pHSG575, resulting in $pHSG\_TatB_{C.g.}^{-n}$ (n being the number of C-terminally truncated amino acids), and transformed into *E. coli* BØD (Δ*tatB*). The transformed strains were cultivated overnight, then diluted and streaked onto LB agar plates containing 4% SDS. This was done to test for functionality of the resulting mutant Tat translo-

10. Calculated using the local pairwise alignment tool EMBOSS matcher (McWilliam et al, 2013), based on BLOSUM62 (BLOcks SUbstitution Matrix), an evidence-based substitution matrix for aligning evolutionarily divergent protein sequences.

cases regarding the translocation of the natural periplasmic Tat-substrates AmiA and AmiC (as described on page 48) which are necessary for growth on SDS-containing media.

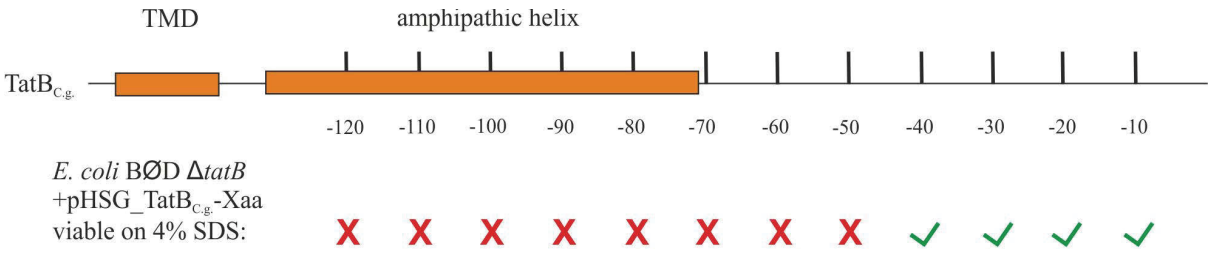

Figure 32: Truncation analysis of *C. glutamicum* TatB. Twelve TatB$_{C.g.}^{-n}$ truncations were constructed by C-terminally deleting *n* amino acids (n=10, 20, 30,...120). These TatB$_{C.g.}^{-n}$ variants were tested for functionality by expressing them in *E. coli* BØD (Δ*tatB*). Overnight cultures of transformed strains were diluted and streaked onto LB agar plates containing 4% SDS. Only cells expressing TatB$_{C.g.}^{-n}$ variants able to complement *E. coli* TatB function are able to grow on SDS (check marked in green).

Only the truncation of a maximum of 40 amino acids allowed growth on 4% SDS-containing agar plates (depicted in figure 32) which leads to the conclusion that truncations of >40 amino acids either leads to an unfunctional translocase or at least to a translocase which is not capable of exporting sufficient amounts of the *E. coli* amidases to support growth on SDS.
Next, three of the TatB$_{C.g.}$ variants which were functional in the SDS assay, TatB$_{C.g.}$-20, TatB$_{C.g.}$-30, and TatB$_{C.g.}$-40, as well as TatB$_{C.g.}$-50 and TatB$_{C.g.}$-60 which were not functional in the SDS assay were tested for their translocation capabilities of an artificial substrate in the presence of TorD. They were compared for translocation of TorA^{SP}-MalE into the periplasm against wild-type TatB$_{C.g.}$.
For this purpose, the *E. coli tatB*-mutant BØD (*malE*$^-$) was transformed with the substrate vector pBBR_TorA-MalE, TatB$_{C.g.}$ on pHSG_TatB$_{C.g.}$ or the truncated TatB variants on pHSG_TatB$_{C.g.}^{-n}$ as well as either TorD on pTrSp_TorD or, as expression control, GFP on pTrSp_GFP. These strains were cultivated overnight, diluted to an OD$_{600nm}$ of 0,1 and then streaked onto minimal medium agar plates containing maltose as sole carbon source.
The growth of these strains on maltose minimal medium is depicted in figure 33. The negative controls, *E. coli* wild-type strain MC4100 not expressing the substrate (1) and *E. coli* Δ*tatB* with empty vector pHSG575 not expressing a TatB molecule (2), are unable to grow on maltose minimal medium. The small cell papillae which are visible (2) were infrequently observed after long incubation times of maltose minimal medium agar plates. They were not considered as normal *E. coli* growth and are possibly due to bifunctional TatA suppressor mutations. The positive control, wild-type strain MC4100 expressing the substrate TorA^{SP}-MalE, is able to grow in absence (3) and in presence (4) of TorD. As seen before (see page 57), the *E. coli tatB*-mutant strain expressing the substrate TorA^{SP}-MalE as well as wild-type TatB$_{C.g.}$ is unable to grow in presence of TorD (5).
The *tatB*-mutant strains expressing the three truncated variants of TatB$_{C.g.}$ which allowed growth on SDS, TatB$_{C.g.}$-20, TatB$_{C.g.}$-30 and TatB$_{C.g.}$-40, show the same growth phenotype on maltose minimal medium as when wild-type TatB$_{C.g.}$ is expressed. They show growth comparable to the wild-type strain in absence of TorD (8, 10, 12) and are unable to grow in presence of TorD (7, 9, 11). The *tatB*-mutant strain expressing the two TatB$_{C.g.}$-truncations which did not allow growth in presence of SDS when expressed in a *tatB*-mutant strain, TatB$_{C.g.}$-50 and TatB$_{C.g.}$-60, also show growth in absence of TorD when expressing TorA^{SP}-MalE (14, 16) although less well than the wild-type strain. In presence of TorD the *tatB*-mutant strains complemented with TatB$_{C.g.}$-50 and TatB$_{C.g.}$-60 are also unable to grow (13, 15). This means that the C-terminal truncation of up to 40 amino acids from TatB$_{C.g.}$ does not alter

the capability of the resulting translocase to export the substrate TorA^{SP}-MalE in absence of TorD. A truncation of up to 60 amino acids from TatB$_{C.g.}$ results in translocases which allow residual translocation of TorA^{SP}-MalE in absence of TorD sufficient for limited growth.
The truncation of the C-terminus of TatB$_{C.g.}$ did not lead to a TatB variant that, when expressed in a *tatB*-mutant strain expressing the substrate TorA^{SP}-MalE, allowed growth in presence of TorD. That is a strong indication that the extreme C-terminus of *C. glutamicum* TatB does not possess a specific residue or a structure that prevents an interaction of the translocase with the TorA^{SP}-substrate/ TorD complex necessary for the release of TorD.

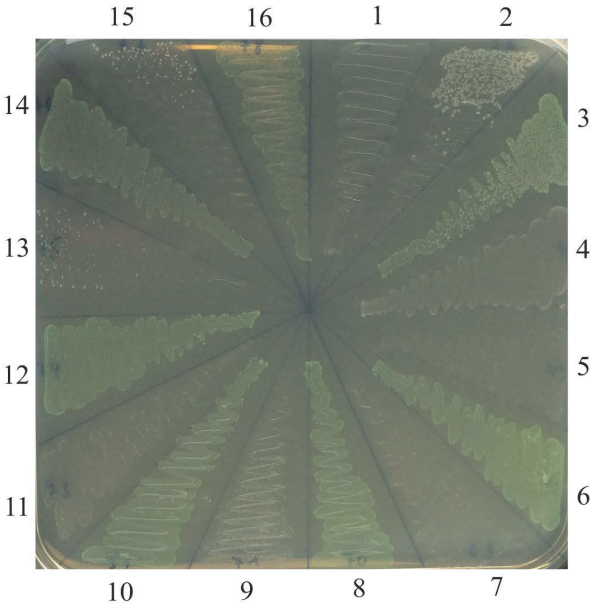

		pBBR	pHSG	pTrSp	growth on MM
1	MC4100	-	-	-	-
2	BØD	TorA^{SP}-MalE	-	-	-
3	MC4100 Δ*malE*		-	GFP	++
4			-	TorD	++
5	BØD Δ*malE*	TorA^{SP}-MalE	TatB$_{C.g.}$ wt	TorD	-
6				GFP	++
7			TatB$_{C.g.}$ -20aa	TorD	-
8				GFP	++
9			TatB$_{C.g.}$ -30aa	TorD	-
10				GFP	++
11			TatB$_{C.g.}$ -40aa	TorD	-
12				GFP	++
13			TatB$_{C.g.}$ -50aa	TorD	-
14				GFP	+
15			TatB$_{C.g.}$ -60aa	TorD	-
16				GFP	+

Figure 33: *E. coli* cells expressing truncated TatB$_{C.g.}$ variants cultivated on a maltose minimal medium agar plate to analyze the export of the maltose binding protein TorA^{SP}-MalE *in situ*. Strains are transformed with expression vectors according to the table. The strains were cultivated overnight, diluted to an OD$_{600nm}$ of 0,1, streaked onto the plates and incubated for ~48 hours at 37ºC (++ wild-type growth, + limited growth, - no growth).

To analyze the *de facto* exported amounts of MalE, EDTA-lysozyme spheroblast fractionations were made. For this, the *E. coli tatB*-mutant BØD (*malE*$^-$) complemented with wild-type TatB$_{C.g.}$ was compared with the *tatB*-mutant strain complemented with truncated versions TatB$_{C.g.}$-20, TatB$_{C.g.}$-40 and TatB$_{C.g.}$-60.
Figure 34 shows that in absence of TorD, the *E. coli tatB*-mutant strain BØD complemented with (wild-type) TatB$_{C.g.}$ exports TorA^{SP}-MalE into the periplasm (lane 3). Likewise, the complementation of the *tatB*-mutant strain with the truncated variants, TatB$_{C.g.}$-20 and TatB$_{C.g.}$-40, allows comparable export into the periplasm (lanes 5 and 7). The *tatB*-mutant strain complemented with TatB$_{C.g.}$-60 only has a very small amount of MalE in the periplasm (lane 9).
In presence of TorD, the *tatB*-mutant strain complemented with TatB$_{C.g.}$ exhibits an export block of MalE into the periplasm (lane 2). As observed before, an accumulation of TorA^{SP}-MalE precursor in

the cytoplasm/membrane fraction is found as well as some precursor in the periplasmic fraction. The *tatB*-mutant strains complemented with either $TatB_{C.g.}$-20 or $TatB_{C.g.}$-40 show a similar behavior in presence of TorD (lanes 4 and 6). The cytoplasm/ membrane fractions show an accumulation of $TorA^{SP}$-MalE precursor and small amounts of precursor are found also in the periplasmic fractions. The *tatB*-mutant strain complemented with $TatB_{C.g.}$-60 also shows an accumulation of $TorA^{SP}$-MalE precursor in the cytoplasmic fraction (lane 8), although the amount is smaller than that in the other strains. The presence of $TorA^{SP}$-MalE precursor in the periplasmic fractions of strains expressing TorD is again probably due to some cell lysis which occured during the fractionation.

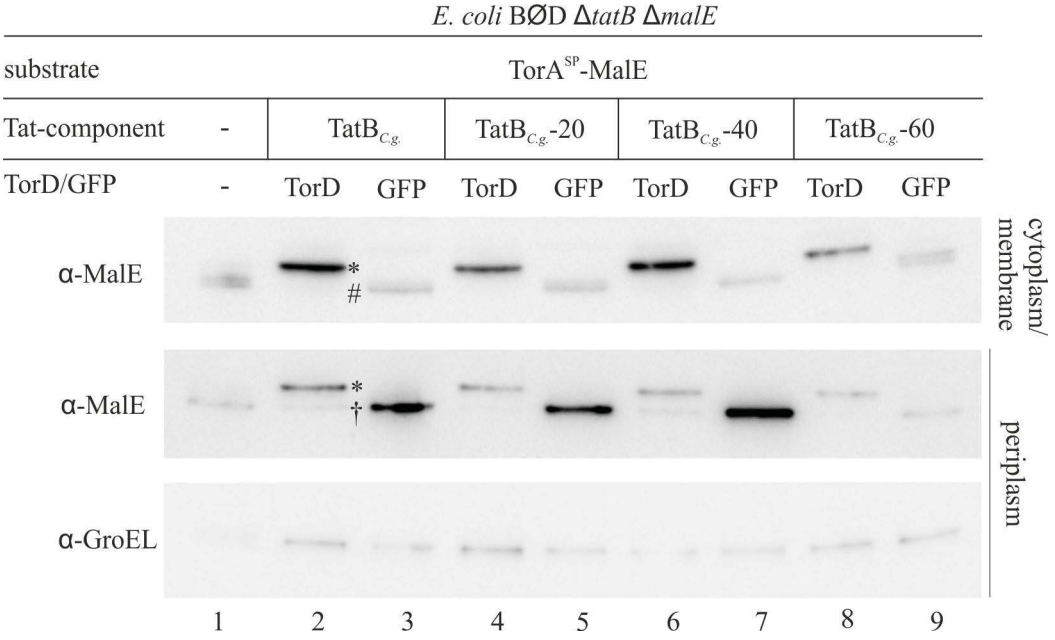

Figure 34: *E. coli tatB*-mutant strains expressing truncated versions of $TatB_{C.g.}$ and $TorA^{SP}$-MalE exhibit an export block in presence of TorD. Periplasmic and combined cytoplasmic/ membrane fractions were subjected to SDS-PAGE and subsequently Western blotted. The top Western blot depicts the cytoplasmic fractions, the middle and the bottom blots the periplasmic fractions. The two upper blots were incubated with an antibody against the maltose binding protein MalE and the bottom blot with an antibody against GroEL (to evaluate cell lysis occurring during the preparation). Lanes 1 to 8 show the *E. coli tatB*-mutant BØD Δ*malE*. All strains have been transformed with three plasmids according to the top of the figure. Of the cytoplasmic/membrane fraction 10 µg and of the periplasmic fraction 2 µg of protein were applied to SDS-PAGE. The asterisk (*) denotes the precursor $TorA^{SP}$-MalE, the obelisk (†) the mature MalE and the hash (#) a degradation product of $TorA^{SP}$-MalE.

In conclusion, the extreme C-terminus of $TatB_{C.g.}$ does not seem to contain a residue or structural element which prevents an interaction of the $TatB_{C.g.}$-containing translocase with the $TorA^{SP}$-MalE/ TorD complex. At least, this can be stated for the C-terminal 40 amino acids. This approach could not determine whether a critical residue of this sort exists further towards the N-terminus of $TatB_{C.g.}$ as shorter truncations abolished the export capabilities of the resulting translocases for the endogenous amidases and $TorA^{SP}$-MalE.

3.2.3.2 Hybrid molecules of $TatB_{E.c.}$ and $TatB_{C.g.}$

After excluding the involvement of the C-terminal 40 amino acids of $TatB_{C.g.}$ in preventing a release of TorD from $TorA^{SP}$-MalE, the next approach targeted the amphipathic helix of TatB. The amphipath-

ic helix, which is oriented along the inside of the cytoplasmic membrane, is a part of the TatBC receptor complex which is exposed to the cytoplasm. Thus it is conceivable that it could play an active role in the recognition of the TorA^{SP}-substrate/ TorD complex before the substrate is released and the signal peptide is bound by the receptor complex prior to translocation. As mentioned above (see page 64f.), the two TatB molecules of *E. coli* and *C. glutamicum* show some grave differences regarding amino acid usage, charge distribution and the α-helical sub-segmentation of the amphipathic helix (see figure 35).

To determine whether the amphipathic helix of TatB$_{C.g.}$ is negatively involved in an interaction between TatB and TorD, hybrid TatB molecules were constructed. The aim was to define whether the amphipathic helix of TatB$_{C.g.}$ contains a segment which prevents the release of TorD from the TorA^{SP}-substrate. Or, the other way around, whether TatB$_{E.c.}$ contains a segment which is necessary for this release mechanism.

Four TatB$_{E.c.}$-TatB$_{C.g.}$ hybrid molecules were constructed, based on the predictions of α-helical segments of the two amphipathic helices, in all of which the transmembrane domain and invariant glycine residue G21 of TatB$_{E.c.}$ was present. TatBE.c.$_{21}$C.g.$_{139}$ is composed of the *E. coli* transmembrane domain, whereas the amphipathic helix and the C-terminus are from the *C. glutamicum* TatB. TatBE.c.$_{54}$C.g.$_{100}$ and TatBE.c.$_{72}$C.g.$_{82}$ have a mixed *E. coli/C. glutamicum* amphipathic helix. TatBE.c.$_{95}$C.g.$_{70}$ has the *E. coli* amphipathic helix and the *C. glutamicum* extreme C-terminus (also see figure 35). These four hybrids were cloned into the base vector pHSG575 resulting in IPTG-inducible vectors pHSG_TatBE.c.$_{21}$C.g.$_{139}$, pHSG_TatBE.c.$_{54}$C.g.$_{100}$, pHSG_TatBE.c.$_{72}$C.g.$_{82}$ and pHSG_TatBE.c.$_{95}$C.g.$_{70}$.

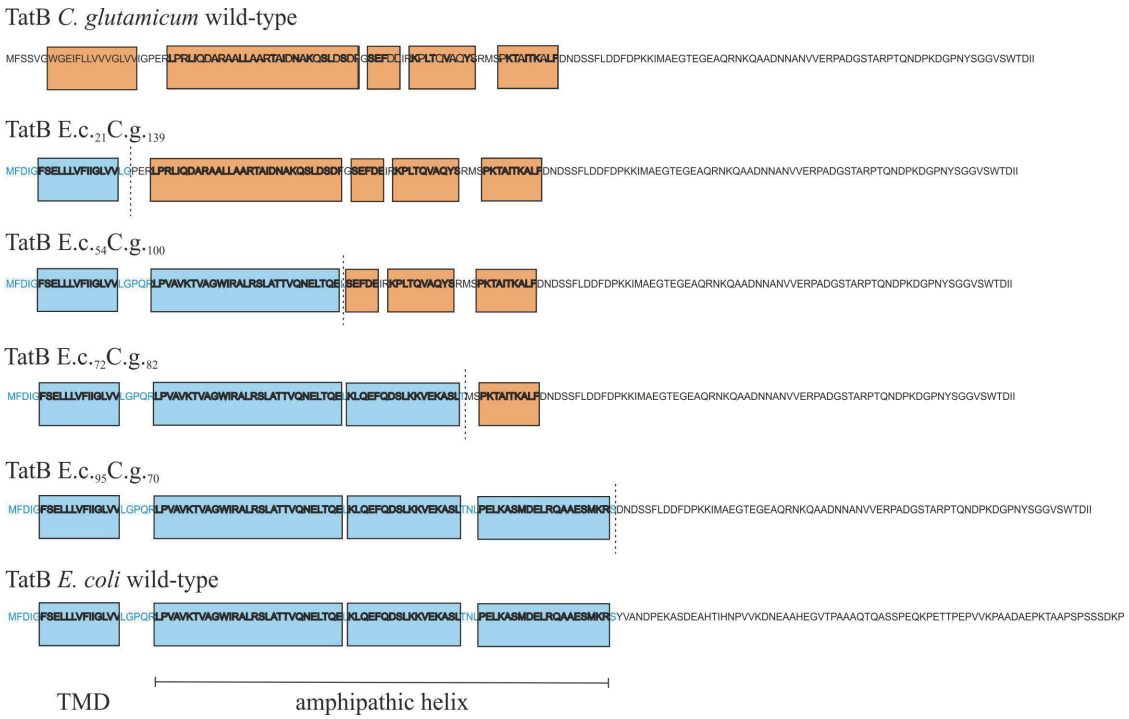

Figure 35: Wild-type and hybrid molecules of TatB from *C. glutamicum* (orange) and *E. coli* (blue). The boxes represent predicted α-helical segments within the molecule, the first α-helix toward the N-terminus being the transmembrane domain of TatB. The other following α-helices together comprise the amphipathic helix which is located within the cytoplasm. (Prediction of α-helices was carried out using PSIPRED v3.3 Protein Sequence Analysis Workbench http://bioinf.cs.ucl.ac.uk/psipred/)

E. coli BØD Δ*tatB* was transformed with these four vectors for the expression of the TatB hybrid molecules as well as the substrate $TorA^{SP}$-MalE on pBBR_TorA-MalE and either pTrSp_TorD or pTrSp_GFP for expression of either TorD or GFP. The resulting strains were first checked for growth on maltose minimal medium (see figure 36). In the absence of TorD all four *E. coli tatB*-mutant strains expressing the hybrid TatB molecules were able to grow comparable to the wild-type (sectors 2, 4, 6 and 8). In the presence of TorD, the *tatB*-mutant strain expressing the four TatB hybrid molecules showed no signs of growth after 24 hours. After incubation of the minimal medium agar plates for 72 hours (as seen in figure 36) the two hybrids $TatBE.c._{21}C.g._{139}$, which has the full *C. glutamicum* amphipathic helix, and $TatBE.c._{54}C.g._{100}$, which has half of the *C. glutamicum* amphipathic helix, were unable to grow save the occasional development of tiny papillae on the agar plates which were not considered as real "growth" (sectors 1 and 3). After 72 hours, complementation of the *tatB*-mutant strain with the two TatB hybrids carrying a majority or all of the *E. coli* amphipathic helix, $TatBE.c._{72}C.g._{82}$ and $TatBE.c._{95}C.g._{70}$ showed very weak signs of growth in presence of TorD (sectors 5 and 7). In a multitude of experiments carried out independently, these signs of very weak growth in the form of a thin opaque cell layer (as seen in figure 36) presented a tendency towards the TatB hybrid molecule containing the complete amphipathic helix of *E. coli* TatB ($TatBE.c._{95}C.g._{70}$) promoting slightly better growth when expressed in the *tatB*-mutant strain in presence of TorD.

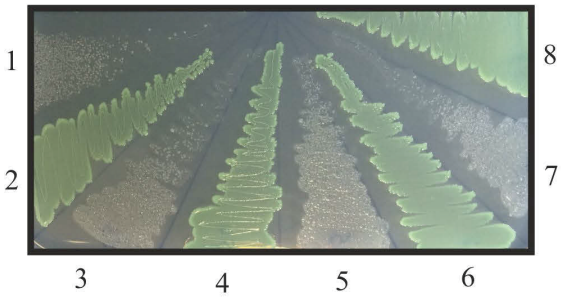

		pBBR	pHSG	pTrS	growth on MM
1	BØD Δ*tatB* Δ*malE*	$TorA^{SP}$-MalE	$TatBE.c._{21}C.g._{139}$	TorD	-
2				GFP	++
3			$TatBE.c._{54}C.g._{100}$	TorD	-
4				GFP	++
5			$TatBE.c._{72}C.g._{82}$	TorD	+
6				GFP	++
7			$TatBE.c._{95}C.g._{70}$	TorD	+
8				GFP	++

Figure 36: Growth of *E. coli* BØD Δ*tatB* Δ*malE* complemented with different hybrid *E. coli/ C. glutamicum* TatB molecules on minimal medium agar plates containing maltose as sole carbon source. Strains were transformed according to table in figure, cultivated overnight, diluted to an OD_{600nm} of 0,1, streaked onto the agar plates and incubated at 37ºC for ~72 hours (++ wild-type growth + limited growth - no growth).

Next, a fractionation into periplasmic and combined cytoplasmic/ membrane fraction of the *tatB*-mutant strains expressing the four $TatB_{E.c.}$-$TatB_{C.g.}$ hybrids was carried out to investigate the actual amounts of expressed and exported $TorA^{SP}$-MalE. Figure 37 shows this fractionation.
Expression of the first hybrid $TatBE.c._{21}C.g._{139}$, of which only the transmembrane domain is of *E. coli* origin shows good export of MalE into the periplasm in absence of TorD (lane 2) and a full export block in presence of TorD (lane 1). Expression of $TatBE.c._{54}C.g._{100}$, which has half of the *E. coli* and half of the *C. glutamicum* amphipathic helix allowed slightly stronger export of MalE into the periplasm in absence of TorD (lane 4) and a very small amount of exported MalE in the periplasm in the presence of TorD (lane 3). Expression of $TatBE.c._{72}C.g._{82}$ which has around ¾ of the *E. coli* amphipathic helix is comparable to $TatBE.c._{54}C.g._{100}$: good export of MalE into the periplasm in the absence of TorD (lane 6) and a small amount of exported MalE in the presence of TorD (lane 5). The ex-

pression of the TatB hybrid with the full *E. coli* amphipathic helix TatBE.c.$_{95}$C.g.$_{70}$ shows the best export in the absence of TorD (lane 8). When TorD is present, export is still limited but the exported amount of MalE is at least three-fold higher (lane 7) in comparison to when the hybrid TatBE.c.$_{54}$C.g.$_{100}$ is expressed.

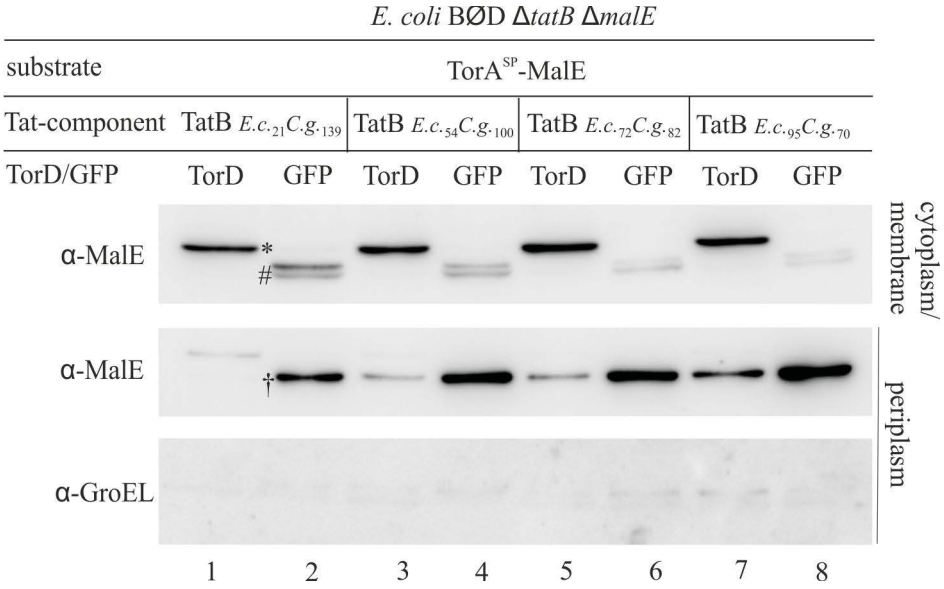

Figure 37: Fractionation of *E. coli tatB*-mutant strains expressing *E. coli/ C. glutamicum* hybrid TatB molecules and TorA^{SP}-MalE. Isolated fractions were subjected to SDS-PAGE and subsequently Western blotted. The top Western blot depicts the cytoplasmic fractions, the middle and bottom blots the periplasmic fractions. The two upper blots were incubated with an antibody against the maltose binding protein MalE and the bottom blot with an antibody against GroEL (to evaluate cell lysis occurring during the preparation). All strains have been transformed with three plasmids according to the top of the figure. Of the cytoplasmic/membrane fraction 10 µg and of the periplasmic fraction 2 µg of protein were applied to SDS-PAGE. The asterisk (*) denotes the precursor TorA^{SP}-MalE, the obelisk (†) the mature MalE and the hash (#) a degradation product of TorA^{SP}-MalE.

Comparing the protein data of expression of the four hybrids with each other, a clear tendency can be seen towards better export when the TatB molecule used for complementation is to a larger proportion composed of *E. coli* sequence. Firstly, the amount of exported MalE in absence of TorD, which is a good indicator for the *de facto* efficiency of the mutant translocase, rises slightly the more of the TatB hybrid is of *E. coli* origin. Secondly, in presence of TorD, the export block of TorA^{SP}-MalE is less pronounced when the TatB hybrid expressed is composed in majority of *E. coli* sequence.
A conclusion which can be drawn from this fractionation experiment is that the amphipathic helix of *E. coli* generally allows better export in absence of TorD. The translocation efficiency in presence of TorD indicates that the cytoplasmically located amphipathic helix of TatB could indeed play a role in a theoretical interaction of TorD-bound TorA^{SP}-substrate with the Tat-translocase, required for release of the substrate. Nevertheless, it has to be considered whether the overall translocation efficiency (observed in absence of TorD) stands in direct correlation to the strength of the export block in presence of TorD.
This would suggest that a Tat-translocase with a lowered export efficiency, for example by the presence of a non-native TatB molecule in the translocase such as TatB$_{C.g.}$ or one of the TatB hybrid molecules, is *per se* deficient TorD release. The reason for this could be that the translocase needs a certain threshhold translocation dynamics to be able to compete with TorD for the TorA signal peptide.

3.2.4 Mutagenesis of *tatB* indicates that $TatB_{C.g.}$ presence might be problematic for release of TorD from $TorA^{SP}$-substrate

The experiments in the preceding sections provided evidence for a correlation between translocation efficiency of the translocase and its ability to release TorD from a $TorA^{SP}$-substrate. Nonetheless, it was still to be ascertained whether *C. glutamicum* TatB possesses a specific residue which might prevent an interaction of the translocase with with TorD/ $TorA^{SP}$-substrate complex, preventing TorD release and export of the substrate taking place. An ideal way to localize a single amino acid residue which might be responsible for the failed release of TorD from the TorA signal peptide in presence of $TatB_{C.g.}$ is by directed evolution. For this purpose *C. glutamicum tatB* as well as the TatB hybrid gene *tatBE.c.*$_{21}$*C.g.*$_{139}$ (see figure 32 for a schematic depiction of the resulting TatB molecule), the gene product which has the transmembrane domain of *E. coli* and the C-terminal part from *C. glutamicum,* were mutagenized by error prone PCR. This is a PCR method which provokes the incorporation of errors into the amplified DNA sequence and is a powerful and well established method to generate mutant libraries with a defined rate of base substitutions (Daugherty et al., 2000).
The mutant libraries of *tatB* were generated using the GeneMorph II kit from Agilent. By adjusting the amount of target DNA used for the PCR reaction, a theoretical mutation frequency of 4.5 - 9 mutations/kb was achieved. After ligation of the PCR products into the backbone of the expression vector pHSG, two libraries with a total number of ~20.000 muteins each were generated.
The *E. coli tatB*-mutant BØD was transformed with the substrate vector pBBR_TorA-MalE and pTrSp_TorD and then with the libraries of mutagenized $TatB_{C.g.}$ and TatBE.c.$_{21}$C.g.$_{139}$ by electroporation. Directly after regeneration, the cells were plated onto minimal medium agar plates to select for clones that can overcome the TorD-induced block of $TorA^{SP}$-MalE export and gain the ability to grow on minimal medium containing maltose as sole carbon source.
After four days, on each of the maltose minimal medium selection plates around 50-60 clones of varying sizes were visible. First, all clones were restreaked onto fresh minimal medium plates to confirm the growth phenotype. In this step, especially the very small colonies which were picked did not grow again. Then, the pHSG vector of the remaining clones containing mutagenized $TatB_{C.g.}$ or TatBE.c.$_{21}$C.g.$_{139}$ was separated and isolated from the other two vectors pBBR_TorA-MalE and pTrSp_TorD.
Next, an *E. coli tat*-mutant-strain DADE (Δ*tatABCE* Δ*malE*) was transformed with the purified substrate vector pBBR_TorA-MalE from every single clone. This was done to verify that the observed growth phenotype of the generated gain-of-function mutant strains on maltose minimal medium is in fact dependent on a modification of the Tat translocase and not on a mutation of the TorA signal peptide of the substrate $TorA^{SP}$-MalE. The strictly Tat-dependent TorA signal peptide possesses a "Sec-avoidance signal", basic amino acid residues within the c-region ($TorA^{SP}$ has two arginine residues at positions 35 and 36). A mutation within this Sec-avoidance signal renders the substrate susceptible for export via the Sec pathway (Bogsch et al., 1997; Blaudeck et al., 2005). Should a mutation within the Sec-avoidance signal of the TorA signal peptide have occured, the *tat*-deficient strain DADE transformed with the isolated pBBR_TorA-MalE substrate vectors should have been able to grow on maltose minimal medium due to export of MalE via the Sec-pathway. This was not the case.
After the possibility of mutations within the signal peptide of the substrate $TorA^{SP}$-MalE had been excluded, the pHSG vectors carrying the generated TatB mutants were again used to transform the *E. coli tatB*-mutant strain BØD together with the substrate vector pHSG_TorA-MalE and pTrSp_TorD. These strains were cultivated overday and then again streaked onto minimal medium plates containing maltose as carbon source to confirm the gain-of-function growth phenotypes in presence of TorD.

The vectors containing the mutagenized variants of *tatB*$_{C.g.}$ and *tatBE.c.*$_{21}$*C.g.*$_{139}$ were sequenced to identify the generated mutations. Finally, to rule out the possibility of mutations within the vector-backbone, the 8 remaining *tatB* mutants were recloned into a fresh pHSG575 expression vector backbone. These plasmids were again used to transform the *E. coli tatB*-mutant BØD (together with substrate TorA^{SP}-MalE and TorD), cultivated overnight and streaked onto maltose minimal medium.
Of eight reconstructed TatB mutants, four each based upon TatB$_{C.g.}$ and TatBE.c.$_{21}$C.g.$_{139}$, only three had a significantly reproducible growth phenotype on maltose minimal medium. These will be discussed here in more detail. An overview of the obtained mutations is found in figure 38 below.

	base vector	**pos./exch.**	**mutations**
X3	TatB$_{C.g.}$ wt	2 *t* ▷ *c* 183 *a* ▷ *t* 190 *a* ▷ *g* 362 *c* ▷ *t*	start codon mutation to ACG E61D K64E A121V
	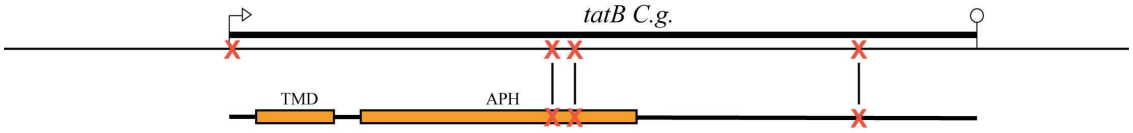		
Z3	TatBE.c.$_{21}$C.g.$_{139}$	162 *t* ▷ *c* 175 *g* ▷ *a* 316 *g* ▷ *t*	silent E58K nonsense: stop-codon leads to C-terminal 52 aa not being translated
	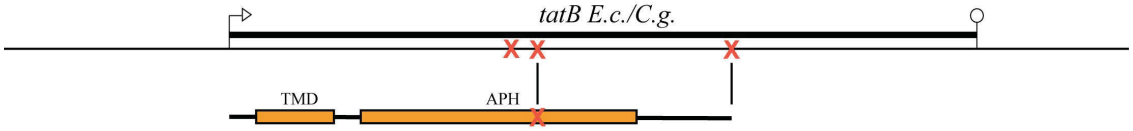		
Z4	TatBE.c.$_{21}$C.g.$_{139}$	-2 *g* ▷ *c* 53 *t* ▷ *c*	mutation in linker between SD and AUG start codon V18A in transmembrane domain
	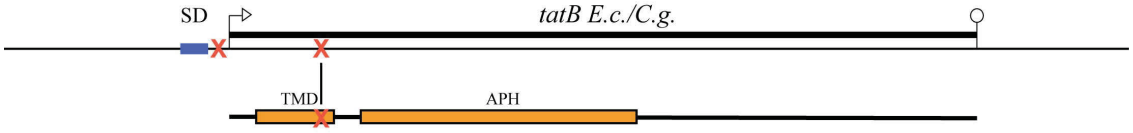		

Figure 38: Overview of mutations obtained by mutagenesis of *tatB*$_{C.g.}$ and *tatBE.c.*$_{21}$*C.g.*$_{139}$ (top line: DNA level) and their consequences on protein level (bottom line: protein). TMD: transmembrane domain, APH: amphipathic helix, SD: Shine-Dalgarno sequence.

The first mutant TatB molecule that promoted reproducible growth on maltose minimal medium when expressing it together with TorA^{SP}-MalE and TorD in an *E. coli tatB*-mutant strain was termed TatB$_{X3}$. It is based upon mutagenized wild-type *tatB*$_{C.g.}$. In figure 39 the growth of an *E. coli tatB*-mutant transformed with TatB$_{X3}$, the substrate TorA^{SP}-MalE and either TorD or GFP on maltose minimal medium can be seen. The growth in absence of TorD (sector 8) is nearly as good as that of the wild-type strain (3). The growth of the TatB$_{X3}$ complemented *tatB*-mutant strain in presence of TorD (7), the phenotype that was selected for, is not reduced compared to the control without TorD (8) but slightly weaker than the wild-type strain expressing TorD (2).

TatB$_{X3}$ has four point mutations. The first one is possibly the most noticeable: the wild-type AUG start codon has been altered to ACG. An ACG start codon is uncommonly found within prokaryotes. In *E. coli*, although not occurring naturally, this alternative start codon is described to support translation initiation at 1-3 % compared to an AUG start codon (Barrick et al., 1994; Sussman et al., 1996). In eukaryotes, alternative start codons are found more often but usually also only support low expression levels of the relevant gene product (Boeck and Kolakofsky, 1994). Two amino acid substitutions are found in the middle of the amphipathic helix: E61D which exchanges a negatively charged glutamic acid for the slightly smaller but also negatively charged aspartic acid and K64E which exchanges a positively charged lysine for a negatively charged glutamic acid. The glutamic acid residue at position 61 in TatB$_{C.g.}$, which has been mutated to an aspartic acid residue in TatB$_{X3}$, could be the equivalent of the conserved E58 residue of *E. coli* which has been descibed as critical for the functionality of the translocase (Hicks et al., 2003). Furthermore, a mutation A121V in the unstructured C-terminus exchanges an alanine for a valine residue, which are both hydrophobic.
The consequences of the mutations within the amphipathic helix and the C-terminus of TatB$_{X3}$ for the functionality of the mutant TatB molecule within the translocase are difficult to evaluate but could have a serious negative effect on the functionality of the TatB$_{X3}$-containing translocase. Taken together with the start codon mutation which probably drastically reduces the amount of synthesized TatB$_{X3}$, an indication was obtained towards selection pressure in presence of TorD reducing the amount and possibly the activity of a problematic TatB molecule. It is unlikely that TatB expression was abolished altogether because the uncomplemented *tatB*-mutant strain is unable to grow on maltose minimal medium (5).

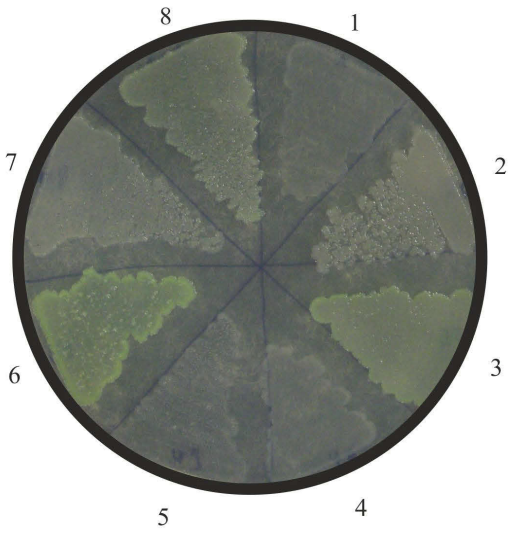

		pBBR	pHSG	pTrSp	growth on MM
1	MC4100 WT Δ*malE*	-	-	-	-
2		TorA-MalE	-	TorD	++
3			-	GFP	++
4	BØD Δ*tatB* Δ*malE*	TorA-MalE	-	-	-
5			TatB$_{C.g.}$	TorD	-
6				GFP	++
7			$_{cp}$TatB$_{X3}$	TorD	+
8				GFP	+

Figure 39: *E. coli tatB*-mutant strain expressing mutant TatB$_{X3}$ (based upon TatB$_{C.g.}$) which promotes growth in presence of TorD. Screening for export of TorA^{SP}-MalE *in situ* on maltose minimal medium agar plates. The *E. coli* strains were transformed according to the table in the figure, grown overnight in LB-medium, diluted to an OD=0,1 and subsequently streaked onto maltose minimal medium agar plates. Incubation occured at 37ºC for ~48 hours (++ wild-type growth + limited growth - no growth)..

The second gain-of-function TatB mutant molecule which allowed growth on maltose minimal medi-

um when expressed together with $TorA^{SP}$-MalE and TorD in a *tatB*-mutant strain was termed $TatB_{Z3}$. It is based upon the TatB-hybrid molecule $TatB_{E.c.21C.g.139}$ which has the transmembrane domain of *E. coli* and the full amphipathic helix and C-terminus of *C. glutamicum*. The growth of an *E. coli tatB*-mutant transformed with $TatB_{Z3}$ and the substrate $TorA^{SP}$-MalE can be seen in figure 40. In absence of TorD (sector 8), growth on minimal medium is nearly as good as that of the wild-type strain control (3). In presence of TorD (7), no limitation in growth compared to the strain with TorD (8) can be seen, even though the growth of the wild-type strain control in presence of TorD (2) is still better.

The sequencing identified three mutations in the *tatBE.c.21C.g.139* gene: one silent mutation at position 162 which alters the serine codon from AGT to AGC. The inspection of a codon usage database[11] showed that AGC is the two-fold preferred codon for serine in *E. coli* K12. Furthermore, $TatB_{Z3}$ has a mutation within the amphipathic helix resulting in E58K which exchanges the acidic glutamate for a basic lysine. The glutamate residues of the *E. coli* TatB amphipathic helix (positions 49, 53, 58) have been shown to be highly important for TatB functionality. When the amino acid sequence of the amphipathic helix is modeled three-dimensionally, they are all three located to one side of the helix and have been discussed to act as an interaction interface during the recognition process of the signal peptide (Hicks et al., 2003). Both wild-type $TatB_{C.g.}$ as well as the hybrid molecule $TatB_{E.c.21C.g.139}$ have two glutamate residues in the center of the amphipathic helix at positions 58 and 61. Using a bioinformatic tool[12] to map the secondary structure of α-helices it showed that in the *C. glutamicum* amphipathic helix these are also oriented towards one side of the helix. Thus, a mutation E58K could possibly have a strong effect on TatB functionality. Lastly a nonsense mutation was present at position 316 that leads to a TGA stop codon resulting in a TatB molecule truncated by the last 52 amino acid residues.

Again, the implications of the mutation E58K within the amphipathic helix of $TatB_{Z3}$ for the functionality of the TatB molecule are hard to evaluate. The silent mutation at position 162 is probably without major consequences. Noticeable is the mutation at position 316 which results in a TGA stop-codon leading to a C-terminal truncation of $TatB_{Z3}$ by 52 amino acids. As could be shown above (see page 66f.), the C-terminal truncation of more than 40 amino acids from $TatB_{C.g.}$ leads to a molecule that, when used to complement a *tatB*-mutant strain, is, although not able to support export of the endogenous amidases necessary for growth on SDS-containing media, able to export the artificial substrate $TorA^{SP}$-MalE in amounts high enough to allow very limited growth on maltose minimal medium (see figure 33). For this reason, it seems likely that in conjunction with the mutation E58K a TatB molecule was generated which has a severely reduced activity within the translocase.

The third gain-of-function mutant TatB molecule $TatB_{Z4}$ is also based upon $TatB_{E.c.21C.g.139}$. Figure 41 shows the growth of the *E. coli tatB*-mutant BØD with $TatB_{Z4}$ and $TorA^{SP}$-MalE on maltose minimal medium plates. In the absence of TorD (sector 8), growth is nearly good as that of the wild-type strain control (3). In the presence of TorD (7), no restriction compared to the control without TorD is apparent, although the wild-type control without TorD still grows better (2).

In $TatB_{Z4}$ two mutations were found. The first one is actually upstream of the *tatB* gene at position -2. Whether this mutation is influential is hard to say. Mutations upstream of the Shine Dalgarno sequence in the 5' untranslated region have been shown to sometimes have a serious effect on the translation initiation frequency because of altered mRNA secondary structure leading to an impaired recognition by the translation apparatus (Coleman et al., 1985). The second mutation leads to V18A found at the cytoplasmically oriented end of the transmembrane domain. A mutation of an amino acid

11. Codon Usage Database; Kazuza, Japan: http://www.kazusa.or.jp/codon/

12. EMBOSS pepwheel; European Bioinformatics Institute, UK http://emboss.bioinformatics.nl/

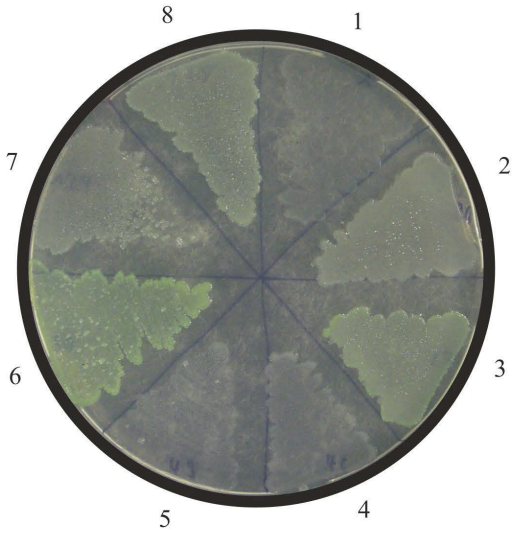

		pBBR	pHSG	pTrSp	growth on MM
1	MC4100 WT Δ*malE*	-	-	-	-
2		TorA-MalE	-	TorD	++
3			-	GFP	++
4	BØD Δ*tatB* Δ*malE*	TorA-MalE	-	-	-
5			$TatB_{C.g.}$	TorD	-
6				GFP	++
7			$_{ep}TatB_{Z3}$	TorD	+
8				GFP	+

Figure 40: *E. coli tatB*-mutant strain expressing mutant $TatB_{Z3}$ (based upon $TatB_{E.c.21C.g.139}$) which promotes growth in presence of TorD. Selection for export of $TorA^{SP}$-MalE *in situ* on maltose minimal medium agar plates. The *E. coli* strains were transformed according to the table in the figure, grown overnight in LB-medium, diluted to an OD=0,1 and subsequently streaked onto maltose minimal medium agar plates. Incubation occured at 37ºC for ~48 hours (++ wild-type growth + limited growth - no growth).

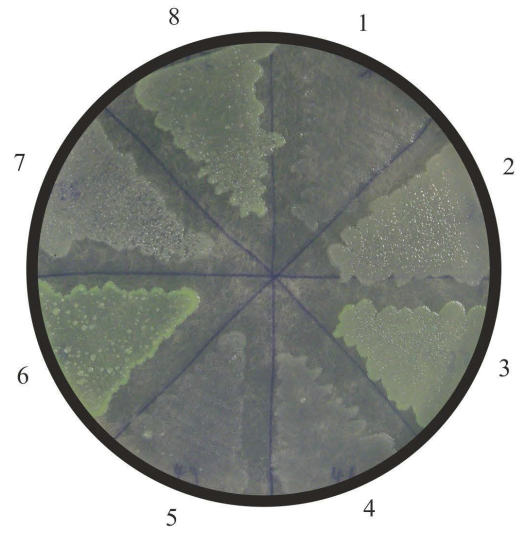

		pBBR	pHSG	pTrSp	growth on MM
1	MC4100 WT Δ*malE*	-	-	-	-
2		TorA-MalE	-	TorD	++
3			-	GFP	++
4	BØD Δ*tatB* Δ*malE*	TorA-MalE	-	-	-
5			$TatB_{C.g.}$	TorD	-
6				GFP	++
7			$_{ep}TatB_{Z4}$	TorD	+
8				GFP	+

Figure 41: *E. coli tatB*-mutant strain expressing mutant $TatB_{Z4}$ (based upon $TatB_{E.c.21C.g.139}$) which promotes growth in presence of TorD. Selection for export of $TorA^{SP}$-MalE *in situ* on maltose minimal medium agar plates. The *E. coli* strains were transformed according to the table in the figure, grown overnight in LB-medium, diluted to an OD=0,1 and subsequently streaked onto maltose minimal medium agar plates. Incubation occured at 37ºC for ~48 hours (++ wild-type growth + limited growth - no growth).

at position 18 of TatB has not yet been described. What is known is that mutations in the hinge region

between transmembrane domain and amphipathic helix at positions L20, G21 and P22 in *E. coli* are critical for the function of the translocase (Hicks et al., 2003).
Under the assumption that the mutation at position -2 of $TatB_{Z4}$ has a negative effect on translation initiation, the amount of this TatB molecule would be reduced in the cell. If this reduction of TatB biosynthesis was drastic enough, the $TatB_{Z4}$ mutant would be analogous to the mutant TatB molecule $TatB_{X3}$ which is probably expressed at a low level. Additionally, the mutation within its transmembrane domain could have an effect on the functionality of the molecule within the translocase.
In summary, the common characteristic of these three suppressor mutants is that they indicate either being expressed at low expression levels or carry mutations within the amphipathic helix or transmembrane domain which could lead to very limited functionality in Tat-dependent translocation. These results suggest that under presence of TorD and the applied selection pressure, a reduction in the amount and activity of $TatB_{C.g.}$ or $TatB_{E.c.21C.g.139}$ had occured.
$TorA^{SP}$-MalE is a highly sensitive reporter enzyme and it could be shown that when *E. coli* TatAC are overexpressed from a plasmid in an *E. coli tat*$^-$ strain, limited growth on maltose minimal medium is possible (Blaudeck et al., 2005). As the *tatB*-mutant strain used for the above experiments (which contains genomically encoded TatAC) is unable to grow on maltose minimal when not complemented with a TatB molecule, it can be deduced that the observed growth cannot be via a TatAC translocase and at least small amounts of the generated mutant TatB molecules are made and partake within the translocase. These low functionality or low abundance TatB molecules which support just enough export of MalE into the periplasm to allow growth on maltose minimal medium are not influenced by the presence of TorD. Two conclusions can be drawn from theses mutagenesis experiments: Firstly, both $TatB_{C.g.}$- and $TatBE.c._{21}C.g._{139}$-presence within the translocase are problematic when TorD is present and selection pressure leads to a minimization of this negative influence within the translocase. Secondly, the expression of TorD in a *tatB*-mutant strain expressing any of the above described mutant TatB molecules does not seem to have a negative influence (in comparison to the situation without TorD) any more. This indicates that, at the expense of overall translocation efficiency, the resulting translocases gain the ability to better cope with the presence of TorD. One possible explanation for this could be that while these translocases are slow and ineffective, they could have an advantage over translocases containing unmutagenized $TatB_{C.g.}$, in for example having a slightly higher efficiency in the binding of free signal peptides or the association of the substrate to the translocase.

3.2.5 TatB-presence is not absolutely necessary for the release of TorD from $TorA^{SP}$-MalE

Three mutant TatB molecules were described in the previous section that in presence of TorD led to growth on maltose minimal medium, when expressed in an *E. coli tatB*-mutant strain. What distinguished these *tatB* variants was that they exhibited mutations which indicate that they might either reduce TatB-function or lead to very low expression levels. For this reason, it was hypothesized that $TatB_{C.g.}$ (or hybrid $TatBE.c._{21}C.g._{139}$) presence in the Tat-translocase could be a hindrance for export of a $TorA^{SP}$-substrate in the presence of the REMP TorD.
To be able to test the effect of TorD coexpression in the complete absence of TatB, the following growth experiments were carried out in an *E. coli* strain with a complete deletion of all *tat*-genes (DADE Δ*tatABCDE* Δ*malE*). To simulate the wild-type situation, the *tat*$^-$ strain was complemented with TatABCE, expressed from the IPTG-inducible vector pHSG_TatABCE. To obtain a constellation of the Tat translocase in which TatB is absent, analogous to the assumed situation after mutagenesis of $TatB_{C.g.}$ (see page 73ff.), *E. coli* DADE was complemented with pHSG_TatAC for expression of TatA

and TatC. A TatAC translocase does, in principal, not allow translocation of Tat-dependent substrates. An exception is the artificial substrate TorA^{SP}-MalE which can be exported in small amounts and allows growth on maltose minimal medium provided that TatAC are overexpressed from a plasmid (Blaudeck et al., 2005). Further translocases tested for coexpression of TorD are two efficient TatAC minimal translocases which were selected after chemical mutagenesis (Blaudeck et al., 2005). These minimal translocases TatAC$_{M2}$ (TatA: G3D) and TatAC$_{M5}$ (TatA: I6S) carry mutations in the extreme N-terminus of TatA which renders these components bifunctional i.e. able to functionally compensate for the absence of TatB functionally (also see introduction page 8). An *E. coli* Δ*tat* strain expressing the artificial translocase TatAC$_{M5}$ is able to export TorA^{SP}-MalE in an amount of approximately 40% in comparison to the strain complemented with the whole translocase TatABCE. TatAC$_{M2}$ expression allows around 20% export of TorA^{SP}-MalE in comparison to TatABCE (Blaudeck et al., 2005).

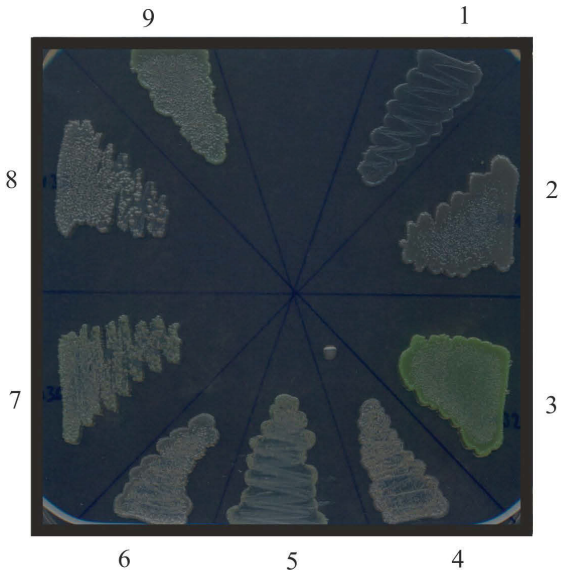

		pBBR	pHSG	pTrSp	growth on MM
1	DADE Δ*tat* Δ*malE*	-	-	-	-
2		TorA-MalE	TatABCE	TorD	++
3				GFP	++
4			TatAC$_{WT}$	TorD	+
5				GFP	+
6			TatAC$_{M2}$	TorD	++
7				GFP	++
8			TatAC$_{M5}$	TorD	++
9				GFP	++

Figure 42: The *E. coli* strain DADE (Δ*tatABCDE* Δ*malE*) expressing artificial TatAC translocases is not affected by TorD coexpression. Growth on maltose minimal medium of strains expressing TorA^{SP}-MalE (transformed with vectors according to table). Strains were cultivated overnight, diluted to an OD$_{600nm}$ of 0,1, streaked onto the agar plates and incubated at 37ºC for ~48 hours (+ limited growth ++ moderate growth +++ wild-type growth).

The growth of the *E. coli* DADE (Δ*tatABCDE* Δ*malE*) strain expressing TorA^{SP}-MalE and minimal translocases with bifunctional TatA proteins in presence of TorD are shown in figure 42. The *E. coli* Δ*tat* strain complemented with the entire translocase TatABCE grows well in presence (sector 2) or in absence (3) of TorD. The complementation of the *E. coli* DADE strain with unaltered TatAC allows limited growth on maltose minimal medium (5) and the presence of TorD does not inhibit this growth (4). The same applies to the *E. coli* DADE strain expressing either of the two minimal translocases with bifunctional TatA molecules TatAC$_{M2}$ and TatAC$_{M5}$. In absence of TorD, the growth of these two strains (7, 9) is better than that of the strain expressing unaltered TatAC (5) but not as good as the positive control expressing the whole operon TatABCE (3). Nonetheless, the coexpression of TorD also has no influence on the growth of these strains on maltose minimal medium (6, 8).
Obviously the absence of TatB reduces the efficiency of the relevant strains to export TorA^{SP}-MalE but this reduction in translocation efficiency does not seem to have an influence on the strains to release TorD from the TorA signal peptide of MalE. More importantly, these growth experiments indi-

cate that TatB is not functionally necessary within the translocase to mediate this release mechanism in an active sense.

3.2.6 Conclusion II: Disturbing the integrity of the Tat-translocase results in incompatibility with TorD

The release of TorD from the TorA signal peptide requires a reasonably well functioning Tat-translocase. Impairing the integrity of the translocase reduces its ability to compete with TorD for free signal peptides of the $TorA^{SP}$-substrate and translocate it. The translocase integrity can be disturbed by several factors. For instance by the presence of the heterologous TatB molecule from *C. glutamicum* within the translocase. Although $TatB_{C.g.}$ is able to substitute for missing *E. coli* TatB, the obvious differences in structure, amino acid composition and amphipathic helix substructure make it inferior to the evolutionarily optimized homologous molecule in conjunction with *E. coli* TatAC when TorD is present. A further disturbance of translocase integrity seems to result from the overexpression itself of TatB molecules in an *E. coli tatB*-mutant. Possibly, this results in a faulty stochiometry of Tat-components. The relationship between translocase efficiency and the ability of the strain to export the $TorA^{SP}$-substrate could be shown by the expression of *E. coli/C. glutamicum* hybrid TatB molecules. The more the TatB molecule resembles the homologous *E. coli* TatB protein, the higher the export efficiency in absence of TorD and the lower the export block effect in presence of TorD. Vice versa, the more the TatB molecule resembles the *C. glutamicum* TatB protein the lower the export efficiency in absence of TorD and a stronger export block in presence of TorD.
Regarding the postulated release mechanism of TorD, the experiments carried out in this work were not able to define a specific residue or secondary structure within $TatB_{C.g.}$ which could be involved. Neither in negatively preventing release of the substrate by TorD nor positively missing within the molecule and thereby precluding productive interaction of the $TatB_{C.g.}$-containing translocase with the TorD/$TorA^{SP}$-substrate complex to mediate the release of TorD from the substrate. In the contrary, it seems that for this postulated release mechanism TatB does in fact not necessarily need to be present which would indicate that the TatB molecule does not partake in a specific release mechanism.
It seems likely that a kinetic partitioning of free $TorA^{SP}$-substrate molecules between (re)binding to TorD and binding to the TatBC receptor complex exists. Supposedly, TorD exhibits a mechanism in which the $TorA^{SP}$-substrate molecule is repeatedly bound and released. Translocation of the $TorA^{SP}$-substrate can thus only occur when TorD is not blocking the signal peptide which both TorD and the Tat-translocase require for recognition. It is furthermore likely that to achieve a beneficial effect out of TorD coexpression a ratio of TorD:$TorA^{SP}$-substrate molecules has to be in favor of the substrate to prevent titration away from the translocase.

4. Discussion

4.1. *Corynebacterium glutamicum* possesses an ABC-type Tat-translocase

The majority of Gram-positive bacteria belong to the phylum of low G/C-content *Firmicutes* such as the classes of *Bacilli* or *Clostridia*. In most cases, their genomes contain at least one copy of *tatA* and one copy of *tatC* which are usually found within a *tatAC* operon (Simone et al., 2013). The Tat-dependent protein translocation of these organisms is performed by a TatAC-type "minimal-translocase" in which a bifunctional TatA protein is also able to fulfill the role assigned to TatB in Gram-negative bacteria. The vast majority of Gram-negative bacterial genomes on the other hand, such as the members of the class of γ-*Proteobacteria* like *Salmonella ssp.* or *Escherichia ssp.*, contain a copy of *tatB* which is, with very few exceptions, found in a *tatABC* operon architecture (Simone et al., 2013) and translocation occurs via a TatABC-type translocase. In these organisms TatB is necessary for full functionality of the translocase because the mechanistic roles of TatA and TatB within the translocation process are clearly different (Sargent et al., 1999).
In contrast, the genomes of high G/C-content Gram-positive bacteria belonging to the class of *Actinobacteria,* such as *Mycobacterium ssp., Rhodococcus ssp., Nocardia ssp.* or *Corynebacterium ssp.* contain a *tatAC* operon, reminiscent of the situation in low G/C Gram-positive bacteria, as well as a monocistronic *tatB* gene elsewhere in the genome[13]. Noticeably, in *Mycobacterium tuberculosis* the deletion of *tatB* is not possible, indicating the essentiality of the Tat-pathway and the importance of TatB for the functioning of the pathway in this pathogenic organism (Saint-Joanis et al., 2006). These results strongly suggest than an ABC-type Tat-translocase might be the functional unit for Tat-dependent protein translocation in the actinobacterium *M. tuberculosis.*
A somewhat different scenario was published by Kikuchi et al. (2006) for another member of the actinobacteria, *C. glutamicum*, in which *tatA* and *tatC* are encoded in a *tatAC* operon (*cg1685, cg1684*) and elsewhere on the genome a copy of a *tatB* homologue (*cg1273*) as well as an additional copy of *tatA* (*tatE; cg3381*) are found. While the *tatE* gene is probably only a cryptic gene duplication of *tatA* and the corresponding gene products are redundant in function, the role of *tatB* was yet unclear. The first comprehensive characterization of Tat-dependent translocation in *C. glutamicum* by Kikuchi et al. (2006) showed that the deletion of either of the genes *tatA* or *tatC* led to a serious growth defect of the corresponding deletion mutant strains in comparison to the wild-type strain. A *tatB*-mutant strain on the other hand grew nearly as well as the wild-type strain control. They also tested for the export of a plasmid-expressed heterologous substrate $TorA^{SP}$-GFP, the signal peptide of the *E. coli* TMAO reductase TorA fused to the green fluorescent protein. Both the *tatA*- and the *tatC*-mutant were unable to secrete this strictly Tat-dependent substrate. In contrast, the *tatB*-mutant strain showed significantly reduced but nevertheless substantial translocation of the substrate $TorA^{SP}$-GFP (Kikuchi et al., 2006). Judging from these results, several possible conclusions could be drawn. Considering that the growth inhibition observed in the *tatA*- and *tatC*-mutants is due to a physiologically important natural substrate not being able to be exported via the Tat-pathway, it seems self-evident that TatB is either not or only marginally involved in the translocation of this substrate. The same applies to the secretion of

13. See genome database http://www.kegg.jp.

TorA^{SP}-GFP. While the presence of TatB seems beneficial, it seems not to be essential for the translocation.

In summary, the results of Kikuchi et al. (2006) suggest that, in contrast to *M. tuberculosis*, *C. glutamicum* might utilize a TatAC-type translocase, as found in low-G/C genome containing Gram-positive bacteria. The role of TatB remains unclear although it seems to fulfill a function which is beneficial for Tat-dependent translocation. In *E. coli* for example, the absence of TatB precludes the translocation of most natural substrates although a rest translocation activity can be observed for some artificial substrates providing the assay used is sensitive enough (Sargent et al., 1999; Ize et al., 2002; Blaudeck et al., 2005). Looking at the growth phenotypes of the *C. glutamicum tat*-mutants as described by Kikuchi et al. (2006), a TatAC minimal translocase seems sufficient to efficiently export the natural substrate that is required for unimpaired growth. Regarding the export of TorA^{SP}-GFP, a TatAC minimal translocase also seems sufficient for at least basal export levels. These findings of Kikuchi et al. (2006) were more than surprising since, as mentioned above, for the close relative of *C. glutamicum*, the also diderm-mycolate actinobacterium *M. tuberculosis*, the essentiality of TatB not only for Tat-dependent translocation but also for viability was demonstrated (Saint-Joanis et al., 2006).

However, one further possibility also has to be considered. In the low G/C-content Gram-positive bacterium *B. subtilis*, three copies of *tatA* and two copies of *tatC* are found within the genome. $TatA_YC_Y$ is the main translocase expressed under all conditions and $TatA_DC_D$ is solely expressed under conditions of phosphate starvation (Jongbloed et al., 2004). Furthermore a fifth subunit $TatA_C$ has been identified to which yet neither a physiological translocase nor a natural substrate could be assigned (Monteferrante et al., 2012a). The discovery of two Tat-translocases working in parallel was quite spectacular and in following investigations it turned out that not only these two combinations of TatA and TatC, namely $TatA_YC_Y$ and $TatA_DC_D$, could form a functional translocase. While functionality for a $TatA_YC_D$ translocase could not be shown (Barnett et al., 2008), a $TatA_DC_Y$ translocase was functional when $TatA_D$ was expressed at high levels in a *B subtilis* $tatA_Y$-mutant (Eijlander et al., 2009). Both $TatA_CC_Y$ and $TatA_CC_D$ translocases were functional when heterologously expressed in an *E. coli* Δ*tatABCDE* background (Monteferrante et al., 2012a). Furthermore, it was shown in yeast-2-hybrid interaction analyses that all three TatA molecules of *B. subtilis* could form not only homo- but also heterodimers (Monteferrante et al., 2012a). Taken together, these findings imply the theoretical possibility of a most intricate network of TatA and TatC subunits forming specific translocases for specific substrates in *B subtilis*.

Back to the unclear role of *C. glutamicum* TatB, this also means that the possibility of not only a TatAC but also a "TatBC" translocase for specific substrates has to be taken into consideration. This assumption is based on the knowledge that TatA and TatB molecules, although fulfilling different mechanistic roles in ABC-type Tat-translocases, are closely related in structure. It should be taken into consideration that possibly, *C. glutamicum* Cg1273 (putative TatB) might in fact be a further *C. glutamicum* TatA molecule. If Cg1273 would also be bifunctional, as the results of Kikuchi et al. (2006) suggest for the *C. glutamicum* TatA molecule, this could mean the presence of a second minimal translocase (sloppily termed "TatBC"-translocase for means of better understanding). In summary, based on the contradicting results described for *M. tuberculosis* and *C. glutamicum*, it is unclear what kind of Tat translocase is in fact utilized in *Actinobacteria.*

The aim of this work was to get a deeper insight into the role of the putative *C. glutamicum* TatB protein and to clarify the actual subunit composition of the active endogenous Tat-translocase(s). Surprisingly, the reconstruction and characterization of *C. glutamicum tatAC*, *tatA/E* and *tatB* mutants revealed severe differences to the findings of Kikuchi et al. (2006). Other than described, a *C. glutamicum tatB*-mutant strain showed a severe growth defect, comparable to that of the *tatAC*- or

tatA/E-mutant strains (see figure 11) which implies that TatB is after all essential for the membrane translocation of the physiologically important substrate. To eliminate the possibility of this *tatB*-mutant strain growth phenotype being due to secondary mutations obtained during the deletion procedure, three *C. glutamicum tatB*-mutants were constructed independently using two different in-frame deletion-vector systems. All three Δ*tatB* strains behaved identical in the way described above which demonstrates, with certainty, the importance of TatB in *C. glutamicum* Tat-dependent translocation.
Also, the obtained results regarding the secretion capabilities of *C. glutamicum tat*-mutant strains with respect to the secretion of heterologous substrates stand in contradiction to Kikuchi et al. (2006). In the present work, two different substrates were tested for translocation: $TorA^{SP}$-GFP (figure 14), the *E. coli* signal peptide of TMAO reductase fused to the green fluorescent protein and $PhoD_{C.g.}{}^{SP}$-GFP (figure 15), a homologous signal peptide of *C. glutamicum* alkaline phosphatase PhoD fused to the green fluorescent protein. It was found that the three *C. glutamicum tat*-mutant strains, Δ*tatAC,* Δ*tatA/E* and Δ*tatB* were equally unable to export either of these substrates. Importantly and in stark contrast to the results described by Kikuchi et al. (2006), no residual translocation of these substrates in the *tatB*-mutant strain was observed, leading to the conclusion that TatB presence is absolutely necessary for their translocation.
Why the *C. glutamicum tatB*-mutant strain of Kikuchi et al. (2006) behaves so fundamentally different to the *tatB*-mutant strain constructed in this work can only be speculated upon. It has to be noted that the wild-type strain in this study, *C. glutamicum* ATCC 13032, differs from the strain *C. glutamicum* ATCC 13869 used by Kikuchi et al. (2006). Importantly, it has to be noted that *C. glutamicum* ATCC 13869 is a biotechnologically relevant production strain (for current european patents on this strain see Date et al., 2002 or Kikuchi et al., 2009) that has undergone extensive chemical mutagenesis with MNNG (Date et al., 2004). MNNG (1-methyl-2-nitro-1-nitrosoguanidine) is a strong alkylating reagent leading to transition mutations by addition of an alkyl group to the O^6 of guanine or the O^4 of thymine. This harsh mutagenic treatment could have resulted in mutations within the *tat*-genes leading, for example, to a bifunctional TatA molecule that can, at least partially, compensate for the loss of the TatB function. In line with this, Blaudeck et al. (2005) could demonstrate that only one or two mutations within the extreme N-terminus of TatA in *E. coli* render this TatA molecule bifunctional and thus able to substitute for TatB function.
Taken together, this study clearly shows that *C. glutamicum* TatB, like TatA and TatC, is absolutely necessary for export of the physiologically important substrate responsible for the delayed growth phenotype in *tat*-mutants as well as for export of two artificial substrates, $TorA^{SP}$-GFP and $PhoD_{C.g.}{}^{SP}$-GFP. This leads to the conclusion that *C. glutamicum* ATCC 13032 possesses a Tat-translocase of the ABC-type as found in most Gram-negative prokaryotes. Taken together with the finding that *M. tuberculosis* also relies on a TatB molecule for a functioning translocase (Saint-Joanis et al., 2006), it seems likely that TatABC-type translocases are the functional units for Tat-dependent protein translocation throughout the phylum *Actinobacteria*.

4.1.1 The physiologically important *C.glutamicum* Rieske protein is translocated Tat-dependently

The deletion of either *tatA/E, tatB,* or *tatC* leads to inhibited growth of *C. glutamicum* (see figure 11). For several other organisms, it could be shown that they suffer from a similar growth defect under aerobic growth conditions upon deletion of the *tat*-genes (Luo et al., 2013; Wagley et al., 2014). Due to the nature of proteins associated with respiratory chains to contain co-factors, it seems obvious that some of these might rely on the Tat-translocase for export or membrane integration. Molik et al.

(2001) in fact showed that the Tat-translocase is responsible for the integration of the Fe/S-cluster containing Rieske protein, a subunit of the cytochrome b_6/f complex, into the thylakoid membrane of plant chloroplasts. In the Gram-negative *Proteobacteria Paracoccus denitrificans*, *Legionella pneumophila* and *Shewanella oneidensis,* it could subsequently further be demonstrated that the assembly of the cofactor-containing Rieske protein is also strictly Tat-dependent in these bacteria (Bachmann et al., 2006; De Buck et al., 2007; Luo et al., 2013).
Recently, the Tat-dependent membrane integration of the Rieske protein of *Streptomyces coelicolor*, belonging to the subclass of *Actinobacterideae* just like *C. glutamicum*, was firstly shown for a Gram-positive bacterium (Keller et al., 2012; Hopkins et al., 2014). Interestingly, and other than in Gram-negative and low-G/C content Gram-positive bacteria, the membrane integration of the Rieske protein in *S. coelicolor* is a two-step process involving the general Sec translocation pathway as well as the Tat-pathway. The Rieske protein of *S. coelicolor* possesses three transmembrane domains, the first two of which are inserted into the cytoplasmic membrane by the Sec translocase. Following this first integration process, the association with the iron-sulfur-complex takes place intracellularly. In the final step, an integral Tat consensus motif located just in front of the third transmembrane domain is recognized by the Tat-translocase and the mature cofactor-containing domain of the Rieske protein is translocated to the trans side of the membrane into its active conformation (Keller et al., 2012).
The Rieske protein QcrA of *C. glutamicum*, just like the one in *S. coelicolor,* has three transmembrane domains. A global sequence comparison reveals that this is presumably a unique feature of *actinobacterial* Rieske proteins, which seem to have evolved differently than Rieske proteins of other bacteria (Schmidt and Shaw, 2001). QcrA is part of the bc_1-aa_3 supercomplex of the aerobic respiratory chain which is composed of a menaquinol:cytochrome c oxidoreductase (cytochrome bc_1 complex) and a cytochrome aa_3 oxidase (Niebisch and Bott, 2001; Niebisch and Bott, 2003). The physiological importance of QcrA becomes apparent in a *qcrA*-mutant strain which exhibits a very strong growth defect, identical to that of *tatAC*, *tatB* or *tatA/E* mutant strains (see figure 16). This ultimately led to locating an internal Tat consensus motif in front of the third transmembrane domain of *C. glutamicum* QcrA (see protein sequence in figure 17). To verify that the membrane integration of the Rieske protein QcrA also takes place in a Tat-dependent manner in *C. glutamicum*, a variant of QcrA with two lysine residues instead of two arginine residues in the internal Tat-motiv was constructed. Translocation of a substrate with a Tat signal peptide altered in such way is strongly impaired (Berks et al., 2003). Next, it was shown that wild-type $QcrA_{RR}$ but not mutated $QcrA_{KK}$ was able to complement a *C. glutamicum* Δ*qcrA* strain in its growth defect (figure 18). This is strong evidence that mislocalized QcrA is the Tat substrate responsible for the growth defect of *C. glutamicum tat*-mutants and that an intact Tat apparatus is necessary for the membrane integration. Until now, the cooperative membrane integration of Rieske proteins by both the Sec- and the Tat-pathway has only been demonstrated in *Actinobacteria*. The Tat-pathway and its function in Rieske protein membrane integration is, for example, a prerequisite for the pathogenicity of *Burkholderia thailandensis* (Wagley et al., 2014). In the Gram-negative bacterium *Rhizobium leguminosarum* it is essential for symbiosis with pea plants (Meloni et al., 2003) and the cyanobacterium *Synechocystis* integrates a total of three Rieske proteins via the Tat-pathway (Aldridge et al., 2008).
To strengthen the point of *C. glutamicum* possessing an ABC-type Tat-translocase, the necessity of TatB involvement in QcrA membrane integration had to be shown. As discussed in the previous chapter, the growth phenotype of the *C. glutamicum tatB*-mutant of Kikuchi et al. (2006) did not exhibit the growth defect observed for a *tatA*- or *tatC*-mutant which would imply TatB not being needed for membrane integration of the Rieske protein. The *tatB*-mutant constructed for this work on the other hand showed the same growth deficit as *tatAC*- or *tatA/E*-mutants, indicating that TatB is in fact ab-

solutely required for membrane integration of QcrA. Therefore, a *qcrA/tatB* double-mutant was finally constructed and tested for possible complementation by wild-type QcrA (figure 19). As the growth phenotype of the double mutant, other than the *qcrA* single mutant, could not be reverted to the growth of the wild-type strain, it can now definitely be concluded that the presence of TatB is mandatory for the membrane integration of QcrA. This finding strongly supports the view that *C. glutamicum* utilizes an ABC-type translocase for Tat-dependent protein translocation.

4.1.2 *C. glutamicum* TatB is not bifunctional and thus a *bona fide* TatB protein

TatB has a very specific function within the translocation process of TatABC-style translocases such as the one in Gram-negative bacteria like *E. coli* or in the thylakoid membranes of plant chloroplasts. This TatB function can clearly be distinguished from the mechanistic function of TatA. Together with TatC, TatB forms a TatBC receptor complex within the membrane. This TatBC complex has a 1:1 stochiometry of TatB to TatC molecules (Bolhuis et al., 2001). During the initiation of the translocation process, the signal peptide of the substrate is bound by this receptor complex (Cline and Mori, 2001). Crosslinking studies have shown that while TatC binds to the Tat consensus motif which contains the arginine pair, TatB has contact to a large proportion of the signal peptide (Fröbel et al., 2012). Only after binding of the substrate by the TatBC complex, a recruitment of TatA multimers takes place (Dabney-Smith et al., 2006; Dabney-Smith and Cline, 2009). The TatA oligomers of varying size are responsible for forming the protein conducting channel through which the export substrate is transported across the membrane (Gohlke et al., 2005). Alternatively, according to another theory, TatA multimers result in a local weakening of the membrane through which the substrate is pulled out of the cytoplasm (Rodriguez et al., 2013).
In *E. coli,* the two proteins TatA and TatB resemble each other closely in amino acid sequence, both bearing one transmembrane domain followed by an amphipathic helix and both having an N-out/ C-in topology (Koch et al., 2012). Although an *E. coli tatB*-mutant cannot be complemented by TatA and vice versa (Sargent et al., 1999), one or two mutations within the extreme N-terminus of TatA are sufficient to convert TatA into a bifunctional Tat component that, besides the TatA function, is also able to fulfill the role of TatB (Blaudeck et al., 2005). For its role within the TatBC complex in binding the signal peptide of the substrate, TatB's critical features are found within the N-terminus and the transmembrane domain (Blaudeck et al., 2005; Barnett et al., 2011). The feature critical for functionality of TatA on the other hand seems to be the amphipathic helix as could be shown by generation of loss-of-function TatA mutations (Hicks et al., 2005) or by cysteine scanning mutagenesis (Greene et al., 2007).
To obtain further evidence that the Tat-translocase of *C. glutamicum* is functionally a translocase of the ABC-type, it was tested whether $TatB_{C.g.}$ could fulfill the distinct function of *E. coli* TatB in an *E. coli tatB*-mutant strain. Barnett et al. (2008) could demonstrate the bifunctionality of *B. subtilis* $TatA_D$ by showing that both an *E. coli tatA*/E- and a *tatB*-mutant could be restored in their secretion capabilities when $TatA_D$ was expressed *in trans*. Analogous to this approach, $TatB_{C.g.}$ was expressed in an *E. coli tatB*-mutant (see figure 20). When assayed for growth on solid media containing 4% SDS, $TatB_{C.g.}$ could fully complement the *tatB*-mutant strain for export of the endogenous amidases AmiA and AmiC which are strictly Tat-dependently exported and necessary for growth of *E. coli* on SDS-containing media (Bernhardt and de Boer, 2003). This shows that *C. glutamicum* TatB can indeed substitute for *E. coli* TatB. In parallel, it could also be shown that *C. glutamicum* TatA is not able to fulfill *E. coli* TatB function.

Further evidence against a bifunctionality of *C. glutamicum* TatB was the expression of $TatB_{C.g.}$ in an *E. coli tatA/E*-mutant (see figure 21). Due to the fact that $TatB_{C.g.}$ was unable to complement this *tatA/E*-mutant, the conclusion can be drawn that the function of TatA, namely the formation of the protein translocation channel, cannot be fulfilled by $TatB_{C.g.}$, at least not in *E. coli*. Nevertheless, these results are no final evidence against a $TatB_{C.g.}$ bifunctionality as it cannot be totally excluded that $TatB_{C.g.}$ behaves differently in *C. glutamicum*, i.e. that it is able to fulfill TatA function when present in its native environment. But regarding this result in conjunction with the growth and export experiments with the *tatB*- and *tatA/E*-mutant strains outlined above, a coherent elimination of $TatB_{C.g.}$ bifunctionality has been demonstrated. Surprisingly, the control experiment of $TatA_{C.g.}$ expression in an *E. coli tatA/E* mutant did not lead to growth on SDS either. To test whether expression of $TatA_{C.g.}$ actually takes place whole cell extracts of the *E. coli tatB*-mutant with the $TatA_{C.g.}$-expression vector were made and conspicuous bands, not appearing in the empty vector control, analyzed by MALDI-TOF for the presence of TatA. It was unsuccessful to identify $TatA_{C.g.}$ in this approach but a strong induction of the *E. coli* phage shock protein PspA in relation to the control strains could be seen. PspA, a membrane-stress response protein, has been shown to be induced in *E. coli* upon elevated levels of (homologous) TatA as overexpression of this membrane protein leads to a destabilization of the membrane. Also TatA and PspA can be co-purified under these conditions (Mehner et al., 2012). Although this is only indirect evidence, the expression of $TatA_{C.g.}$ in *E. coli* Δ*tatA/E* is thus likely to take place. Presumably, $TatA_{C.g.}$ is simply not compatible with the *E. coli* TatBC receptor complex so that the recruitment of $TatA_{C.g.}$ oligomers after binding of the substrate to the receptor complex does not take place.
The inability of $TatA_{C.g.}$ to complement the *E. coli tatA/E*-mutant strain for TatA function of course somewhat weakens the conclusion of $TatB_{C.g.}$ not being able to fulfill TatA-function in *E. coli*. It could theoretically be possible that also $TatB_{C.g.}$, although capable of fulfilling TatB-function in an *E. coli tatB*-mutant, also has TatA-functionality (i.e. is bifunctional) but not in combination with the *E. coli* TatBC receptor complex for the same reasons of incompatibility just like $TatA_{C.g.}$. However, this is considered highly unlikely when regarding these results in combination with the inability of a *C. glutamicum tatA/E* mutant to translocate $TorA^{SP}$-substrates as well as to translocate QcrA.
In summary, strong evidence for a *C. glutamicum* Tat-translocase of the ABC-type has been presented as it could be shown that TatB is essential for the translocation of the physiologically important Tat-substrate QcrA and artificial $TorA^{SP}$-substrates. In support of this finding, an analogy to the *E. coli* ABC-type translocase could be demonstrated by showing that $TatB_{C.g.}$ functionally corresponds to *E. coli* TatB and is as such a *per definitionem* TatB protein.

4.2. Impairing translocase integrity results in incompatibility with the REMP TorD

The cytoplasmic *Escherichia coli* redox enzyme maturation protein (REMP) TorD is a crucial player in the biogenesis of the Tat-dependently exported periplasmic TMAO reductase TorA (Pommier et al., 1998; Ilbert et al., 2003). The *torCAD* operon of *E. coli* constitutes the main anaerobic pathway for the reduction of trimethylamine-N-oxide to trimethylamine (Jourlin et al., 1996). Herein, the chaperone TorD, which is highly specific for the TorA signal peptide, protects *apo*TorA from premature proteolysis and premature export before the cytoplasmic integration of a molybdenum cofactor has taken place and mature TorA is translocated via the Tat-pathway. Although the deletion of *torD* does not completely impair this pathway, a significant reduction of TorA reductase activity can be measured

(Pommier et al., 1998).
The translocation of misassembled or malfolded substrates constitutes a waste of energy for the cell. For this reason, it has been suggested that the Tat-translocase possesses an intrinsic folding quality control mechanism which prevents the export of substrates which are either not folded correctly or have been misassembled, i.e. are missing a necessary co-factor or have not oligomerized properly (DeLisa et al., 2003). For specific complex co-factor containing substrates it has been suggested that REMPs, such as TorD, fulfill an additional quality control mechanism which was termed "Tat-proof-reading" (Sargent, 2007). It was initially thought that this mechanism would only apply for the specific substrates of the respective REMP. Then, Li et al. (2006) reported that a coexpression of TorD and a fusion of the TorA signal peptide to GFP ($TorA^{SP}$-GFP) led to a two to four-fold increase in the amount of exported GFP in *E. coli*. The ability to increase the quantity and quality of an exported heterologous substrate of course opened up the question whether TorD coexpression could be applied beneficially in a biotechnological protein production background .

4.2.1 Export block of $TorA^{SP}$-substrates in *C. glutamicum* upon coexpression of TorD

On the basis of the finding of Li et al. (2006) and in the light of a possible biotechnological applicability, it was tested whether TorD and $TorA^{SP}$-GFP coexpression leads to the same beneficial effect in *C. glutamicum* (Brundiek, 2008). Unexpectedly, instead of increasing the translocation efficiency, this led to a complete block of $TorA^{SP}$-GFP export. This resulted in the hypothesis that the release of TorD from the signal peptide of $TorA^{SP}$-GFP does not take place because the *C. glutamicum* Tat-translocase might be unable to interact with the chaperone substrate complex.
In *E. coli* under native conditions, a release of the TorD-bound substrate TorA obviously takes place. The precise mechanism of how this release is triggered is to date unknown, although several clues have been elaborated. The *E. coli* REMP DmsD, the specific chaperone for the DMSO reductase DmsA, could be shown to interact with components of the Tat-translocase (Papish et al., 2003; Kostecki et al., 2010), which made it likely that this could also be the case for the functionally closely related REMP TorD. It has furthermore been speculated that a GTP-hydrolysis event could play a regulatory role, as a TorD dimer shows light GTP hydrolysis activity *in vitro* (Hatzixanthis et al., 2005; Guymer et al., 2010). Also, it has been shown that in *E. coli* TorD binds the TorA signal peptide very efficiently, albeit not in the highly conserved N-region (which contains the twin-arginine consensus motif) but in the hydrophobic h-region (Hatzixanthis et al., 2005; Shanmugham et al., 2012). This could possibly leave the n-region of the TorA signal peptide exposed so that a competition for signal peptide binding with the TatBC receptor complex takes place, which specifically binds the, twin-arginine consensus motif containing, n-region of Tat signal peptides (Fröbel et al., 2012). Recently, it has also been suggested that the maturation process of TorA itself could be involved in the native release mechanism. It could also be shown that signal-peptide-less TorA binds to TorD, which indicates that TorA is not only bound by its signal peptide but also by protein parts that lie within the *apo*-protein (Dow et al., 2013). A conformational change of TorA, after incorporating the molybdenum cofactor, could thus be another trigger mechanism to release TorD and initiate translocation via the Tat-pathway.
However the release mechanism actually works, based on the reults of Brundiek (2008) it was hypothesized that the Tat-translocase of *C. glutamicum* might be unable to mediate this release of TorD from the TorA signal peptide of $TorA^{SP}$-GFP, leading to the observed export block. Next, it was tried to identify a specific Tat-component responsible for this failed release. Of different conditions tested,

only the additional coexpression of the *E. coli* Tat-translocase components TatABC in the *C. glutamicum* wild-type strain expressing TorD and TorA^{SP}-GFP led to a cancelation of the export block (Brundiek, 2008). These results suggested that the *E. coli* Tat-translocase, other than the Tat-translocase of *C. glutamicum*, is able to carry out the hypothetical interaction with the TorD/ TorA^{SP}-GFP complex to mediate the release of the chaperone and transfer the substrate to the translocase.
But one further finding of Brundiek (2008) makes this interpretation at least questionable. As discussed before, until a few years ago, the presence of a *tatB* gene in *C. glutamicum* was still unknown (Dilks et al., 2003). This resulted in Meissner (2005) constructing a Tat-deficient *C. glutamicum* strain Δ*tatAC*. Although the Tat-pathway of this strain is completely defective, the genome still contains a copy of *tatB* and *tatE*. As these two genes are not encoded in an operon with *tatAC* and found in relative distance in the genome, expression of the gene products TatB and TatE in the Δ*tatAC* strain still takes place. H. Brundiek expressed the *E. coli* Tat-components in this *C. glutamicum tatAC*-mutant strain with the aim of restoring Tat-dependent export. Neither the expression of *E. coli* TatABC nor TatAC in *C. glutamicum* Δ*tatAC* led to such a restoration. This was explained by the formation of "mix-translocases" which are Tat-translocases composed in part of homologous (genomically encoded *C. glutamicum* TatB, TatE) and heterologous (plasmid based *E. coli* TatABC) Tat components. It was concluded, that, as *E. coli* TatAC is unable to complement the *C. glutamicum tatAC*-mutant, a mixed translocase composed of $TatAC_{E.c.}$ and $TatB_{C.g.}$ is not functional in *C. glutamicum* and, furthermore, that the expression of $TatABC_{E.c.}$ does not lead to Tat-dependent export in *C. glutamicum* Δ*tatAC* due to the presence of genomically encoded $TatB_{C.g.}$ (Brundiek, 2008).
These results and the fact that the TorD-induced export block of TorA^{SP}-GFP in the *C. glutamicum* wild-type strain could only be cancelled when the *E. coli* translocase TatABC was coexpressed imposes two questions:

- Is the *E. coli* Tat-translocase, which is expressed *in trans* in the *C. glutamicum* wild-type strain and leads to TorD release in fact active? Or does the *E. coli* translocase only mediate the release of the chaperone from the TorA signal peptide and translocation takes place via the endogenous *C. glutamicum* translocase?
- Does TatB play a role in this mechanism? On the one hand, export of TorA^{SP}-GFP in the presence of TorD was only observed when plasmid-expressed *E. coli* TatB was present additionally to homologous *C. glutamicum* TatB. On the other hand, the TorD-induced export block has only been observed in *C. glutamicum* strains with a presence of genomically encoded TatB.

These questions highlighted the need for an alternative approach with a clean genetic background in which there is no simultaneous presence of the same Tat-component from two different organisms. When expressing the complete *C. glutamicum* Tat-translocase TatACBE together with the substrate TorA^{SP}-MalE and the REMP TorD in an *E. coli tat*-mutant (Δ*tatABCE* Δ*malE*), no growth occured on minimal medium agar plates containing maltose as sole carbon source (see figure 22). This confirmed that indeed an incompatibility between the translocase of *C. glutamicum* and TorD, prohibiting the export of the substrate TorA^{SP}-MalE, also exists in a clean genetic situation. Since the previous work by Brundiek (2008) had strongly suggested that nature of the TatB protein might be the actual cause for this incompatibility, the role of this Tat cmoponent (if any) for the release of TorD from TorA^{SP}-substrates was investigated in further detail.

4.2.2 An interaction of TatB with the TorD/substrate complex is not necessary to release TorD from the substrate

The mechanism of how the REMP TorD is released from its TorA^{SP}-substrate had been suggested to

rely on an interaction of the Tat-translocase with the TorD/TorA^{SP}-substrate complex. It had been stipulated by the results of Brundiek (2008) that the TatB molecule of *C. glutamicum* could be responsible for this interaction not taking place. The reason for this might be that $TatB_{C.g.}$, other than homologous $TatB_{E.c.}$, is either unable to mediate a specific interaction because it misses a specific residue or structure or otherwise for some reason prevents this postulated interaction from taking place.

To investigate the involvement of TatB, it was tested what effect the coexpression of TorD has on TorA^{SP}-MalE export in a system where TatB is not present at all. For this purpose three different *E. coli* translocases devoid of a TatB molecule were tested in an *E. coli tat*-mutant (Δ*tatABCE* Δ*malE*) for export of MalE: Firstly, the expression of two artificial *E. coli* "minimal translocases" $TatAC_{M2}$ and $TatAC_{M5}$. Both contain TatA molecules which possess single amino acid substitutions in their extreme N-terminus (located at the periplasmic side of the membrane) thus rendering the TatA molecules bifunctional, i.e. able to both form the protein conducting channel and to fulfill the TatB function within the TatBC receptor complex (Blaudeck et al., 2005). The expression of these two artificial minimal translocases $TatAC_{M2}$ and $TatAC_{M5}$ in an *E. coli tat*$^-$ strain allows for significant export of TorA^{SP}-MalE. Additionally, to test the effect of TorD coexpression in complete absence of a Tat molecule even remotely possessing TatB function, unaltered wild-type TatAC (with "monofunctional" TatA) was expressed in an *E. coli tat*- strain. This strain has a very residual TorA^{SP}-MalE translocation activity. More importantly, the additional expression of TorD did not lead to an export block in any of these strains (see figure 42) which indicates that TatB presence is not ultimately necessary for the release of TorD from the TorA signal peptide.

This finding disproves the hypothesis of Brundiek (2008) of strict TatB involvement in a postulated release mechanism which requires an interaction of the Tat-translocase with a TorD/TorA^{SP}-substrate complex. In fact, it stands to reason whether an interaction of this sort is necessary at all to mediate the release of REMP chaperones from their respective substrates.

Among the wide variety of molecular chaperones which have been observed in nature, a differentiation between energy-dependent foldases and energy-independent holdases is made (Hartl and Hayer-Hartl, 2002). Although TorD has been shown to bind GTP *in vitro*, it has no hydrolytic activity (Hatzixanthis et al., 2005; Guymer et al., 2010). Chaperones categorized as holdases and not showing catalytic activity are termed as holding chaperones (Mattoo and Goloubinoff, 2014). A well-studied *E. coli* holding chaperone which functions ATP-independently is the cytosolic SecB. SecB is an export specific chaperone that plays an important role in preventing premature folding of substrates destined for translocation via the Sec pathway (Ullers et al., 2004). It fulfills this function by repetitive cycles of binding and releasing its substrate termed kinetic partitioning (Diamond and Randall, 1997; Topping and Randall, 1997). This simply means that an equilibrium between the bound and un-bound substrate exists depending on whether the free energy of rebinding the substrate or of aggregation/folding is higher.

Due to the nature of TorD, especially in the light of its small size and it not possessing any known catalytic activity, it is likely that a similar mechanism of reiterative binding/release cycles occurs. It has been suggested that a conformational change of the native TorD-substrate TorA after folding and successful incorporation of the molybdenum cofactor could trigger the release of TorD from TorA (Dow et al., 2013). This conformational change then results in TorD preferentially not binding the mature TorA anymore and translocation via the Tat machinery occurring. However, this does not explain how the release of TorD from artificial substrates bearing the TorA signal peptide is mediated. It is likely that for substrates like TorA^{SP}-GFP used in the studies of Li et al. (2006), Brundiek (2008) and also in this study, the state of the equilibrium between bound and un-bound substrate ultimately determines when and how much of the substrate can be recognized by the translocase via its unmasked signal

peptide.

4.2.3 TorD efficiently binds the artificial substrate TorA^{SP}-MalE

In *E. coli,* the chaperone TorD is highly specific for its only known substrate, the trimethylamine-N-oxide reductase TorA (Ilbert et al., 2004). Its major function is to protect its substrate *apo*TorA from premature proteolysis and to prevent export before the molybdenum cofactor has been integrated and the mature protein is ready for export into the periplasm. It could be shown that Lon protease degrades *apo*TorA and that Lon protease and the chaperone TorD compete for binding of *apo*TorA in *E. coli.* Once the cofactor has been integrated, Lon protease does not bind TorA anymore, indicating that the protease probably targets the catalytic site (Redelberger et al., 2013). Exactly such a protection of Tat-substrates from premature proteolysis would be beneficial in the industrial production of heterologous proteins (provided the substrate is efficiently released from TorD).
And indeed, the coexpression of all three tested TorA signal peptide fusions to model substrates, TorA^{SP}-Bla, TorA^{SP}-MalE and TorA^{SP}-GFP, together with TorD leads to a massive accumulation of precursor protein within the cytoplasm in all strains tested (see figures 25, 27 and 28). This accumulation clearly demonstrates that TorD binds not only to its natural substrate TorA but also to artificial substrates bearing the TorA signal peptide and effectively protects them from intracellular proteolysis. It could furthermore be shown that *Strep*-tagged TorD can be crosslinked *in vivo* to its artificial substrate TorA^{SP}-MalE. Complexes composed 1:1 of TorD and TorA^{SP}-MalE molecules can be identified within the cytosol (see figure 29).
It has to be considered that the amount of TorD expressed from pTrSp, a derivative of the high-copy vector pTrc99A, is possibly much higher than the amount of TorD expressed under native conditions in *E. coli*. This could lead to a competition between the chaperone TorD in the cytoplasm and the TatBC receptor complex in the cytoplasmic membrane for free TorA signal peptides - presumably in favor of TorD. The expression vector pTrSp, from which TorD is expressed, has a high copy number of around 30-40 copies per cell (Amann et al., 1988) and pBBR, the plasmid from which the TorA^{SP}-substrates are expressed has a medium to high copy number of around 15-30 copies per cell (Kovach et al., 1995), TorD is therefore at all times most likely in great excess to the TorA^{SP}-substrate. This can also be seen by the abundance of TorD in a Coomassie stained SDS gel (see figures 23 and 29). The choice of expressing higher amounts of the REMP TorD than of the TorA^{SP}-substrate was intentional. This ensured that substrate molecules in the cell were always complexed by TorD and the experiments targeted at understanding the TorD release process would not be biased by TorA^{SP}-substrates not bound by TorD being directly translocated.
The high amount of protected TorA^{SP}-substrate precursor within the cells upon TorD coexpression most probably does not correlate to the amounts of TorD-protected TorA under normal conditions in *E. coli*. It is more likely that under natural conditions in *E. coli*, upon presence of TMAO, a fine-tuned amount of these two proteins according to demand is expressed (Ansaldi et al., 2007) and the intracellular retention of TorA by TorD only occurs as long as it takes for TorA to fully mature. As mentioned before, it has recently been suggested that the completion of TorA maturation might result in a conformational change of TorA which could be a trigger for the release by TorD (Dow et al., 2013).
The excess of the REMP TorD over its TorA^{SP}-substrate, which was generated by the chosen expression vectors in this work, probably also explains the discrepancy to the findings of Li et al. (2006). In their study, the coexpression of TorD had resulted in a two- to four-fold increase in the amount of exported TorA^{SP}-GFP (Li et al., 2006). In the present work however, the coexpression of TorD and TorA^{SP}-GFP in the *E. coli* wild-type strain resulted in a slight decrease in the amount of exported GFP

(see figure 28). An explanation for this seeming contradiction might be that Li et al. (2006) expressed the substrate $TorA^{SP}$-GFP from a pBAD-based fully arabinose-induced expression vector with a high copy number (Guzman et al., 1995) while expressing TorD from a constitutively expressed pACYC184-derived vector with a low copy number (Bartolome et al., 1991). This presumably resulted in an intracellular ratio of TorD:$TorA^{SP}$-substrate opposite to the one in this work. In the work of Li et al. (2006), the net increase of exported GFP possibly resulted from the protection of a greater subfraction of totally synthesized $TorA^{SP}$-GFP substrate from intracellular proteolysis compared to the situation where no TorD is coexpressed. Additionally, due to the number of substrate molecules within the cell being higher than TorD molecules, the resulting state of the equilibrium between bound and unbound substrate molecules was probably more in favor of TorD-free $TorA^{SP}$-GFP molecules that, due to the unmasked signal peptide, can be recognized and exported by the Tat-translocase.

4.2.4 Quantity and quality of the expressed TatB protein determine how well $TorA^{SP}$-substrate is translocated in presence of TorD

The question remains why the coexpression of TorD and a $TorA^{SP}$-substrate in the *C. glutamicum* wild-type strain results in an export block and what role *C. glutamicum* TatB plays herein. All data that were obtained to identify a residue or structure within $TatB_{C.g.}$ responsible for the observed export block point towards the efficiency of the expressed translocase as being the main determining factor for how well translocation takes place in presence of TorD. The TorD-induced export block was reproduced in an *E. coli tatB*-mutant which can be complemented with $TatB_{E.c.}$ or heterologous $TatB_{C.g.}$ (see figure 20). Three artificial substrates bearing the signal peptide of the *E. coli* TMAO reductase TorA were tested. All three substrates, $TorA^{SP}$-Bla (TEM1 β-lactamase), $TorA^{SP}$-MalE (maltose binding protein) and $TorA^{SP}$-GFP (green fluorescent protein) were blocked completely in presence of TorD when the Δ*tatB* strain was complemented with *C. glutamicum* TatB (see figures 25, 27 and 28). In absence of TorD, $TorA^{SP}$-MalE and $TorA^{SP}$-GFP were exported very efficiently. $TorA^{SP}$-Bla was also translocated but not in the quantity of the other two substrates.

Had this export block only manifested itself when the Δ*tatB* strain was complemented with $TatB_{C.g.}$, there would have been a simple mechanistic explanation for the phenomenon pointing to $TatB_{C.g.}$ being deficient in some sort of interaction with TorD - which would have been in line with the original hypothesis. But as it turned out, the complementation of the *E. coli tatB*-mutant with homologous $TatB_{E.c.}$ also led to, though not blocking export completely, a significant reduction in the amount of exported $TorA^{SP}$-substrate in the presence of TorD (see figures 25, 27 and 28). Interestingly, in the absence of TorD the homologously complemented *tatB*-mutant strain exported all three substrates with even higher efficiency than the wild-type control strain. The reason for this improved export efficiency probably has stochiometrical reasons. Maybe the overexpression of homologous TatB in the *tatB*-mutant strain leads to a slightly increased number of functional TatBC receptor complexes. TatBC receptor complexes consist of TatB and TatC molecules in a 1:1 ratio and each complex consists of 6-8 molecules each (Bolhuis et al., 2001; Tarry et al., 2009). Before assembly in TatBC receptor complexes, both TatB and TatC have been shown to appear in the cytoplasmic membrane as homomultimeric complexes and it has been suggested that a homomultimeric TatC complex serves as a scaffold for the association of TatB molecules (Behrendt et al., 2007; Orriss et al., 2007). Now, in the *E. coli tatB*-mutant strain BØD, the deletion of *tatB* from the *tatABC* operon moves the *tatC* gene from the third (in the wild-type operon) to the second position of the operon *tatAC*. It has been shown that a relationship between the distance of a gene from the beginning of the mRNA and the rate of its translation into protein exists (Lim et al., 2011). This would suggest that in a *tatB*-mutant strain a slightly increased

number of TatC molecules is synthesized. Taken together with an ample supply of plasmid-expressed TatB molecules, a higher number of TatBC receptor complexes is assembled in the membrane resulting in increased export.

It was originally hypothesized that a difference between the *C. glutamicum* and the *E. coli* Tat translocase disallowed the release of TorD from the signal peptide of $TorA^{SP}$-GFP in presence of $TatB_{C.g.}$ (Brundiek, 2008). The differences between the two TatB molecules have been commented on (page 64ff), namely a different amino acid usage, charge distribution and α-helical substructure of the amphipathic helix with the two molecules exhibiting a sequence identity of 23,57%. The two TatB molecules have a decreasing homology from the N- to the C-terminal end (TatB pairwise alignment in figure 30). The unstructured C-terminal ends of $TatB_{E.c.}$ and $TatB_{C.g.}$ show the lowest homology and were thus considered to be a region in which $TatB_{C.g.}$ might either contain or miss a specific feature which could be responsible for the inability of a $TatB_{C.g.}$-containing translocase to export $TorA^{SP}$-substrates in the presence of TorD. To identify whether $TatB_{C.g.}$ has a C-terminally located feature that is responsible for the export block observed in the presence of TorD, a C-terminal truncation analysis was carried out. This revealed that the C-terminal 40 amino acids are not necessary for translocation of $TorA^{SP}$-MalE (in absence of TorD); a result that is in line with the finding that the extreme C-terminus of *E. coli* TatB is not necessary for export of the natural *E. coli* substrates TorA and SufI (Lee et al., 2002). Furthermore, the C-terminal truncation analysis of $TatB_{C.g.}$ revealed that a deletion of up to 40 amino acids did not reduce the strength of the export block of $TorA^{SP}$-MalE in presence of TorD (see figure 34). This suggests that the C-terminal 40 amino acids of $TatB_{C.g.}$ do not play a role in preventing export of $TorA^{SP}$-substrates in presence of TorD

After excluding the possibility of the extreme C-terminus of $TatB_{C.g.}$ playing a role in the TorD-induced export block of $TorA^{SP}$-substrates, the amphipathic helices of the TatB molecules were compared. Once again looking at the alignment, the homology of this crucial part of the TatB molecules is low to medium. Two residues that were identified as critical for functionality of *E. coli* TatB, G21 in the hinge-region between transmembrane domain and amphipathic helix and P26 at the beginning of the amphipathic helix (Hicks et al., 2003) are also found in *C. glutamicum* TatB (here: G22 and P27 respectively). Of three glutamic acid residues, which are essential for TatB functionality in *E. coli* (E49, E53 and E58) (Hicks et al., 2003), only two are found in *C. glutamicum* (here: E58 and E61). The homology of the amphipathic helices of the two TatB molecules also decreases from N- to C-terminal end. Noticeable is the differing substructure of predicted α-helical segments which constitute the amphipathic helix. This led to the construction of four hybrid TatB molecules bearing an *E. coli* N-terminus, a *C. glutamicum* C-terminus and variable lengths of the amphipathic helices of $TatB_{E.c.}$ and $TatB_{C.g.}$ (see figure 35).

In presence of TorD, Tat-translocases containing these TatB hybrid molecules exhibited a TorD-induced export block of $TorA^{SP}$-MalE of different strength (see figure 37). The TatB hybrid $TatBE.c._{21}C.g._{139}$, which has the transmembrane domain of *E. coli* and the complete amphipathic helix of *C. glutamicum* resulted in a total export block just like the wild-type $TatB_{C.g.}$ molecule. The other three TatB hybrids had an ascending proportion of *E. coli* amphipathic helix with $TatBE.c._{95}C.g._{70}$ bearing the complete transmembrane domain and amphipathic helix of *E. coli* and only the unstructured C-terminus of *C. glutamicum.* The translocation capabilities in absence and in presence of TorD of Tat-translocases containing these hybrid TatB molecules, composed of an *E. coli* N-terminus and a *C. glutamicum* C-terminus, strongly suggest an interrelationship between translocation efficiency and the strength of the TorD-induced export block of $TorA^{SP}$-MalE. The larger the proportion of the amphipathic helix is derived from *E. coli* TatB*,* the better the export of $TorA^{SP}$-MalE is in absence of TorD. Vice versa, in presence of TorD, the export block of $TorA^{SP}$-MalE is weaker the more the TatB

hybrid molecule resembles the homologous *E. coli* TatB protein (see figure 37). This indicates that the export of $TorA^{SP}$-MalE in presence of TorD requires a certain fidelity of the translocase. Also, not surprisingly, a translocase containing the evolutionarily adapted homologous TatB molecule functions more efficiently than when it contains the "foreign" *C. glutamicum* TatB molecule.
It is known that the Tat-translocase is highly susceptible to changes in Tat-component stochiometry. While the overexpression of the whole Tat-translocase can be beneficial for example to improve the yield of SufI in *E. coli* (Yahr and Wickner, 2001), the sole overexpression of TatA in the *E. coli* wild-type strain leads to a slight reduction in the amount of translocated protein (Sargent et al., 1999; Lee et al., 2006). The overexpression of TatB alone in the *E. coli* wild-type strain on the other hand even results in a complete defect of Tat-dependent translocation (Sargent et al., 1999). As mentioned before, prior to assembly of the TatBC receptor complexes, both TatB and TatC are found in higher-number homooligomers within the membrane (Behrendt et al., 2007; Orriss et al., 2007). During assembly of the TatBC receptor complex within the membrane, TatB associates to a scaffold made up of 6-8 TatC molecules (Behrendt et al., 2007; Orriss et al., 2007), with the assembled receptor complex containing a final 1:1 stochiometry of TatB to TatC molecules (Bolhuis et al., 2001). The receptor complex has a ring-like core which is composed of TatC molecules and the TatB molecules are associate to the outside of this ring (Tarry et al., 2009). Although this complex has a theoretical number of one signal peptide binding pocket per TatC molecule, a structural analysis of the TatBC receptor complex by single-particle electron microscopy revealed that the complex only possesses one or two functional binding sites which are localized at two adjacent TatC molecules (Tarry et al., 2009).
Consequently, both the alteration of the amount of available TatB molecules as well as the quality of these TatB molecules could have severe consequences for the assembly of the TatBC receptor complex. The first problem, the presence of increased amounts of TatB due to overexpression from a plasmid in an *E. coli tatB*-mutant strain, could lead to a suboptimal stochiometry of Tat components available within the membrane for the assembly of the TatBC receptor complex.
As discussed above, the increased amount of exported $TorA^{SP}$-substrate in absence of TorD in an *E. coli tatB*-mutant strain complemented with either $TatB_{E.c.}$ or $TatB_{C.g.}$ can be explained by the increased amount of TatC expressed in a *tatB*-mutant strain. The reduced length of the *tatAC* operon (due to *tatB* deletion) increases translational initiation of *tatC* in comparison to the wild-type *tatABC* operon. This could result in a higher overall number of TatBC receptor complexes resulting in an increased export of $TorA^{SP}$-substrates. The fact that a higher number of receptor complexes does not necessarily mean that these are more efficient is then seen in presence of TorD where, e.g. a diminished number of functional signal peptide binding sites results in a reduced ability of the translocase to compete for free signal peptides and consequently to an export block of $TorA^{SP}$-substrate.
The implications of the presence of a foreign TatB molecule (such as $TatB_{C.g.}$) on the efficiency of the TatBC receptor complex are even more severe. In this case, in addition to a suboptimal stochiometry of Tat components due to overexpression of TatB, direct protein-protein interactions between TatB and TatC are required. It is known that a physical interaction between TatB and TatC takes place (Kneuper et al., 2012) and it is likely that the evolutionarily optimized TatB molecule of *E. coli* does this more efficiently than a heterologous TatB molecule such as $TatB_{C.g.}$. This could likely result in a TatBC receptor complex containing a foreign TatB molecule having a reduced efficiency in signal peptide binding. In absence of TorD, the $TatB_{C.g.}$-containing translocase is able to export amounts of $TorA^{SP}$-substrate comparable to those of the wild-type strain. But when TorD is present in the cell, the translocase has to compete with TorD for binding of free signal peptides of the $TorA^{SP}$-substrate and then the reduced efficiency of the $TatB_{C.g.}$-containing translocase in comparison to the wild-type translocase becomes apparent.

How problematic the presence of the "foreign" *C. glutamicum* TatB molecule within the translocase is when TorD and a $TorA^{SP}$-substrate are coexpressed also becomes apparent when regarding the results of *tatB* mutagenesis. The mutagenesis of $TatB_{C.g.}$ and $TatBE.c._{21}C.g._{139}$, which was carried out to identify suppressor mutations which allow translocation of $TorA^{SP}$-MalE in presence of TorD delivered an interesting result. All three characterized mutant TatB molecules (see figure 38 for a detailed overview of the obtained mutations) were indicative to be strongly reduced in functionality like $TatB_{Z3}$ (C-terminal truncation of 52 amino acids) or severely reduced in the amounts of expressed protein like $TatB_{X3}$ (highly uncommon ACG start codon) or $TatB_{Z4}$ (mutation in linker between Shine-Dalgarno sequence and start codon). The fact that selection pressure for export of the maltose binding protein on maltose minimal medium in presence of TorD results in the strains deactivating $TatB_{C.g.}$ points towards the presence of these foreign TatB molecules being highly problematic within the translocase. Translocases containing either $TatB_{X3}$, $TatB_{Z3}$ or $TatB_{Z4}$ are significantly reduced in their efficiency in translocating $TorA^{SP}$-MalE in comparison to the wild-type translocase (see figures 39, 40 and 41) even in absence of TorD. The fact that the additional expression of TorD does not negatively influence the amount of translocated $TorA^{SP}$-MalE can probably also be explained by the efficiency of signal peptide binding of the TatBC receptor complexes containing these mutant TatB molecules. It could be speculated that while these mutant-TatB molecule containing translocase are slow and have a low translocation turnover in absence of TorD, the additional presence of TorD does not influence the amount of translocated $TorA^{SP}$-MalE because they have an increased binding affinity to the TorA signal peptide in comparison to the wild-type TatBC receptor complex.
In addition, it is known that export of the highly sensitive reporter protein $TorA^{SP}$-MalE can occur via a TatAC translocase in an *E. coli tat*-strain when TatAC is overexpressed from a plasmid (Blaudeck et al., 2005). This finding could also be demonstrated in this study (see figure 42). Because the level of TatA and TatC is not sufficiently high in an uncomplemented *E. coli tatB*-mutant strain, the export of $TorA^{SP}$-MalE does not not suffice for growth on maltose minimal medium (see e.g. figure 26). Nonetheless, this demonstrates that in the *tatB*-mutant strains expressing either of the mutant TatB molecules the translocation of $TorA^{SP}$-MalE could occur with only a marginal involvement of TatB within the process of signal peptide binding.

4.2.5 A kinetic partitioning between binding to TorD and export via the Tat-translocase determines the amount of exported $TorA^{SP}$-substrate

The original aim of this work was to find out whether an interaction between the Tat-translocase and a TorD/$TorA^{SP}$-substrate complex is strictly required for the release of TorD from the substrate. Herein, especially the involvement of the TatB molecule in such a putative interaction was investigated. Taken together, all data obtained however point towards the view that such an interaction is in fact not required for TorD release. Rather, it seems likely that the small cytoplasmic chaperone TorD exhibits reiterative cycles of binding and releasing its substrate, provided that the substrate is in its finally folded state. Subsequently, the kinetic partitioning of the chaperone-free $TorA^{SP}$-substrate between (re)binding to TorD and productive binding to the TatBC receptor complex of the translocase most likely ultimately determines how much of the substrate is actually translocated across the membrane (schematically depicted in figure 43).

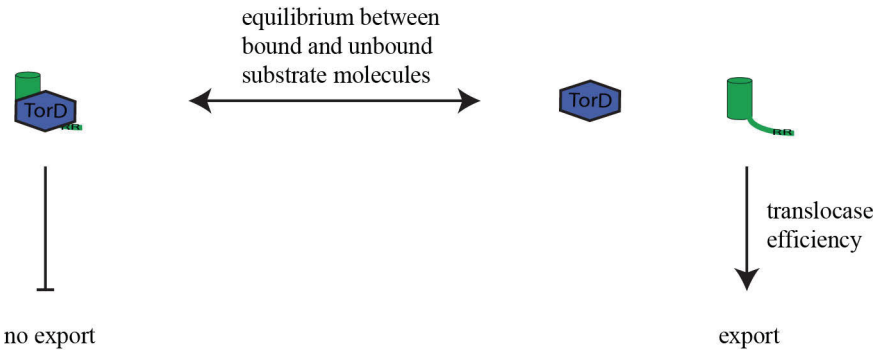

Figure 43: Kinetic partitioning of free TorA^{SP}-substrate molecules between (re)-binding of TorD and transfer to the TatBC receptor of the Tat translocase is strongly dependent upon the efficiency of the Tat-translocase.

The affinity of TorD for the native TorA protein has been determined by isothermal titration calorimetry to have an apparent K_D of around 59 nM (Buchanan et al., 2008) and for a synthetic peptide comprising amino acids 2-22 of the TorA signal peptide an apparent K_D of around 76 µM (Hatzixanthis et al., 2005). The substrate binding interaction of the wild-type *E. coli* Tat translocase in purified membrane fractions with the *E. coli* Tat substrate pre-SufI on the other hand has an apparent K_D of 7-23 nM, measured with an *in vitro* FRET assay (fluorescence resonance energy transfer) (Whitaker et al., 2012). Under the assumption that the signal peptide of TorA exhibits a comparable affinity to the TatBC receptor complex as pre-SufI, it can be deduced that the affinity of free TorA signal peptides for binding to the substrate binding pocket of the Tat translocase is higher than for binding to the REMP TorD.

As discussed in the previous section, the presence of a non-native TatB molecule such as $TatB_{C.g.}$ in the TatBC receptor complex most likely reduces this affinity of the receptor complex to bind the TorA signal peptide. Taken together with a high amount of intracellular TorD, this explains the observed export block of TorA^{SP}-substrates in presence of TorD because it reduces the likeliness of the Tat translocase to bind free signal peptides. In other words, a kinetic partitioning of TorA^{SP}-substrate molecules with unmasked signal peptides between (re)binding to TorD and productive binding to the TatBC receptor complex is moved in favor of binding to TorD the lower the signal peptide binding efficiency of the expressed translocase is. This ultimately also explains why the coexpression of TorD in the *C. glutamicum* wild-type strain, as observed by Brundiek (2008), results in an export block of TorA^{SP}-substrates. The wild-type *C. glutamicum* Tat translocase obviously exhibits an affinity towards the free TorA signal peptide which is not high enough when having to compete with high concentrations of intracellular TorD for binding of it.

Summary

The twin-arginine translocation (Tat) pathway facilitates the translocation of fully folded, co-factor associated, or even oligomerized proteins across the cytoplasmic membrane of bacteria and the thylakoid membrane of plant chloroplasts. In Gram-negative bacteria such as *Escherichia coli* and plant chloroplasts, an ABC-type translocase is found in which three different translocase components (TatA, TatB and TatC) perform distinct functions. Whereas oligomers of TatA constitute the actual protein conducting channel, the components TatB and TatC together form a receptor complex which is responsible for recognizing the signal peptides of the Tat-substrates. In most low-G/C Gram-positive bacteria on the other hand, an AC-type translocase is found in which a bifunctional TatA component can both partake in signal peptide recognition in the receptor complex as well as in the formation of the protein conducting channel across the membrane.

In this work, it could be shown that in the biotechnologically important high-G/C Gram-positive model organism *Corynebacterium glutamicum* a translocase of the ABC-type is used as the functional unit for Tat-dependent translocation. This was achieved by showing the involvement of *C. glutamicum* TatB in the translocation of model Tat-substrates. Furthermore, it could be demonstrated that the *C. glutamicum* Rieske protein QcrA, a component of the cytochrome bc_1 complex of the main respiratory chain which contains an iron-sulfur cluster, is integrated into the cytoplasmic membrane in a Tat-dependent manner. Under aerobic growth conditions, the deletion of either the *tatAC* operon or the monocistronically localized *tatB* gene results in a comparable growth inhibition, showing the equal importance of all three Tat components. By demonstrating that a *C. glutamicum qcrA* mutant but not a *qcrA/tatB* double mutant can be complemented with QcrA *in trans* it was proven that TatB presence is absolutely essential for the assembly of this important Tat substrate. Finally, it was shown that *C. glutamicum* $TatB_{C.g.}$ is a *bona fide* TatB as it can complement for TatB function in an *E. coli tatB*-mutant strain, but not for TatA function in a *tatA*-mutant strain. Since in the ABC-type Tat-translocase of *E. coli*, TatB fulfills a dedicated role as an essential component of the receptor complex which is clearly different from the translocation-pore function of TatA, this finding demonstrated that $TatB_{C.g.}$ is not bifunctional and further confirmed that *C. glutamicum*, and most likely other *Actinobacteria* as well, utilize a Gram-negative style, ABC-type Tat-translocase.

Coexpression of the *E. coli* redox enzyme maturation protein TorD has been reported as an option to increase Tat-dependent export of heterologous substrates bearing the signal peptide of the TMAO reductase TorA through protection from intracellular proteolysis. However, in this work it was found that when TorD was expressed in *C. glutamicum* or in an *E. coli tatB*-mutant strain expressing *C. glutamicum* TatB, this resulted in a complete export block of $TorA^{SP}$-substrates. These findings led to the hypothesis that the release of the TorD chaperone from the $TorA^{SP}$-substrate might be actively triggered by an interaction between TatB and the TorD/$TorA^{SP}$-substrate complex and that this function of TatB (if existent) might be precluded by the presence of the foreign *C. glutamicum* TatB. Based on this hypothesis, a possible active involvement of TatB in TorD release was investigated. Surprisingly and in contrast to the original hypothesis, it was found that the presence of TatB is not strictly required for the release of TorD from the TorD/$TorA^{SP}$-substrate complex, suggesting that in fact no active release mechanism involving an interaction with the Tat translocase exists. Rather, both the quantity and/or nature of TatB seem to have an indirect influence on how well export of $TorA^{SP}$-substrates in the presence of TorD can take place. The analysis of Tat translocases containing hybrid *E. coli*/ *C. glutamicum* TatB proteins revealed an interrelationship between translocase efficiency and export of $TorA^{SP}$-containing substrates in the presence of TorD, strongly suggesting that a kinetic partitioning of free $TorA^{SP}$-substrate between (re)binding to TorD and transfer to the signal peptide-binding pocket in the TatBC receptor complex ultimately determines how much $TorA^{SP}$-substrate can actually be translocated across the membrane in the presence of given concentrations of the TorD chaperone.

Zusammenfassung

Der twin-arginine translocation (Tat)-Weg erlaubt die Translokation vollständig gefalteter, Kofaktor-haltiger und oligomerisierter Proteine über die zytoplasmatische Membran von Bakterien und die Thylakoidmembran von Pflanzenchloroplasten. In Gram-negativen Bakterien wie *Escherichia coli* und Pflanzenchloroplasten wird eine ABC-Typ Translokase verwendet die aus drei Komponenten besteht (TatA, TatB und TatC) welche distinkte Funktionen erfüllen. TatA Multimere bilden die eigentliche Translokationspore und TatB und TatC zusammen einen Rezeptorkomplex, der für die Erkennung des Signalpeptides des Tat-Substrates verantwortlich ist. In den meisten niedrig G/C-haltigen Gram-positiven Bakterien existiert eine AC-Typ Translokase, in der ein bifunktionales TatA Molekül sowohl im Rezeptorkomplex in der Signalpeptid Erkennung wirkt als auch den Translokationkanal über die Membran bilden kann.

In dieser Arbeit wurde gezeigt, dass der biotechnologisch wichtige, hoch G/C-haltige, Gram-positive Modellorganismus *Corynebacterium glutamicum* eine Translokase des ABC-Typs für seine Tat-abhängige Translokation verwendet. Dies wurde durch die notwendige Beteiligung von *C. glutamicum* TatB bei der Translokation von Modell Tat-Substraten gezeigt. Weiterhin konnte gezeigt werden, dass der Membraneinbau des *C. glutamicum* Rieske Proteins QcrA, einer Eisen-Schwefel-Cluster haltigen Komponente des Cytochrom bc_1 Komplexes der Hauptatmungskette, Tat-abhängig erfolgt. Unter aeroben Wachstumsbedingungen führt die Deletion des *tatAC* Operons oder des monocistronisch lokalisierten *tatB* zu einer vergleichbaren Wachstumsinhibierung, was auf die gleichwertige Wichtigkeit der drei Tat-Komponente hinweist. Dadurch, dass eine *C. glutamicum qcrA*-Mutante, nicht aber eine *qcrA/tatB* Doppelmutante mit QcrA *in trans* komplementiert werden kann, konnte gezeigt werden, dass TatB für die Assemblierung dieses wichtigen Tat-Substrates zwingend notwendig ist.

Desweitern wurde gezeigt, dass *C. glutamicum* $TatB_{C.g.}$ ein *bona fide* TatB ist, da es für TatB-Funktion in einer *E. coli tatB*-Mutante, aber nicht für TatA-Funktion in einer *tatA*-Mutante komplementieren kann. In der ABC-Typ Translokase von *E. coli* erfüllt TatB eine dezidierte Funktion als essentielle Komponente des Rezeptorkomplex, welche klar von der Translokationskanal-bildenden Funktion von TatA differenziert werden kann. Dieser Befund demonstriert, dass $TatB_{C.g.}$ nicht bifunktional ist, und ist eine weitere Bestätigung dafür, dass *C. glutamicum* und höchstwahrscheinlich alle *Actinobacterien* eine ABC-Typ Translokase, wie in Gram-negativen Bakterien, verwenden.

Es wurde berichtet, dass Koexpression des *E. coli* Redoxenzym Reifungsprotein (REMP) TorD den Export heterologer Substrate mit dem Signalpeptid der TMAO Reduktase TorA, durch Schutz vor intrazellulärer Proteolyse, verbessern kann. In dieser Arbeit wurde gezeigt, dass Expression von TorD in *C. glutamicum* oder in einem *E. coli tatB*-Mutantenstamm der *C. glutamicum* TatB exprimiert, zu einem vollständigen Exportblock von $TorA^{SP}$-Substraten führt. Dieser Befund führte zu der Hypothese, dass die Ablösung des Chaperons TorD vom $TorA^{SP}$-Substrat einen aktiven Mechanismus in Form einer Interaktion zwischen TatB und dem TorD/$TorA^{SP}$-Substratkomplex benötigt und diese Funktion (falls existent) in Anwesenheit von *C. glutamicum* TatB nicht stattfindet. Basierend auf dieser Annahme wurde eine mögliche aktive Beteiligung von TatB am TorD-Ablöseprozess untersucht. Unerwarteterweise und im Widerspruch zu der ursprünglichen Hypothese, konnte gezeigt werden, dass die Anwesenheit von TatB für eine Ablösung von TorD vom $TorA^{SP}$-Substratkomplex nicht zwingend notwendig ist was darauf hinweist, dass es keinen aktiven Ablösemechanismus gibt, der eine Interaktion mit der Tat Translokase voraussetzt. Vielmehr scheinen sowohl die Quantität und/oder die Qualität von TatB einen indirekten Einfluss darauf zu haben wie gut $TorA^{SP}$-Substrate in Anwesenheit von TorD exportiert werden. Die Analyse von, *E. coli/ C.glutamicum*-hybrid TatB Proteinen enthaltenden, Tat Translokasen wiesen auf eine Wechselbeziehung zwischen Translokaseeffizienz und Export von $TorA^{SP}$-Substraten in Anwesenheit von TorD hin. Dies deutet darauf hin, dass eine kinetische Partitionierung freier $TorA^{SP}$-Substrate zwischen Bindung an TorD und Transfer zur Signalpeptid-Bindetasche des TatBC Rezeptorkomplexes letztendlich darüber entscheidet wie viel $TorA^{SP}$-Substrat, bei gegebener Menge des TorD Chaperons, über die Membran transloziert werden kann.

5. Bibliography

Adrio, J.L., and Demain, A.L. (2014) Microbial Enzymes: Tools for Biotechnological Processes. *Biomolecules*, 4:117-139.

Alami, M., Luke, I., Deitermann, S., Eisner, G., Koch, H.G., Brunner, J., and Muller, M. (2003) Differential interactions between a twin-arginine signal peptide and its translocase in *Escherichia coli*. *Mol Cell*, 12:937-946.

Alder, N.N., and Theg, S.M. (2003) Energetics of protein transport across biological membranes. a study of the thylakoid ΔpH-dependent/cpTat pathway. *Cell*, 112:231-242.

Aldridge, C., Spence, E., Kirkilionis, M.A., Frigerio, L., and Robinson, C. (2008) Tat-dependent targeting of Rieske iron-sulphur proteins to both the plasma and thylakoid membranes in the cyanobacterium *Synechocystis* PCC6803. *Mol Microbiol*, 70:140-150.

Amann, E., Ochs, B., and Abel, K.J. (1988) Tightly regulated *tac* promoter vectors useful for the expression of unfused and fused proteins in *Escherichia coli*. *Gene*, 69:301-315.

Ansaldi, M., Theraulaz, L., Baraquet, C., Panis, G., and Mejean, V. (2007) Aerobic TMAO respiration in *Escherichia coli*. *Mol Microbiol*, 66:484-494.

Babu, M.M., Priya, M.L., Selvan, A.T., Madera, M., Gough, J., Aravind, L., and Sankaran, K. (2006) A database of bacterial lipoproteins (DOLOP) with functional assignments to predicted lipoproteins. *J Bacteriol*, 188:2761-2773.

Bachmann, J., Bauer, B., Zwicker, K., Ludwig, B., and Anderka, O. (2006) The Rieske protein from *Paracoccus denitrificans* is inserted into the cytoplasmic membrane by the twin-arginine translocase. *FEBS J*, 273:4817-4830.

Baglieri, J., Beck, D., Vasisht, N., Smith, C.J., and Robinson, C. (2012) Structure of TatA paralog, TatE, suggests a structurally homogeneous form of Tat protein translocase that transports folded proteins of differing diameter. *J Biol Chem*, 287:7335-7344.

Bansal-Mutalik, R., and Nikaido, H. (2011) Quantitative lipid composition of cell envelopes of *Corynebacterium glutamicum* elucidated through reverse micelle extraction. *Proc Natl Acad Sci U S A*, 108:15360-15365.

Barnett, J.P., Eijlander, R.T., Kuipers, O.P., and Robinson, C. (2008) A minimal Tat system from a gram-positive organism: a bifunctional TatA subunit participates in discrete TatAC and TatA complexes. *J Biol Chem*, 283:2534-2542.

Barnett, J.P., Lawrence, J., Mendel, S., and Robinson, C. (2011) Expression of the bifunctional *Bacillus subtilis* TatAd protein in *Escherichia coli* reveals distinct TatA/B-family and TatB-specific domains. *Arch Microbiol*, 193:583-594.

Barrick, D., Villanueba, K., Childs, J., Kalil, R., Schneider, T.D., Lawrence, C.E., Gold, L., and Stormo, G.D. (1994) Quantitative analysis of ribosome binding sites in *E.coli*. *Nucleic Acids Res*, 22:1287-1295.

Bartolome, B., Jubete, Y., Martinez, E., and de la Cruz, F. (1991) Construction and properties of a family of pACYC184-derived cloning vectors compatible with pBR322 and its derivatives. *Gene*, 102:75-78.

Bayan, N., Houssin, C., Chami, M., and Leblon, G. (2003) Mycomembrane and S-layer: two important structures of *Corynebacterium glutamicum* cell envelope with promising biotechnology applications. *J Biotechnol*, 104:55-67.

Bechtluft, P., van Leeuwen, R.G., Tyreman, M., Tomkiewicz, D., Nouwen, N., Tepper, H.L., Driessen, A.J., and Tans, S.J. (2007) Direct observation of chaperone-induced changes in a protein folding pathway. *Science*, 318:1458-1461.

Behrendt, J., Lindenstrauss, U., and Bruser, T. (2007) The TatBC complex formation suppresses a modular TatB-multimerization in *Escherichia coli. FEBS Lett*, 581:4085-4090.

Bendtsen, J.D., Nielsen, H., Widdick, D., Palmer, T., and Brunak, S. (2005) Prediction of twin-arginine signal peptides. *BMC Bioinformatics*, 6:167.

Berks, B.C., Palmer, T., and Sargent, F. (2003) The Tat protein translocation pathway and its role in microbial physiology. *Adv Microb Physiol*, 47:187-254.

Bernhardt, T.G., and de Boer, P.A. (2003) The *Escherichia coli* amidase AmiC is a periplasmic septal ring component exported via the twin-arginine transport pathway. *Mol Microbiol*, 48:1171-1182.

Bertani, G. (1951) Studies on lysogenesis. I. The mode of phage liberation by lysogenic *Escherichia coli*. *J Bacteriol*, 62:293-300.

Billman-Jacobe, H., Wang, L., Kortt, A., Stewart, D., and Radford, A. (1995) Expression and secretion of heterologous proteases by *Corynebacterium glutamicum. Appl Environ Microbiol*, 61:1610-1613.

Blaudeck, A.N. (2001) Charakterisierung der Tat-abhängigen Proteintranslokation in Gram-negativen Bakterien.

Blaudeck, N., Kreutzenbeck, P., Freudl, R., and Sprenger, G.A. (2003) Genetic analysis of pathway specificity during posttranslational protein translocation across the *Escherichia coli* plasma membrane. *J Bacteriol*, 185:2811-2819.

Blaudeck, N., Kreutzenbeck, P., Müller, M., Sprenger, G.A., and Freudl, R. (2005) Isolation and characterization of bifunctional *Escherichia coli* TatA mutant proteins that allow efficient Tat-dependent protein translocation in the absence of TatB. *J Biol Chem*, 280:3426-3432.

Boeck, R., and Kolakofsky, D. (1994) Positions +5 and +6 can be major determinants of the efficiency of non-AUG initiation codons for protein synthesis. *EMBO J*, 13:3608-3617.

Bogsch, E., Brink, S., and Robinson, C. (1997) Pathway specificity for a ΔpH-dependent precursor thylakoid lumen protein is governed by a 'Sec-avoidance' motif in the transfer peptide and a 'Sec-incompatible' mature protein. *EMBO J*, 16:3851-3859.

Bogsch, E.G., Sargent, F., Stanley, N.R., Berks, B.C., Robinson, C., and Palmer, T. (1998) An essential component of a novel bacterial protein export system with homologues in plastids and mitochondria. *J Biol Chem*, 273:18003-18006.

Bolhuis, A., Mathers, J.E., Thomas, J.D., Barrett, C.M., and Robinson, C. (2001) TatB and TatC form a functional and structural unit of the twin-arginine translocase from *Escherichia coli*. *J Biol Chem*, 276:20213-20219.

Bordes, P., Cirinesi, A.M., Ummels, R., Sala, A., Sakr, S., Bitter, W., and Genevaux, P. (2011) SecB-like chaperone controls a toxin-antitoxin stress-responsive system in *Mycobacterium tuberculosis. Proc Natl Acad Sci U S A*, 108:8438-8443.

Bradford, M.M. (1976) A rapid and sensitive method for the quantitation of microgram quantities of protein utilizing the principle of protein-dye binding. *Anal Biochem*, 72:248-254.

Brundiek, H. (2008) Etablierung und Optimierung der sekretorischen Gewinnung von thermostabilen Lipasen in Gram-positiven Bakterien.

Brüser, T., and Sanders, C. (2003) An alternative model of the twin arginine translocation system. *Microbiol Res*, 158:7-17.

Bruser, T., Yano, T., Brune, D.C., and Daldal, F. (2003) Membrane targeting of a folded and cofactor-containing protein. *Eur J Biochem*, 270:1211-1221.

Buchan, D.W., Minneci, F., Nugent, T.C., Bryson, K., and Jones, D.T. (2013) Scalable web services for the PSIPRED Protein Analysis Workbench. *Nucleic Acids Res*, 41:349-357.

Buchanan, G., Maillard, J., Nabuurs, S.B., Richardson, D.J., Palmer, T., and Sargent, F. (2008) Features of a twin-arginine signal peptide required for recognition by a Tat proofreading chaperone. *FEBS Lett*, 582:3979-3984.

Bullock, W.O., Fernandez, J.M., and Short, J.M. (1987) XL-1 Blue : a high efficiency plasmid transforming *recA Escherichia coli* strain with beta-galactosidase selection. *Bio Techniques*, 5:376-379.

Casadaban, M.J. (1976) Transposition and fusion of the *lac* genes to selected promoters in *Escherichia coli* using bacteriophage lambda and Mu. *J Mol Biol*, 104:541-555.

Caspers, M., and Freudl, R. (2008) *Corynebacterium glutamicum* possesses two *secA* homologous genes that are essential for viability. *Arch Microbiol*, 189:605-610.

Chaddock, A.M., Mant, A., Karnauchov, I., Brink, S., Herrmann, R.G., Klosgen, R.B., and Robinson, C. (1995) A new type of signal peptide: central role of a twin-arginine motif in transfer signals for the ΔpH-dependent thylakoidal protein translocase. *EMBO J*, 14:2715-2722.

Chattopadhyay, A. (2013) Regulatorische Aspekte der Expression und Sekretion heterologer Proteine in *Corynebacterium glutamicum*.

Cline, K., and Mori, H. (2001) Thylakoid ΔpH-dependent precursor proteins bind to a cpTatC-Hcf106 complex before Tha4-dependent transport. *J Cell Biol*, 154:719-729.

Coleman, J., Inouye, M., and Nakamura, K. (1985) Mutations upstream of the ribosome-binding site affect translational efficiency. *J Mol Biol*, 181:139-143.

Cristóbal, S., de Gier, J.-W., Nielsen, H., and von Heijne, G. (1999) Competition between Sec-and TAT-dependent protein translocation in *Escherichia coli*. *EMBO J*, 18:2982-2990.

Dabney-Smith, C., and Cline, K. (2009) Clustering of C-terminal stromal domains of Tha4 homo-oligomers during translocation by the Tat protein transport system. *Mol Biol Cell*, 20:2060-2069.

Dabney-Smith, C., Mori, H., and Cline, K. (2006) Oligomers of Tha4 organize at the thylakoid Tat translocase during protein transport. *J Biol Chem*, 281:5476-5483.

Dalbey, R.E., Wang, P., and Kuhn, A. (2011) Assembly of bacterial inner membrane proteins. *Annu Rev Biochem*, 80:161-187.

Date, M., Itaya, H., Matsui, H., and Kikuchi, Y. (2006) Secretion of human epidermal growth factor by *Corynebacterium glutamicum*. *Lett Appl Microbiol*, 42:66-70.

Date, M., Kikuchi, Y., Matsui, H., Umezawa, Y., and Yokoyama, K. (2002) Process for producing transglutaminase. *Ajinomoto Co. Inc.* European patent EP1219713A1

Date, M., Yokoyama, K., Umezawa, Y., Matsui, H., and Kikuchi, Y. (2004) High level expression of *Streptomyces mobaraensis* transglutaminase in *Corynebacterium glutamicum* using a

chimeric pro-region from *Streptomyces cinnamoneus* transglutaminase. *J Biotechnol*, 110:219-226.

Daugherty, P.S., Chen, G., Iverson, B.L., and Georgiou, G. (2000) Quantitative analysis of the effect of the mutation frequency on the affinity maturation of single chain Fv antibodies. *Proc Natl Acad Sci U S A*, 97:2029-2034.

De Buck, E., Lammertyn, E., and Anne, J. (2008) The importance of the twin-arginine translocation pathway for bacterial virulence. *Trends Microbiol*, 16:442-453.

De Buck, E., Vranckx, L., Meyen, E., Maes, L., Vandersmissen, L., Anné, J., and Lammertyn, E. (2007) The twin-arginine translocation pathway is necessary for correct membrane insertion of the Rieske Fe/S protein in *Legionella pneumophila*. *FEBS Lett*, 581:259-264.

DeLisa, M.P., Tullman, D., and Georgiou, G. (2003) Folding quality control in the export of proteins by the bacterial twin-arginine translocation pathway. *Proc Natl Acad Sci U S A*, 100:6115-6120.

Desvaux, M., Hebraud, M., Talon, R., and Henderson, I.R. (2009) Secretion and subcellular localizations of bacterial proteins: a semantic awareness issue. *Trends Microbiol*, 17:139-145.

Diamond, D.L., and Randall, L.L. (1997) Kinetic partitioning. Poising SecB to favor association with a rapidly folding ligand. *J Biol Chem*, 272:28994-28998.

Dilks, K., Rose, R.W., Hartmann, E., and Pohlschroder, M. (2003) Prokaryotic utilization of the twin-arginine translocation pathway: a genomic survey. *J Bacteriol*, 185:1478-1483.

Dow, J.M., Gabel, F., Sargent, F., and Palmer, T. (2013) Characterization of a pre-export enzyme-chaperone complex on the twin-arginine transport pathway. *J Biochem*, 452:57-66.

du Plessis, D.J.F., Nouwen, N., and Driessen, A.J.M. (2010) The Sec translocase. *Biochim Biophys Acta*,

Dyall, S.D., Brown, M.T., and Johnson, P.J. (2004) Ancient invasions: from endosymbionts to organelles. *Science*, 304:253-257.

Eijlander, R.T., Jongbloed, J.D.H., and Kuipers, O.P. (2009) Relaxed specificity of the *Bacillus subtilis* TatAdCd translocase in Tat-dependent protein secretion. *J Bacteriol*, 191:196-202.

Eikmanns, B.J., Thum-Schmitz, N., Eggeling, L., Lüdtke, K.U., and Sahm, H. (1994) Nucleotide sequence, expression and transcriptional analysis of the *Corynebacterium glutamicum gltA* gene encoding citrate synthase. *Microbiology*, 140:1817-1828.

Fisher, A.C., and DeLisa, M.P. (2008) Laboratory evolution of fast-folding green fluorescent protein using secretory pathway quality control. *PLoS One*, 3:e2351.

Fisher, A.C., Kim, W., and DeLisa, M.P. (2006) Genetic selection for protein solubility enabled by the folding quality control feature of the twin-arginine translocation pathway. *Protein Sci*, 15:449-458.

Fleckenstein, S. (2013) Untersuchungen zur Membranintegrität während der Tat-abhängigen Proteintranslokation in *Escherichia coli*.

Freudl, R. (2013) Leaving home ain't easy: protein export systems in Gram-positive bacteria. *Res Microbiol*, 164:664-674.

Fröbel, J., Rose, P., Lausberg, F., Blümmel, A.-S., Freudl, R., and Müller, M. (2012) Transmembrane insertion of twin-arginine signal peptides is driven by TatC and regulated by TatB. *Nat Commun*, 3:1311.

Gay, P., Le Coq, D., Steinmetz, M., Berkelman, T., and Kado, C.I. (1985) Positive selection procedure for entrapment of insertion sequence elements in gram-negative bacteria. *J Bacteriol*, 164:918-921.

Genest, O., Ilbert, M., Méjean, V., and Iobbi-Nivol, C. (2005) TorD, an essential chaperone for TorA molybdoenzyme maturation at high temperature. *J Biol Chem*, 280:15644-15648.

Genest, O., Neumann, M., Seduk, F., Stöcklein, W., Méjean, V., Leimkühler, S., and Iobbi-Nivol, C. (2008) Dedicated metallochaperone connects apoenzyme and molybdenum cofactor biosynthesis components. *J Biol Chem*, 283:21433-21440.

Gerard, F., and Cline, K. (2007) The thylakoid proton gradient promotes an advanced stage of signal peptide binding deep within the Tat pathway receptor complex. *J Biol Chem*, 282:5263-5272.

Gohlke, U., Pullan, L., McDevitt, C.A., Porcelli, I., de Leeuw, E., Palmer, T., Saibil, H.R., and Berks, B.C. (2005) The TatA component of the twin-arginine protein transport system forms channel complexes of variable diameter. *Proc Natl Acad Sci U S A*, 102:10482-10486.

Gram, H.C.J. (1884) Über die isolirte Färbung der *Schizomyceten* in Schnitt- und Trockenpräparaten. *Fortschr Med*, 2:185-189.

Greene, N.P., Porcelli, I., Buchanan, G., Hicks, M.G., Schermann, S.M., Palmer, T., and Berks, B.C. (2007) Cysteine scanning mutagenesis and disulfide mapping studies of the TatA component of the bacterial twin arginine translocase. *J Biol Chem*, 282:23937-23945.

Guymer, D., Maillard, J., Agacan, M.F., Brearley, C.A., and Sargent, F. (2010) Intrinsic GTPase activity of a bacterial twin-arginine translocation proofreading chaperone induced by domain swapping. *FEBS J*, 277:511-525.

Guzman, L.M., Belin, D., Carson, M.J., and Beckwith, J. (1995) Tight regulation, modulation, and high-level expression by vectors containing the arabinose PBAD promoter. *J Bacteriol*, 177:4121-4130.

Hanahan, D. (1983) Studies on transformation of *Escherichia coli* with plasmids. *J Mol Biol*, 166:557-580.

Hansmeier, N., Albersmeier, A., Tauch, A., Damberg, T., Ros, R., Anselmetti, D., Puhler, A., and Kalinowski, J. (2006) The surface (S)-layer gene *cspB* of *Corynebacterium glutamicum* is transcriptionally activated by a LuxR-type regulator and located on a 6 kb genomic island absent from the type strain ATCC 13032. *Microbiology*, 152:923-935.

Hartl, F.U., and Hayer-Hartl, M. (2002) Molecular chaperones in the cytosol: from nascent chain to folded protein. *Science*, 295:1852-1858.

Hatzixanthis, K., Clarke, T.A., Oubrie, A., Richardson, D.J., Turner, R.J., and Sargent, F. (2005) Signal peptide-chaperone interactions on the twin-arginine protein transport pathway. *Proc Natl Acad Sci U S A*, 102:8460-8465.

Heim, R., Cubitt, A.B., and Tsien, R.Y. (1995) Improved green fluorescence. *Nature*, 373(6516):663-664.

Hicks, M.G., Guymer, D., Buchanan, G., Widdick, D.A., Caldelari, I., Berks, B.C., and Palmer, T. (2006) Formation of functional Tat translocases from heterologous components. *BMC Microbiol*, 6:64.

Hicks, M.G., de Leeuw, E., Porcelli, I., Buchanan, G., Berks, B.C., and Palmer, T. (2003) The *Escherichia coli* twin-arginine translocase: conserved residues of TatA and TatB family components involved in protein transport. *FEBS Lett*, 539:61-67.

Hicks, M.G., Lee, P.A., Georgiou, G., Berks, B.C., and Palmer, T. (2005) Positive selection for loss-of-function *tat* mutations identifies critical residues required for TatA activity. *J Bacteriol*, 187:2920-2925.

Hoffelder, M., Raasch, K., van Ooyen, J., and Eggeling, L. (2010) The E2 domain of OdhA of *Corynebacterium glutamicum* has succinyltransferase activity dependent on lipoyl residues of the acetyltransferase AceF. *J Bacteriol*, 192:5203-5211.

Hoffmann, C., Leis, A., Niederweis, M., Plitzko, J.M., and Engelhardt, H. (2008) Disclosure of the mycobacterial outer membrane: cryo-electron tomography and vitreous sections reveal the lipid bilayer structure. *Proc Natl Acad Sci U S A*, 105:3963-3967.

Hopkins, A., Buchanan, G., and Palmer, T. (2014) Role of the Twin Arginine Protein Transport Pathway in the Assembly of the S*treptomyces coelicolor* Cytochrome bc1 Complex. *J Bacteriol*, 196:50-59.

Ilbert, M., Méjean, V., Giudici-Orticoni, Marie-Thérèse, Samama, J.-P., and Iobbi-Nivol, C. (2003) Involvement of a mate chaperone (TorD) in the maturation pathway of molybdoenzyme TorA. *J Biol Chem*, 278:28787-28792.

Ilbert, M., Méjean, V., and Iobbi-Nivol, C. (2004) Functional and structural analysis of members of the TorD family, a large chaperone family dedicated to molybdoproteins. *Microbiology*, 150:935-943.

Ize, B., Gerard, F., Zhang, M., Chanal, A., Voulhoux, R., Palmer, T., Filloux, A., and Wu, L.F. (2002) *In vivo* dissection of the Tat translocation pathway in *Escherichia coli*. *J Mol Biol*, 317:327-335.

Jack, R.L., Buchanan, G., Dubini, A., Hatzixanthis, K., Palmer, T., and Sargent, F. (2004) Coordinating assembly and export of complex bacterial proteins. *EMBO J*, 23:3962-3972.

Jack, R.L., Sargent, F., Berks, B.C., Sawers, G., and Palmer, T. (2001) Constitutive expression of *Escherichia coli tat* genes indicates an important role for the twin-arginine translocase during aerobic and anaerobic growth. *J Bacteriol*, 183:1801-1804.

Jarlier, V., and Nikaido, H. (1990) Permeability barrier to hydrophilic solutes in *Mycobacterium chelonei*. *J Bacteriol*, 172:1418-1423.

Jongbloed, J.D.H., Martin, U., Antelmann, H., Hecker, M., Tjalsma, H., Venema, G., Bron, S., van Dijl, J.M., and Müller, J. (2000) TatC is a specificity determinant for protein secretion via the twin-arginine translocation pathway. *J Biol Chem*, 275:41350-41357.

Jongbloed, J.D., Grieger, U., Antelmann, H., Hecker, M., Nijland, R., Bron, S., and van Dijl, J.M. (2004) Two minimal Tat translocases in *Bacillus*. *Mol Microbiol*, 54:1319-1325.

Jourlin, C., Simon, G., Pommier, J., Chippaux, M., and Méjean, V. (1996) The periplasmic TorT protein is required for trimethylamine N-oxide reductase gene induction in *Escherichia coli*. *J Bacteriol*, 178:1219-1223.

Kalinowski, J., Bathe, B., Bartels, D., Bischoff, N., Bott, M., Burkovski, A., Dusch, N., Eggeling, L., Eikmanns, B.J., Gaigalat, L., Goesmann, A., Hartmann, M., Huthmacher, K., Krämer, R., Linke, B., McHardy, A.C., Meyer, F., Möckel, B., Pfefferle, W., Pühler, A., Rey, D.A., Rückert, C., Rupp, O., Sahm, H., Wendisch, V.F., Wiegräbe, I., and Tauch, A. (2003) The complete *Corynebacterium glutamicum* ATCC 13032 genome sequence and its impact on the production of L-aspartate-derived amino acids and vitamins. *J Biotechnol*, 104:5-25.

Kang, D., Gho, Y.S., Suh, M., and Kang, C. (2002) Highly Sensitive and Fast Protein Detection with Coomassie Brilliant Blue in Sodium Dodecyl Sulfate-Polyacrylamide Gel Electrophoresis. *Bull Korean Chem Soc*, 23:1511-1512.

Keilhauer, C., Eggeling, L., and Sahm, H. (1993) Isoleucine synthesis in *Corynebacterium glutamicum*: molecular analysis of the *ilvB-ilvN-ilvC* operon. *J Bacteriol*, 175:5595-5603.

Keller, R., de Keyzer, J., Driessen, A.J.M., and Palmer, T. (2012) Co-operation between different targeting pathways during integration of a membrane protein. *J Cell Biol*,

Kikuchi, Y., Date, M., Umezawa, Y., Yokoyama, K., Heima, H., and Matsui, H. (2009) Method for the secretion and production of protein. *Ajinomoto Co. Inc.* European Patent EP1375664B1

Kikuchi, Y., Date, M., Itaya, H., Matsui, K., and Wu, L.-F. (2006) Functional analysis of the twin-arginine translocation pathway in *Corynebacterium glutamicum* ATCC 13869. *Appl Environ Microbiol*, 72:7183-7192.

Kinoshita, S., Nakayama, K., and Akita, S. (1958) Taxonomical Study of Glutamic Acid Accumulating Bacteria, *Micrococcus glutamicus* nov. sp. *Bull Agr Chem Soc Japan*, 22:176-185.

Kirchner, O., and Tauch, A. (2003) Tools for genetic engineering in the amino acid-producing bacterium *Corynebacterium glutamicum*. *J Biotechnol*, 104:287-299.

Kneuper, H., Maldonado, B., Jager, F., Krehenbrink, M., Buchanan, G., Keller, R., Muller, M., Berks, B.C., and Palmer, T. (2012) Molecular dissection of TatC defines critical regions essential for protein transport and a TatB-TatC contact site. *Mol Microbiol*, 85:945-961.

Koch, S., Fritsch, M.J., Buchanan, G., and Palmer, T. (2012) *Escherichia coli* TatA and TatB proteins have N-out, C-in topology in intact cells. *J Biol Chem*, 287:14420-14431.

Kol, S., Nouwen, N., and Driessen, A.J. (2008) Mechanisms of YidC-mediated insertion and assembly of multimeric membrane protein complexes. *J Biol Chem*, 283:31269-31273.

Kostecki, J.S., Li, H., Turner, R.J., and DeLisa, M.P. (2010) Visualizing interactions along the *Escherichia coli* twin-arginine translocation pathway using protein fragment complementation. *PLoS One*, 5:e9225.

Kovach, M.E., Elzer, P.H., Hill, D.S., Robertson, G.T., Farris, M.A., Roop, R.M., and Peterson, K.M. (1995) Four new derivatives of the broad-host-range cloning vector pBBR1MCS, carrying different antibiotic-resistance cassettes. *Gene*, 166:175-176.

Kreutzenbeck, P.J. (2005) Export von Proteinen mit Zwillingsarginin-Signalsequenzen ueber den Tat-Weg in *Escherichia coli*.

Laemmli, U.K. (1970) Cleavage of structural proteins during the assembly of the head of bacteriophage T4. *Nature*, 227:680-685.

Lausberg, F., Fleckenstein, S., Kreutzenbeck, P., Frobel, J., Rose, P., Muller, M., and Freudl, R. (2012) Genetic evidence for a tight cooperation of TatB and TatC during productive recognition of twin-arginine (Tat) signal peptides in *Escherichia coli. PLoS One*, 7:e39867.

Lee, P.A., Tullman-Ercek, D., and Georgiou, G. (2006) The bacterial twin-arginine translocation pathway. *Annu Rev Microbiol*, 60:373-395.

Lee, P.A., Buchanan, G., Stanley, N.R., Berks, B.C., and Palmer, T. (2002) Truncation analysis of TatA and TatB defines the minimal functional units required for protein translocation. *J Bacteriol*, 184:5871-5879.

Li, S.-Y., Chang, B.-Y., and Lin, S.-C. (2006) Coexpression of TorD enhances the transport of GFP via the TAT pathway. *J Biotechnol*, 122:412-421.

Lim, H.N., Lee, Y., and Hussein, R. (2011) Fundamental relationship between operon organization and gene expression. *Proc Natl Acad Sci U S A*, 108:10626-10631.

Link, A.J., Phillips, D., and Church, G.M. (1997) Methods for generating precise deletions and insertions in the genome of wild-type *Escherichia coli*: application to open reading frame characterization. *J Bacteriol*, 179:6228-6237.

Lüke, I., Handford, J.I., Palmer, T., and Sargent, F. (2009) Proteolytic processing of *Escherichia coli* twin-arginine signal peptides by LepB. *Arch Microbiol*, 191:919-925.

Luo, Q., Dong, Y., Chen, H., and Gao, H. (2013) Mislocalization of Rieske protein PetA predominantly accounts for the aerobic growth defect of *tat* mutants in *Shewanella oneidensis*. *PLoS One*, 8:e62064.

Lycklama a Nijholt, J.A., and Driessen, A.J. (2012) The bacterial Sec-translocase: structure and mechanism. *Phil Trans R Soc B*, 367:1016-1028.

Mattoo, R.U., and Goloubinoff, P. (2014) Molecular chaperones are nanomachines that catalytically unfold misfolded and alternatively folded proteins. *Cell Mol Life Sci*,

McWilliam, H., Li, W., Uludag, M., Squizzato, S., Park, Y.M., Buso, N., Cowley, A.P., and Lopez, R. (2013) Analysis Tool Web Services from the EMBL-EBI. *Nucleic Acids Res*, 41:597-600.

Mehner, D., Osadnik, H., Lünsdorf, H., and Brüser, T. (2012) The Tat system for membrane translocation of folded proteins recruits the membrane-stabilizing Psp machinery in *Escherichia coli*. *J Biol Chem*, 287:27834-27842.

Meissner, D. (2005) Vergleichende Analyse der Sec- und Tat-abhaengigen sekretorischen Proteingewinnung mit Gram-positiven Bakterien als Wirtsorganismen.

Meissner, D., Vollstedt, A., van Dijl, J.M., and Freudl, R. (2007) Comparative analysis of twin-arginine (Tat)-dependent protein secretion of a heterologous model protein (GFP) in three different Gram-positive bacteria. *Appl Microbiol Biotechnol*, 76:633-642.

Mejean, V., Iobbi-Nivol, C., Lepelletier, M., Giordano, G., Chippaux, M., and Pascal, M.C. (1994) TMAO anaerobic respiration in *Escherichia coli*: involvement of the tor operon. *Mol Microbiol*, 11:1169-1179.

Méjean, V., Iobbi-Nivol, C., Lepelletier, M., Giordano, G., Chippaux, M., and Pascal, M.C. (1994) TMAO anaerobic respiration in *Escherichia coli*: involvement of the tor operon. *Mol Microbiol*, 11:1169-1179.

Meloni, S., Rey, L., Sidler, S., Imperial, J., Ruiz-Argueso, T., and Palacios, J.M. (2003) The twin-arginine translocation (Tat) system is essential for *Rhizobium*-legume symbiosis. *Mol Microbiol*, 48:1195-1207.

Molik, S., Karnauchov, I., Weidlich, C., Herrmann, R.G., and Klösgen, R.B. (2001) The Rieske Fe/S Protein of the Cytochromeb 6/f Complex in Chloroplasts. *J Biol Chem*, 276:42761-42766.

Monteferrante, C.G., Baglieri, J., Robinson, C., and van Dijl, J.M. (2012a) TatAc, the third TatA subunit of *Bacillus subtilis*, can form active twin-arginine translocases with the TatCd and TatCy subunits. *Appl Environ Microbiol*, 78:4999-5001.

Monteferrante, C.G., Mackichan, C., Marchadier, E., Prejean, M.-V., Carballido-López, R., and van Dijl, J.M. (2012b) Mapping the twin-arginine protein translocation network of *Bacillus subtilis*. *Proteomics*, Proteomics

Mori, H., Summer, E.J., and Cline, K. (2001) Chloroplast TatC plays a direct role in thylakoid ΔpH-dependent protein transport. *FEBS Lett*, 501:65-68.

Mori, H., and Cline, K. (2002) A twin arginine signal peptide and the pH gradient trigger reversible assembly of the thylakoid ΔpH/Tat translocase. *J Cell Biol*, 157:205-210.

Mullineaux, C.W., Nenninger, A., Ray, N., and Robinson, C. (2006) Diffusion of green fluorescent protein in three cell environments in *Escherichia coli*. *J Bacteriol*, 188:3442-3448.

Niebisch, A., and Bott, M. (2001) Molecular analysis of the cytochrome bc1-aa3 branch of the *Corynebacterium glutamicum* respiratory chain containing an unusual diheme cytochrome c1. *Arch Microbiol*, 175:282-294.

Niebisch, A., and Bott, M. (2003) Purification of a cytochrome bc-aa3 supercomplex with quinol oxidase activity from *Corynebacterium glutamicum*. Identification of a fourth subunity of cytochrome aa3 oxidase and mutational analysis of diheme cytochrome c1. *J Biol Chem*, 278:4339-4346.

Niederweis, M., Danilchanka, O., Huff, J., Hoffmann, C., and Engelhardt, H. (2010) Mycobacterial outer membranes: in search of proteins. *Trends Microbiol*, 18:109-116.

Nikaido, H. (2003) Molecular basis of bacterial outer membrane permeability revisited. *Microbiol Mol Biol Rev*, 67:593-656.

Okibe, N., Suzuki, N., Inui, M., and Yukawa, H. (2011) Efficient markerless gene replacement in *Corynebacterium glutamicum* using a new temperature-sensitive plasmid. *J Microbiol Methods*, 85:155-163.

Orriss, G.L., Tarry, M.J., Ize, B., Sargent, F., Lea, S.M., Palmer, T., and Berks, B.C. (2007) TatBC, TatB, and TatC form structurally autonomous units within the twin arginine protein transport system of *Escherichia coli*. *FEBS Lett*, 581:4091-4097.

Palmer, T., and Berks, B.C. (2012) The twin-arginine translocation (Tat) protein export pathway. *Nat Rev Microbiol*,

Papish, A.L., Ladner, C.L., and Turner, R.J. (2003) The twin-arginine leader-binding protein, DmsD, interacts with the TatB and TatC subunits of the *Escherichia coli* twin-arginine translocase. *J Biol Chem*, 278:32501-32506.

Pappin, D.J., Hojrup, P., and Bleasby, A.J. (1993) Rapid identification of proteins by peptide-mass fingerprinting. *Curr Biol*, 3:327-332.

Perkins, D.N., Pappin, D.J., Creasy, D.M., and Cottrell, J.S. (1999) Probability-based protein identification by searching sequence databases using mass spectrometry data. *Electrophoresis*, 20:3551-3567.

Pett, W., and Lavrov, D.V. (2013) The twin-arginine subunit C in *Oscarella*: origin, evolution, and potential functional significance. *Integr Comp Biol*, 53:495-502.

Pogliano, J.A., and Beckwith, J. (1994) SecD and SecF facilitate protein export in *Escherichia coli. EMBO J*, 13:554-561.

Pommier, J., Méjean, V., Giordano, G., and Iobbi-Nivol, C. (1998) TorD, a cytoplasmic chaperone that interacts with the unfolded trimethylamine N-oxide reductase enzyme (TorA) in *Escherichia coli. J Biol Chem*, 273:16615-16620.

Pop, O., Martin, U., Abel, C., and Muller, J.P. (2002) The twin-arginine signal peptide of PhoD and the TatAd/Cd proteins of *Bacillus subtilis* form an autonomous Tat translocation system. *J Biol Chem*, 277:3268-3273.

Poritz, M.A., Bernstein, H.D., Strub, K., Zopf, D., Wilhelm, H., and Walter, P. (1990) An *E. coli* ribonucleoprotein containing 4.5 S RNA resembles mammalian signal recognition particle. *Science*, 250:1111-1117.

Ramasamy, S., Abrol, R., Suloway, C.J.M., and Clemons, W.M. (2013) The Glove-like Structure of the Conserved Membrane Protein TatC Provides Insight into Signal Sequence Recognition in Twin-Arginine Translocation. *Structure*, 21:777-788.

Redelberger, D., Genest, O., Arabet, D., Mejean, V., Ilbert, M., and Iobbi-Nivol, C. (2013) Quality control of a molybdoenzyme by the Lon protease. *FEBS Lett*, 587:3935-3942.

Rezwan, M., Grau, T., Tschumi, A., and Sander, P. (2007) Lipoprotein synthesis in mycobacteria. *Microbiology*, 153:652-658.

Rodrigue, A., Chanal, A., Beck, K., Muller, M., and Wu, L.F. (1999) Co-translocation of a periplasmic enzyme complex by a hitchhiker mechanism through the bacterial tat pathway. *J Biol Chem*, 274:13223-13228.

Rodriguez, F., Rouse, S.L., Tait, C.E., Harmer, J., Riso, A.D., Timmel, C.R., Sansom, M.S.P., Berks, B.C., and Schnell, J.R. (2013) Structural model for the protein-translocating element of the twin-arginine transport system. *Proc Natl Acad Sci U S A*,

Rojas Contreras, J.A., Pedraza-Reyes, M., Ordonez, L.G., Estrada, N.U., Barba de la Rosa, A.P., and De Leon-Rodriguez, A. (2010) Replicative and integrative plasmids for production of human interferon gamma in *Bacillus subtilis. Plasmid*, 64:170-176.

Rose, R.W., Bruser, T., Kissinger, J.C., and Pohlschroder, M. (2002) Adaptation of protein secretion to extremely high-salt conditions by extensive use of the twin-arginine translocation pathway. *Mol Microbiol*, 45:943-950.

Rusch, S.L., and Kendall, D.A. (2007) Interactions that drive Sec-dependent bacterial protein transport. *Biochemistry*, 46:9665-9673.

Saint-Joanis, B., Demangel, C., Jackson, M., Brodin, P., Marsollier, L., Boshoff, H., and Cole, S.T. (2006) Inactivation of Rv2525c, a substrate of the twin arginine translocation (Tat) system of *Mycobacterium tuberculosis*, increases beta-lactam susceptibility and virulence. *J Bacteriol*, 188:6669-6679.

Sargent, F., Bogsch, E.G., Stanley, N.R., Wexler, M., Robinson, C., Berks, B.C., and Palmer, T. (1998) Overlapping functions of components of a bacterial Sec-independent protein export pathway. *EMBO J*, 17:3640-3650.

Sargent, F., Stanley, N.R., Berks, B.C., and Palmer, T. (1999) Sec-independent protein translocation in *Escherichia coli.* A distinct and pivotal role for the TatB protein. *J Biol Chem*, 274:36073-36082.

Sargent, F. (2007) Constructing the wonders of the bacterial world: biosynthesis of complex enzymes. *Microbiology*, 153:633-651.

Sargent, F., Berks, B.C., and Palmer, T. (2002) Assembly of membrane-bound respiratory complexes by the Tat protein-transport system. *Arch Microbiol*, 178:77-84.

Sarrouh, B., Santos, T.M., Miyoshi, A., Dias, R., and Azevedo, V. (2012) Up-To-Date Insight on Industrial Enzymes Applications and Global Market. *J Bioproces Biotechniq*,

Schaefer, A., Tauch, A., Jaeger, W., Kalinowski, J., Thierbach, G., and Puehler, A. (1994) Small mobilizable multi-purpose cloning vectors derived from the *Escherichia coli* plasmids pK18 and pK19: selection of defined deletions in the chromosome of *Corynebacterium glutamicum. Gene*, 145:69-73.

Scheele, S., Oertel, D., Bongaerts, J., Evers, S., Hellmuth, H., Maurer, K.H., Bott, M., and Freudl, R. (2013) Secretory production of an FAD cofactor-containing cytosolic enzyme (sorbitol-xylitol oxidase from *Streptomyces coelicolor*) using the twin-arginine translocation (Tat) pathway of *Corynebacterium glutamicum*. *Microb Biotechnol*, 6:202-206.

Schmidt, C.L., and Shaw, L. (2001) A comprehensive phylogenetic analysis of Rieske and Rieske-type iron-sulfur proteins. *J Bioenerg Biomembr*, 33:9-26.

Schmidt, F.R. (2004) Recombinant expression systems in the pharmaceutical industry. *Appl Microbiol Biotechnol*, 65:363-372.

Schmidt, T.G., and Skerra, A. (2007) The Strep-tag system for one-step purification and high-affinity detection or capturing of proteins. *Nat Protoc*, 2:1528-1535.

Schulze, R.J., Komar, J., Botte, M., Allen, W.J., Whitehouse, S., Gold, V.A., Lycklama, A.N.J.A., Huard, K., Berger, I., Schaffitzel, C., and Collinson, I. (2014) Membrane protein insertion and proton-motive-force-dependent secretion through the bacterial holo-translocon SecYEG-SecDF-YajC-YidC. *Proc Natl Acad Sci U S A*, 111:4844-4849.

Schwarz, G. (2005) Molybdenum cofactor biosynthesis and deficiency. *Cell Mol Life Sci*, 62:2792-2810.

Scott, J.R., and Barnett, T.C. (2006) Surface proteins of gram-positive bacteria and how they get there. *Annu Rev Microbiol*, 60:397-423.

Settles, A.M., Yonetani, A., Baron, A., Bush, D.R., Cline, K., and Martienssen, R. (1997) Sec-independent protein translocation by the maize Hcf106 protein. *Science*, 278:1467-1470.

Shanmugham, A., Bakayan, A., Völler, P., Grosveld, J., Lill, H., and Bollen, Y.J.M. (2012) The hydrophobic core of twin-arginine signal sequences orchestrates specific binding to Tat-pathway related chaperones. *PLoS One*, 7:e34159.

Sharp, P.A., Sugden, B., and Sambrook, J. (1973) Detection of two restriction endonuclease activities in *Haemophilus parainfluenzae* using analytical agarose-ethidium bromide electrophoresis. *Biochemistry*, 12:3055-3063.

Shimomura, O., Johnson, F.H., and Saiga, Y. (1962) Extraction, purification and properties of aequorin, a bioluminescent protein from the luminous hydromedusan, *Aequorea. J Cell Comp Physiol*, 59:223-239.

Silhavy, T.J., Kahne, D., and Walker, S. (2010) The bacterial cell envelope. *Cold Spring Harb Perspect Biol*, 2:a000414.

Simon, G., Mejean, V., Jourlin, C., Chippaux, M., and Pascal, M.C. (1994) The torR gene of *Escherichia coli* encodes a response regulator protein involved in the expression of the trimethylamine N-oxide reductase genes. *J Bacteriol*, 176:5601-5606.

Simone, D., Bay, D.C., Leach, T., and Turner, R.J. (2013) Diversity and Evolution of Bacterial Twin Arginine Translocase Protein, TatC, Reveals a Protein Secretion System That Is Evolving to Fit Its Environmental Niche. *PLoS One*, 8:e78742.

Stanley, N.R., Palmer, T., and Berks, B.C. (2000) The twin arginine consensus motif of Tat signal peptides is involved in Sec-independent protein targeting in *Escherichia coli. J Biol Chem*, 275:11591-11596.

Sussman, J.K., Simons, E.L., and Simons, R.W. (1996) *Escherichia coli* translation initiation factor 3 discriminates the initiation codon in vivo. *Mol Microbiol*, 21:347-360.

Takeshita, S., Sato, M., Toba, M., Masahashi, W., and Hashimoto-Gotoh, T. (1987) High-copy-number and low-copy-number plasmid vectors for *lacZ* α-complementation and chloramphenicol- or kanamycin-resistance selection. *Gene*, 61:63-74.

Tanaka, S., Lerner, S.A., and Lin, E.C. (1967) Replacement of a phosphoenolpyruvate-dependent phosphotransferase by a nicotinamide adenine dinucleotide-linked dehydrogenase for the utilization of mannitol. *J Bacteriol*, 93:642-648.

Tarry, M.J., Schafer, E., Chen, S., Buchanan, G., Greene, N.P., Lea, S.M., Palmer, T., Saibil, H.R., and Berks, B.C. (2009) Structural analysis of substrate binding by the TatBC component of the twin-arginine protein transport system. *Proc Natl Acad Sci U S A*, 106:13284-13289.

Topping, T.B., and Randall, L.L. (1997) Chaperone SecB from Escherichia coli mediates kinetic partitioning via a dynamic equilibrium with its ligands. *Journal of Biological Chemistry*, 272:19314-19318.

Tranier, S., Mortier-Barriere, I., Ilbert, M., Birck, C., Iobbi-Nivol, C., Mejean, V., and Samama, J.P. (2002) Characterization and multiple molecular forms of TorD from *Shewanella massilia*, the putative chaperone of the molybdoenzyme TorA. *Protein Sci*, 11:2148-2157.

Tranier, S., Iobbi-Nivol, C., Birck, C., Ilbert, M., Mortier-Barrière, I., Méjean, V., and Samama, J.-P. (2003) A novel protein fold and extreme domain swapping in the dimeric TorD chaperone from *Shewanella massilia. Structure*, 11:165-174.

Tsukazaki, T., Mori, H., Echizen, Y., Ishitani, R., Fukai, S., Tanaka, T., Perederina, A., Vassylyev, D.G., Kohno, T., Maturana, A.D., Ito, K., and Nureki, O. (2011) Structure and function of a membrane component SecDF that enhances protein export. *Nature*, 474:235-238.

Tullman-Ercek, D., DeLisa, M.P., Kawarasaki, Y., Iranpour, P., Ribnicky, B., Palmer, T., and Georgiou, G. (2007) Export pathway selectivity of *Escherichia coli* twin arginine translocation signal peptides. *J Biol Chem*, 282:8309-8316.

Turner, R.J., Papish, A.L., and Sargent, F. (2004) Sequence analysis of bacterial redox enzyme maturation proteins (REMPs). *Can J Microbiol*, 50:225-238.

Ullers, R.S., Luirink, J., Harms, N., Schwager, F., Georgopoulos, C., and Genevaux, P. (2004) SecB is a bona fide generalized chaperone in Escherichia coli. *Proc Natl Acad Sci U S A*, 101:7583-7588.

Valent, Q.A., Scotti, P.A., High, S., de Gier, J.W., von Heijne, G., Lentzen, G., Wintermeyer, W., Oudega, B., and Luirink, J. (1998) The *Escherichia coli* SRP and SecB targeting pathways converge at the translocon. *EMBO J*, 17:2504-2512.

van der Rest, M.E., Lange, C., and Molenaar, D. (1999) A heat shock following electroporation induces highly efficient transformation of *Corynebacterium glutamicum* with xenogeneic plasmid DNA. *Appl Microbiol Biotechnol*, 52:541-545.

Varela, C., Rittmann, D., Singh, A., Krumbach, K., Bhatt, K., Eggeling, L., Besra, G.S., and Bhatt, A. (2012) MmpL genes are associated with mycolic acid metabolism in mycobacteria and corynebacteria. *Chem Biol*, 19:498-506.

Vogt, M., Haas, S., Klaffl, S., Polen, T., Eggeling, L., Ooyen, J.V., and Bott, M. (2013) Pushing product formation to its limit: Metabolic engineering of *Corynebacterium glutamicum* for l-leucine overproduction. *Metabolic engineering*, 22:40-52.

Wagley, S., Hemsley, C., Thomas, R., Moule, M.G., Vanaporn, M., Andreae, C., Robinson, M., Goldman, S., Wren, B.W., Butler, C.S., and Titball, R.W. (2014) The twin arginine translocation system is essential for aerobic growth and full virulence of *Burkholderia thailandensis*. *J Bacteriol*, 196:407-416.

Walker, M.B., Roy, L.M., Coleman, E., Voelker, R., and Barkan, A. (1999) The maize *tha4* gene functions in sec-independent protein transport in chloroplasts and is related to *hcf106*, *tatA*, and *tatB*. *J Cell Biol*, 147:267-276.

Watanabe, K., Tsuchida, Y., Okibe, N., Teramoto, H., Suzuki, N., Inui, M., and Yukawa, H. (2009) Scanning the *Corynebacterium glutamicum* R genome for high-efficiency secretion signal sequences. *Microbiology*, 155:741-750.

Wexler, M., Sargent, F., Jack, R.L., Stanley, N.R., Bogsch, E.G., Robinson, C., Berks, B.C., and Palmer, T. (2000) TatD is a cytoplasmic protein with DNase activity. No requirement for TatD family proteins in sec-independent protein export. *J Biol Chem*, 275:16717-16722.

Whitaker, N., Bageshwar, U.K., and Musser, S.M. (2012) Kinetics of precursor interactions with the bacterial Tat translocase detected by real-time FRET. J Biol Chem

Yahr, T.L., and Wickner, W.T. (2001) Functional reconstitution of bacterial Tat translocation *in vitro*. *EMBO J*, 20:2472-2479.

Yen, M.R., Tseng, Y.H., Nguyen, E.H., Wu, L.F., and Saier, M.H.J. (2002) Sequence and phylogenetic analyses of the twin-arginine targeting (Tat) protein export system. *Arch Microbiol*, 177:441-450.

Zhu, L., Klenner, C., Kuhn, A., and Dalbey, R.E. (2012) Both YidC and SecYEG are required for translocation of the periplasmic loops 1 and 2 of the multispanning membrane protein TatC. *J Mol Biol*, 424:354-367.

Zuber, B., Chami, M., Houssin, C., Dubochet, J., Griffiths, G., and Daffé, M. (2008) Direct visualization of the outer membrane of mycobacteria and corynebacteria in their native state. *J Bacteriol*, 190:5672-5680.

Acknowledgement

I would like to express my special appreciation and thanks to my supervisor Prof. Dr. Roland Freudl for his support, discussions, constructive criticism and patience with my writing style.

I would like to thank Prof. Dr. Joachim Ernst for kindly taking on the corefereeship of this work.

For the excellent working conditions at the Institute for Bio- and Geosciences IBG1:Biotechnology, I would like to thank Prof. Dr. Michael Bott.

My special thanks go to all current and previous members of the work goup bacterial protein secretion for creating an excellent working atmosphere. Especially to Astrid Bida with whom I greatly enjoyed sharing a lab bench and who contributed considerably to the finalization of this work but also to: Dr. Frank Lausberg, Dr. Stefan Fleckenstein, Dr. Ava Chattophadyay, Sonja Müller, Dr. Sandra Scheele, Doris Dohmen-Olma and Sarah Jurischka.

Furthermore I would like to thank all members at the IBG1 who were always open for discussions and contributed to quality time during incubation times and while the centrifuge was running (in alphabetical order): Dr. Stefan Binder, Ursula Degner, Helga Etterich, Dr. Kristina Hoffmann, Dr. Abigail Koch-Koerfges, Dr. Andreas Küberl, Jennifer Pahlke, Dr. Georg Schendzielorz, Dr. Jan van Ooyen, Philana van Summeren-Wesenhagen, Dr. Michael Vogt and Sabrina Witthoff.

Most importantly, I would like to thank my parents as well as Timm and Daria who have supported me through thick and thin throughout all these years.

My greatest thanks go to my soul mate Anne without whose boundless loving support I would not be at the place I am now.

Ich versichere hiermit, dass ich die vorliegende Arbeit selbständig angefertigt und keine anderen als die angegebenen Quellen und Hilfsmittel verwendet habe.

Jülich, den 27. Juni 2014